THE CELLULAR RESPONSE OF THE MONGOLIAN GERBIL (*MERIONES UNGUICULATUS*), A NONPERMISSIVE HOST, TO CANINE HEARTWORM (*DIROFILARIA IMMITIS*)

by

ELYSSA JACOB CAMPBELL

(Under the Direction of Andrew R. Moorhead)

ABSTRACT

A comprehensive understanding of *Dirofilaria immitis*, canine heartworm, requires thorough investigation into each life stage to understand not only the mechanisms of parasite establishment within the host, but also host-parasite interaction during establishment. Due to the limited availability of *D. immitis* in research settings, the majority of *in vitro* studies focus on the microfilariae and third-stage larval life stages of the parasite. Current *in vivo D. immitis* research relies on an established infection in a permissive host, and the best animal models for these studies are dogs and ferrets. Rodent animal models are generally preferred by researchers for *in vivo* work due to the nature of the research and economics; however, previous studies have attempted to establish infection in immunocompetent mice, rats, and jirds without success. The studies in this dissertation are innovative for three reasons: Chapter 2 describes the first study to characterize the initial cellular immune response of a nonpermissive host, the Mongolian gerbil, to *D. immitis* intraperitoneal infection. Chapter 3 describes the first study to explore the role of

gerbil peritoneal exudate cells with flow cytometry and is the first to deplete gerbil peritoneal macrophages. Chapter 4 describes differential splicing of SLO-1 that could underlie differences in emodepside activity against relevant *D. immitis* life stages. In the studies of this dissertation, we hypothesized that the establishment of *D. immitis* in the definitive host is determined by that host's immune response to the presence of larvae. The results of these proposed studies will fill in a gap of knowledge regarding the determinants of filarial host specificity. The results also provide insight into the anti-filarial mechanisms of the host, which may be used to discover a preventive and/or therapeutic in the future. Not only will the results of these studies impact the field of canine heartworm research, but they can also lead to more targeted eradication efforts of other types of human and animal infectious filarial diseases.

INDEX WORDS: *Dirofilaria immitis,* canine heartworm, Mongolian gerbil, jird, peritoneal exudate cells, cellular immune response, macrophage, SLO-1

THE CELLULAR RESPONSE OF THE MONGOLIAN GERBIL (*MERIONES UNGUICULATUS*), A NONPERMISSIVE HOST, TO CANINE HEARTWORM (*DIROFILARIA IMMITIS*)

by

ELYSSA JACOB CAMPBELL

B.A., Georgia State University, 2011

A Dissertation Submitted to the Graduate Faculty of the University of Georgia in Partial Fulfillment of the Requirements for the Degree

DOCTOR OF PHILOSOPHY

ATHENS, GEORGIA

2024

THE CELLULAR RESPONSE OF THE MONGOLIAN GERBIL (*MERIONES UNGUICULATUS*), A NONPERMISSIVE HOST, TO CANINE HEARTWORM (*DIROFILARIA IMMITIS*)

by

ELYSSA JACOB CAMPBELL

Major Professor:	Andrew R. Moorhead
Committee:	Kaori Sakamoto
	Michael Dzimianksi
	John Harrington

Electronic Version Approved:

Ronald Walcott
Dean of the Graduate School
The University of Georgia
August 2024

DEDICATION

To my husband, Aaron, thank you for your unwavering support and encouragement.

To my daughter, Mackenna, you will always be my inspiration.

ACKNOWLEDGMENTS

I would like to express my deepest gratitude to the following individuals and organizations whose support and encouragement were invaluable throughout my dissertation journey:

My mentor, Dr. Andy Moorhead, for their guidance, insightful feedback, and steadfast support from the inception to the completion of this dissertation. My Committee Members, Drs. Mike Dzimianski, Kaori Sakamoto, and John Harrington, for their constructive criticism, valuable suggestions, and for challenging me to think critically and creatively. My lab colleagues, Katie Greenway, Leonor Sicalo Gianechini, Sam Hogan, Chris Evans, Yi Chu, Tanya Cooper, Angela Tolbert, Liz Boudreau, and Catherine Pope for their scientific, technical, and moral support. My family, for their love, understanding, and encouragement, which sustained me through the highs and lows of this academic endeavor. Animol Discoveries for their financial support and TRS Labs, Inc., which enabled me to conduct research and complete this dissertation. Drs. Tim Geary and Mostafa Zamanian, for their collaboration, mentorship, and engaging in stimulating discussions.

I am also grateful to all those who have contributed in ways big and small, directly or indirectly, to the completion of this dissertation.

TABLE OF CONTENTS

LIST OF TABLES

LIST OF FIGURES

ABBREVIATIONS

AAM	alternatively activated macrophage
ANOVA	analysis of variance
BALB/c	Bagg Albino mice with the genotype at the color locus of c/c
Bm-CPL-1	cysteine protein inhibitor expressed by *Brugia malayi*
BW	body weight
BSA	bovine serum albumin
C1q	complement component
CAM	classically activated macrophage
CD	cluster of differentiation
CI	confidence interval
CL	clodronate
CRT	calreticulin
ddPCR	droplet digital PCR
Di-CPI	cysteine protein inhibitor expressed by *Dirofilaria immitis*
dpi	days post infection
DNA	deoxyribonucleic acid
DPBS	Dulbecco's phosphate buffered saline
EMO	emodepside
FDA	Federal Drug Administration
GA	Georgia 2
GluCls	glutamate-gated chloride channels
H&E	hematoxylin and eosin stain
HBSS	Hank's balanced salt solution
IA	immature adult
Iba1	ionized calcium-binding adaptor molecule 1
IFN	interferon
IgG	Immunoglobulin G
IGS	International Genetic Standardization
IHC	immunohistochemistry
IL	interleukin
iNOS	inducible nitric oxide synthase
IP	intraperitoneal
IVM	ivermectin
JYD	JYD-34
L3	third-stage larva(e)
L4	fourth-stage larva(e)
LOE	loss of efficacy
MF	microfilaria(e)
MIF	macrophage migration inhibitory factor
ML	macrocyclic lactone

MO	Missouri
MOX	moxidectin
NETs	neutrophil extracellular traps
NIAID	National Institute of Allergy and Infectious Diseases
NIH	National Institute of Health
NRG	NOD-Rag1^{null} IL2rg^{null}
NSG	NOD/ShiLtJ scid gamma
PBMCs	peripheral blood mononuclear cells
PBS	phosphate buffered solution
PCA	principal component analysis
PCR	polymerase chain reaction
PEC	peritoneal exudate cell
RNA	ribonucleic acid
SC	subcutaneous
SCID	severe combined immunodeficiency disease
SLO-1	calcium activated, voltage-dependent potassium channel SLO-1
STAT	Signal Transducer and Activator of Transcription
TGF	transforming growth factor
Th	T helper
TNF	tumor-necrosis factor
UV	ultraviolet

CHAPTER 1

INTRODUCTION AND LITERATURE REVIEW

Principles of infectious diseases

Infectious diseases are defined as an illness, caused by a pathogen, and transmitted from an infected person, animal, or contaminated inanimate object to a susceptible host [1]. A disease requires an infection to not only disrupt the host but damage the host in a way that results in objective and subjective symptoms and signs of illness [1]. Recovery from the infection is considered complete when there is elimination of the agent, and incomplete when there is a latent or chronic infection. A latent infection is defined by agents that remain dormant in host cells and may be reactivated. Alternatively, a chronic infection is due to the persistent presence of the infectious agent within the host [1].

Host susceptibility, environmental factors, and pathogenic agents are three determinants unique to every infectious disease [2]. Host susceptibility to infection by pathogenic agents and disease depends on genetic innate immunity, acquired immunity from exposure or vaccination, age, stress, nutrition, and immunocompromised conditions such as chronic illness or pregnancy [1]. Environmental factors can also determine infection by pathogenic agents and host susceptibility. Physical, social, and behavioral factors determine the transmission of agents, and there are cultural, political, and economic determinants that impact acquired immunity and may contribute to underlying conditions [1]. The infectivity of a pathogenic agent is defined by the number of agents required to infect 50% of the susceptible host population [1], and mediated by the route of inoculation, mode of transmission, and stability outside of the host [3]. There are

four groups of pathogenic agents: viruses, bacteria, fungi, and parasites [1, 3]. Because my dissertation research focuses on nematodes, with some reference to their endosymbiont bacterium, *Wolbachia*, I will only discuss bacteria and parasites here.

Bacteria

Most bacteria that mammals encounter in a lifetime are considered normal flora, which inhabits skin, large intestines, and the mouth; the minority of bacteria that is distinct from normal flora is likely pathogenic [4]. Bacteria typically exist as free-living cells, conducting the majority of their essential metabolic processes internally and only depending on the host for acquiring their nutrition [4]. Although minimal in their morphologic variety, characterized by their shape as rods, cocci, or spirals, bacteria are distinct from one another due to a variety of surface structures that assist in movement and adherence [4]. The objective of bacteria is to multiply, not cause disease [5]. Bacterial virulence factors cause toxicity directly to host cells, allowing the bacteria to invade the host, cause disease, and evade host defenses [4, 5]. The host has nonspecific resistance to the pathogenic bacteria at initial infection and will build specific immunity over time to destroy the bacteria at the next infection [5]. The first cellular response in a host after a bacterial infection, such as with *Shigella*, a causative agent of dysentery, involves macrophages and neutrophils. Macrophages reside in the tissues of the host and neutrophils reside in the blood of a healthy individual until a bacterial infection is detected. Neutrophils are then quickly recruited to the site of infection where they work with macrophages to clear the pathogen through phagocytosis [4]. Due to foundational genetic differences between bacteria and their hosts, antibacterial drugs can inhibit bacterial processes such as DNA replication, transcription, and translation without harming the host [4].

Parasites

Billions of humans and animals are infected with parasites, which are transmitted by blood, food, water, and vectors. Parasites are smaller organisms that live on, within, or at the expense of a larger organism known as the host [6]. The three major classes of parasites are protozoa, arthropods, and helminths. Protozoa are microscopic, unicellular parasites that can reproduce sexually or asexually, prefer moist environments, and can be classified by their motility: flagellates, ciliates, and amoebae [7]. Arthropods are invertebrate parasites, commonly known as ectoparasites, that affect the host by sucking blood or tissue fluids (fleas, lice, mites, and ticks) or by burrowing into skin and orifices (mites, fleas, and flies) [8]. Helminths are multicellular worm-like parasites that are characterized by their external and internal morphology of their developmental stages: egg, larva, and adult [9]. Helminth species exhibit both hermaphroditic and bisexual life histories. The ultimate classification of helminths is based on the egg, larval, and adult stages [9]. The three categories of helminths are trematodes, cestodes, and nematodes, more commonly known as flukes, tapeworms, and roundworms, respectively [9]. Adult nematodes can survive for years in a mammalian host [10] due to their immunomodulatory properties [11], which are due to the molecular communication between the parasite and the host inducing, for example, a lack of response from antigen-specific T cells [12, 13].

Determinants of host specificity

Host specificity refers to the different host species a parasite can infect and is largely dependent on structural (ecological importance), phylogenetic, and geographic specificity [14, 15]. Although host susceptibility factors, such as microbiome, inoculum, sex, temperature,

environment, age, chance, history, immunity, nutrition, and genetics [16], can affect the establishment of a parasite, host susceptibility and specificity are distinct from one another, because the former regards an individual host, and the latter includes the species. One factor of host specificity is the relative ecological importance [15] of the host, known as structural specificity. Soil-transmitted helminths, parasitic worms in the soil that cause gastrointestinal infections, pass their eggs in the feces. These parasites are often transmitted in areas lacking adequate sanitation resulting in soil contamination [17]. Vector-borne parasites differ from soil-transmitted worms because they rely on an intermediate host for the parasite's development, in addition to a definitive host in which the parasite matures to adulthood and reproduces sexually. [6, 18].

Dirofilaria immitis, commonly known as canine heartworm, is generally found in the warmer regions of North and South America, Europe, Asia, and Australia, where transmission of the parasite by the mosquito intermediate host to the canine definitive host can occur for most of the year [19]. Phylogenetic specificity, another factor of host specificity, refers to species that are closely related, often exhibiting comparable biological, behavioral, and physiological characteristics [15, 20]. Hosts susceptible to patent *D. immitis* infection, dogs, wild canids, ferrets, and seals, belong to the suborder Caniformia within the order Carnivora [21, 22]. Patent *D. immitis* infections are defined as the ability of adult worms to produce microfilariae, continuing the ability of the parasite to be transmitted to the mosquito vector. A third factor of host specificity is geography, where the parasite, intermediate host, and definitive host are able to interact [15].

Host specificity of filariae

Relationship between the host and filarial helminth

Filarial pathogens are nematode obligate endoparasites, parasites within the body of a host that always require a host, belonging in the family of *Onchocercidae* within the superfamily Filarioidea [6]. Within the family *Onchocercidae* are the causative agents of important veterinary and human diseases, including canine heartworm (*D. immitis*), lymphatic filariasis (*Wuchereria bancrofti* and *Brugia malayi*), and river blindness (*Onchocerca volvulus*) [6]. Filariae, vector-borne, thread-like, parasitic nematodes, reside in specific tissues of a definitive host depending on the species (Table 1.1). The progeny, microfilariae (MF), are ingested by an arthropod intermediate host, required for transmission of the infective larvae to another definitive host [6]. Pathogens transmitted by invertebrates, such as arthropods, are commonly referred to as vector-borne diseases [6].

Species of Onchocercidae

There are several species of Onchocercidae that infect both animals and humans (Table 1.1). These species are unique in their definitive host, vector, and clinical disease presentation.

Table 1.1
Species of Onchocercidae

Species	Definitive host	Vector	Disease
Brugia malayi	Human	Mosquitoes	Lymphatic filariasis
Brugia timori	Human	Mosquitoes	Lymphatic filariasis
Wuchereria bancrofti	Human	Mosquitoes	Lymphatic filariasis
Loa	Human	Deer flies	Subcutaneous filariasis (loiasis)
Onchocerca volvulus	Human	Blackflies	Subcutaneous filariasis (river blindness)
Mansonella streptocerca	Human Chimpanzee	Biting midge	Subcutaneous filariasis
Mansonella pertans	Human	Biting midge	Cavity filariasis
Mansonella ozzardi	Human	Biting midge Blackflies	Cavity filariasis
Dirofilaria immitis	Dogs	Mosquitoes	Pulmonary dirofilariasis (canine heartworm)
Dirofilaria repens	Dogs	Mosquitoes	Subcutaneous dirofilariasis
Dirofilaria striata	Bobcats	Mosquitoes	Subcutaneous dirofilariasis
Dirofilaria subdermata	Porcupines	Mosquitoes	Subcutaneous dirofilariasis
Dirofilaria tenuis	Raccoons	Mosquitoes	Subcutaneous dirofilariasis
Dirofilaria ursi	Bears	Blackflies	Subcutaneous dirofilariasis
Brugia pahangi	Cats	Mosquitoes	Feline filariasis
Onchocerca ochengi	Bovines	Blackflies	Intradermal onchocerciasis
Acanthocheilonema viteae	Rodents	Soft ticks	Subcutaneous filariasis
Litomosoides sigmodontis	Cotton rats	Rat mite	Cavity filariasis

Notes: Compiled and adapted from [6, 23].

Host-parasite interaction with filariae

In order to survive and reproduce in definitive hosts, filariae must evade the host immune system. One method of immune evasion is immunomodulation, which relies on molecular

interactions between the parasite and the host to create a more favorable environment for development and establishment [24]. Parasites secrete soluble excretory/secretory (E/S) proteins, such as protease inhibitors and cytokine homologs, that have immunomodulatory qualities [12]. Another characteristic of filarial worms is the harboring of the endosymbiotic bacterium, *Wolbachia*, passed transovarially from the female to offspring [25]. Filarial worms can successfully evade the immune system of their host, although they are initially recognized by innate immune cells. Hansen, *et al*. found that the filarial parasite, *Onchocerca ochengi,* releases *Wolbachia*-derived molecules while residing in fibrous nodules, attracting neutrophils. It is only when the *Wolbachia* is cleared by administration of an antibiotic to the host that neutrophils gradually diminish, and eosinophils surround the worms, degranulating their contents onto the surface of the worm. The authors suggest that the *Wolbachia*-induced neutrophilia protects adult *O. ocheng*i from eosinophil degranulation, and that an increased combination of immunological signals by the host may increase the fitness of the parasite [26]. Bovine chemokines that typically attract neutrophils were significantly downregulated in the *Wolbachia*-depleted group, suggesting that the *O. ochengi* attract eosinophils when the endosymbiotic bacteria, *Wolbachia*, is not able to attract neutrophils. There was a clear inverse relationship between neutrophil counts and eosinophil degranulation. When *Wolbachia* was re-introduced in the host, there was a decrease in eosinophils, an increase in neutrophils, and sustained survival of the adult worms [26].

Animal models for filarial parasite research

Filarial worms are host-specific, and *in vivo* models, especially rodent models of filariae in which the rodent is not the definitive host, are not as comparable to the definitive host due to

the distant relatedness of rodents with the latter. Most immunocompetent rodents are not permissive to the establishment of filariae due to factors of host specificity and the rodent immune response, and some adult filariae are too large to be accommodated by the rodent's body cavities or organs [27]. Although *in vitro* testing of novel anti-helminthic compounds on filarial worms can signal promising new drug candidates, the *in vitro* results rarely translate to the activity against the filariae *in vivo* [27]. Aside from macrocyclic lactones (MLs) and cyclodepsipeptides, no new chemical class exhibiting antifilarial properties has emerged despite extensive *in vitro* screening efforts by several researchers. This suggests a significant gap between the efficacy observed *in vitro* and the efficacy against the filarial parasite *in vivo*, especially in the definitive host [27]. Filarial worms are deeply embedded within the host's body, necessitating optimal drug pharmacokinetics for effective penetration. This challenge is unlikely to be adequately addressed using models that employ surrogate hosts or different parasite species, thus requiring careful consideration. It is well-known that anti-filarial therapeutics, like ivermectin, inhibit functional components of the worm. However, it is the host immune response that assists in the removal of the parasite once its functions are inhibited by ivermectin [28]. Albeit, researchers have developed immunocompetent and immunocompromised animal models for production of parasite resources, as well as *in vivo* testing of anti-filarial compounds as shown in Table 1.2.

Table 1.2
Animal models for filarial production and efficacy testing of MLs and cyclooctadepsipeptide emodepside

Species	Definitive host	Animal Model	Immunocompetent
Brugia malayi	Human	Cat	+
		Dog	+
		M. unguiculatus	+
		M. coucha	+
		BALB/c mice	+
		Athymic mice	-
		SCID mice	-
Loa loa	Human	SCID mice	-
Onchocerca volvulus	Human	Bovine	+
Dirofilaria immitis	Dogs	Dog	+
		Ferret	+
		Sprague-Dawley IGS Rat	-
		NSG mice	-
		NRG mice	-
Brugia pahangi	Cats	Dog	+
		Cat	+
		M. unguiculatus	+
		M. coucha	+
		BALB/c mice	+
		Athymic mice	-
		SCID mice	-
Acanthocheilonema vitea	Rodents	*M. coucha*	+
		M. natalensis	+
		M. unguiculatus	+
Litomosoides sigmodontis	Cotton rats	Cotton rats	+
		BALB/c mice	+
		M. coucha	+

Notes: Sources from [27, 29-31].

Significance of *Dirofilaria immitis*

Canine heartworm disease, caused by the filarial nematode *D. immitis*, was diagnosed in almost 200,000 dogs in the United States in the year 2023 [32], although the actual number is

likely underestimated due to owners declining veterinary care and diagnostics. These parasites are transmitted by mosquito vectors. Infectious third-stage larvae (L3) are deposited on the dog's skin during an infected mosquito's blood meal and enter the bite wound to migrate through the cutaneous tissue and molt into fourth-stage larvae (L4). The L4 travel through the tissues and molt one last time into immature adults (IA) between 50- and 58-days post infection [33]. As early as 68 days post-infection [34], the IA establish in the heart and pulmonary arteries, becoming sexually mature adults around 4.5 months post infection and producing MF 6 months post infection [34]. A mosquito ingests blood containing MF from a heartworm-infected dog (Figure 1.1). The MF undergo two molts in the mosquito, developing to L3. These L3 are considered infectious as they have made their way to the head and proboscis of the mosquito. Adult *D. immitis* worms can live between 5-7 years in dogs [33] and cause irreparable clinical and pathological changes to the heart and pulmonary artery, including inflammation, pulmonary hypertension, disruption of vascular integrity, and fibrosis [35].

Figure 1.1
Dirofilaria immitis life cycle

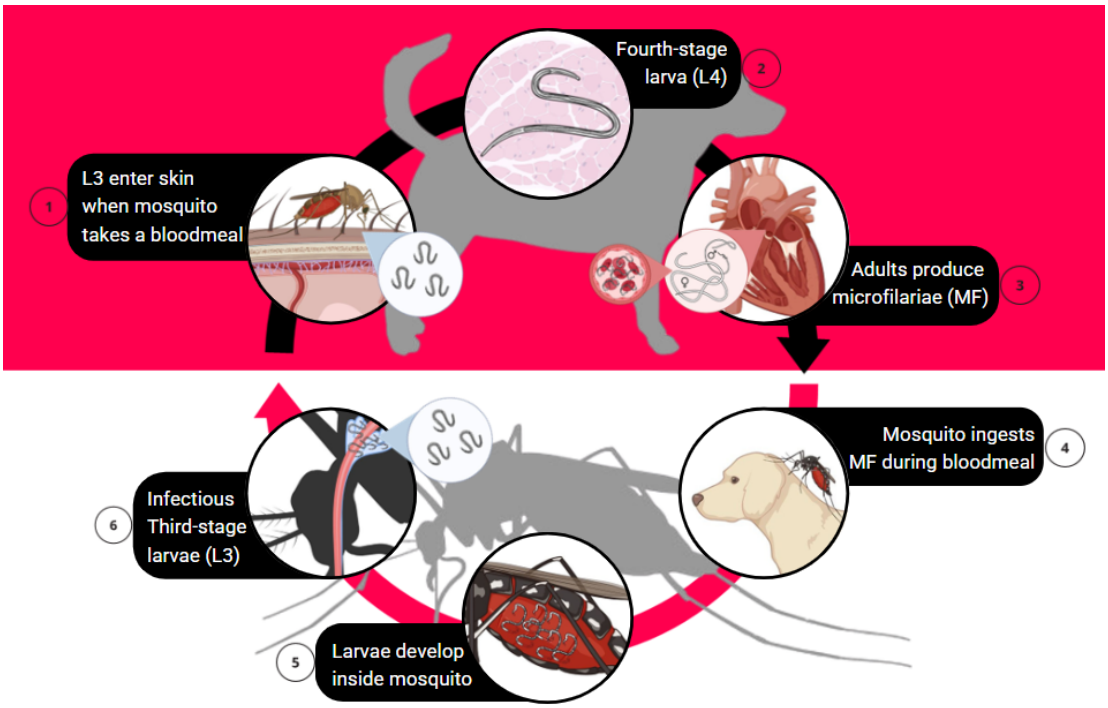

Notes: Made with BioRender.

Elimination attempts of vector-transmitted helminthic diseases have proven unsuccessful to date [36]. An obstacle to eradication may be the many life stages of a parasite, such as *D. immitis,* in the vector intermediate host. Preventives and therapeutics for canine heartworm are lacking in diversity. Currently, all available Federal Drug Administration (FDA)-approved heartworm preventives belong to the drug class ML, which includes ivermectin, selamectin, moxidectin, and milbemycin oxime [37]. An organic arsenical compound, melarsomine dihydrochloride, is the only available therapeutic approved by the FDA in dogs for the killing of adult heartworms and can result in pulmonary thromboembolism when the worms die [38]. Macrocyclic lactones are effective against L3 and L4 stages of *D. immitis* and dogs are susceptible to infection without regular administration of MLs preventives [39]. There is a loss of efficacy concern with ML-resistant *D. immitis* cases increasing in the United States, and since

most of the MLs require some aspect of host immunity to succeed at killing the L3 and L4, there is a need for a new class of drugs that is effective in killing *D. immitis* [37].

A comprehensive understanding of filarial parasites requires thorough investigation into each life stage to understand not only the mechanisms of worm establishment within the host, but also their interaction with the host during establishment. Due to the limited availability of *D. immitis* in research settings, the majority of *in vitro* studies focus on the MF and L3 life stages of the parasite. Although *in vitro* experiments are beneficial for determining the mechanisms of parasite invasion and establishment by the worms, there is a lack of knowledge in the field regarding the host-parasite interaction, specifically the mechanisms of the host that determine the ultimate establishment of the parasite.

Dirofilaria immitis **animal models**

In addition to domestic dogs, *D. immitis* can establish in wild canids, cats, ferrets, marine mammals, and even infect humans [33]. Current *in vivo D. immitis* research relies on an established infection in a permissive host, and the best animal models for these studies are dogs and ferrets. Rodent animal models are generally preferred by researchers for *in vivo* work due to the nature of the research and economics; however, previous studies have attempted to establish infection in immunocompetent mice, rats, and jirds without success [38].

It is challenging to explore the host-parasite interaction of canine heartworm infections, because there are a limited number of animal models for this parasite. Dogs are not a suitable model to study the host-parasite interface because of ethical and financial concerns. Cats are also not a suitable model because of ethical and financial concerns, as well as their inability to produce MF. Rodents are widely considered an ideal animal model for infectious diseases, and

currently, there are three options for *in situ* study of *D. immitis*: the NOD scid gamma (NSG) mouse [31], athymic nude mouse (TRS Labs, unpublished), and steroid-treated Sprague Dawley rats [40].

The NSG mouse is one of the most immunodeficient mouse models used in research [41]. The mouse lacks mature B cells, mature T cells, natural killer cells, and complement, and is also defective for dendritic cells and macrophages [42]. Utilizing an animal model with an ineffective innate immune response and the absence of several immune cells is an approach to analyze a single cell population's response to the presence of *D. immitis* immunomodulation molecules. One method to the aforementioned approach is to inoculate mice with a singular cell type (e.g., neutrophils, eosinophils, or macrophages) via the intraperitoneal route immediately prior to intraperitoneal inoculation with *D. immitis* L3. A peritoneal lavage can be performed at selected times post-inoculation to collect the peritoneal cells and larvae for identification of cell types (possibly a recruitment of new cell types in addition to the singular cell type administered), as well as to observe the development, possible arrested development, or degradation of the larvae [43].

Host cellular immune responses to parasitic infections

Host defenses against a pathogen are known as an immune response [3], and there are two types of immunity to pathogens: innate and adaptive. Innate immunity occurs during the early stages of infection, when immune cells detect and respond to the presence of a pathogen regardless of previous infections by that pathogen. Adaptive, also known as acquired, immunity utilizes immunological memory to send antigen-specific lymphocytes to sites of infection after the antigens have been delivered to lymphoid tissue to prime this response [3].

Once pathogens, like filariae, enter host tissues, they are recognized by mononuclear phagocytes called macrophages. Macrophages circulate through tissues and the body, but are predominantly found in connective tissues, the gastrointestinal tract, the lung, the liver, and the spleen [3]. Due to the establishment of macrophages in tissue, they are the first cell to acknowledge the presence of a pathogen. The macrophage response to a pathogen triggers inflammation, a local accumulation of fluid, plasma proteins, and white blood cells that is initiated by physical injury, infection, or a local immune response [3]. Neutrophils, another phagocyte, predominantly circulate in the blood and are recruited with macrophages to the pathogen in tissues by cell-surface receptors. The role of the macrophages and neutrophils is to recognize, phagocytose, and destroy the pathogen [3]. Circulating monocytes, which will later turn into macrophages, follow the neutrophils to the site of infection, and eosinophils (containing cytotoxic anti-helminthic molecules) [44] and lymphocytes (B and T cells) of the adaptive immune response also arrive to assist in destroying the pathogen [3].

The role of macrophages in host immunity

The activation of macrophages refers to the ability of these cells to change their form and physiology in response to environmental stimuli [45, 46]. These innate cells clear apoptotic cell bodies, regulate the host immune response, and can destroy pathogens [47]. There are three types of activated macrophages: classically activated macrophages (CAMs), alternatively activated (AAMs), and regulatory macrophages. Classically activated macrophages (CAMs) are important to host defense and can propagate inflammatory responses [46]. These macrophages differentiate when signaled by interferon-gamma (IFN-γ), followed by stimulation with tumor necrosis factor-α (TNF-α). Although IFN-γ can be produced by innate immune cells, the activation of T helper 1

(Th1) cells during cell-mediated immunity maintains IFN-γ at a higher level, priming the macrophages for classical activation. In turn, IFN-γ activates transcription factor STAT1/2, which binds to gamma-activated sequences in immune effector genes [46]. Research on *Toxoplasma gondii*, an intracellular protozoan parasite, demonstrated that culturing cells with *T. gondii* suppresses STAT1 gene upregulation responding to signaling from IFN- γ. This suppression is believed to be essential for the parasite's survival and development [48].

The TNF-α cytokine is the second signal for classically activating macrophages. TNF-α is induced by the binding of Toll-like receptors, microbial-sensing proteins [49], by pattern associated molecular patterns (PAMPs) expressed on the surface of pathogens [46]. The combination of PAMPs and cytokines activate the macrophages, when the host is infected with a pathogen. Once the presence of intracellular pathogens signals the activation of macrophages, CAMs metabolize arginine into nitric oxide and express inducible nitric oxide synthase (iNOS) for the killing of intracellular pathogens [46, 47].

Macrophages that have been exposed to cytokines interleukin-4 (IL-4) and/or IL-13 and upregulate expression of mannose receptor CD206 are referred to as alternatively activated macrophages [47, 50]. Alternatively activated macrophages (AAMs) are no better at killing microbes than CAMs and have been suggested to be more susceptible to intracellular infections [51], possibly due to their reduced iNOS production compared to CAMs [47]. They do, however, assist in the process of tissue repair; IL-4 induces arginase activity by converting arginine to ornithine, which is a precursor of collagen and polyamides that are essential for wound healing [47, 52]. Extracellular pathogens, such as helminths, may colonize host tissues, inducing the release of IL-4 and IL-13, and recruiting eosinophils, neutrophils, basophils, and/or natural killer T cells, which then signal the alternative activation of macrophages [50]. However, IL-4 may not

be necessary for inducing AAMs, because helminth-specific antibodies in the presence of helminth antigens have been found to alternatively activate macrophages in the absence of IL-4 [53].

In chronic helminth infections, arginase from AAMs can modulate $CD4^+$ T cell proliferation, controlling excessive fibrosis [47]. Helminths secrete copious amounts of glycosylate protein, which binds to CD206-expressing immune cells such as AAMs; it is suggested that CD206 is a relevant surface marker for AAMs, but its role in helminth infection remains unknown [47]. The binding of helminth glycosylate protein to CD-206 allows the AAMs to recognize the parasites, leading to activation of the transcription factor, Signal Transducer and Activator of Transcription-6 (STAT-6), which assists in expressing signals that result in AAM polarization and proliferation [47].

The complement system and its role in immunity

The complement system is composed of plasma proteins that react with each other to help make pathogens more susceptible to phagocytosis and induce a series of inflammatory responses to fight infection [3]. The body fluid and tissues of the host carry precursor enzymes, zymogens, in the event of infection. In areas of infection, the zymogens are activated, triggering the cascade of inflammatory responses [3]. First, the complement system generates activated complement proteins that bind to pathogens and make them susceptible for phagocytosis. Next, smaller fragments of complement proteins recruit and activate more phagocytes to the site of infection. Lastly, the terminal complement proteins create pores in bacterial membranes to damage them [3].

There are three complement pathways (classical, mannan-binding lectin, and alternative) that can be initiated alone or together to activate the complement cascade on a pathogen's surface [3]. All three pathways follow a cascade of reactions that merge to generate the C3 convertase protease. Succinctly, the three complement pathways are initiated by different complement components, but they all end by generating C3 convertase, which then generates C3b, targeting the pathogen for phagocytosis [3]. Complement pathways are initiated when a complement component binds to the surface of a pathogen: the binding of complement component C1q to antibodies deposited on the pathogen surface initiates the classical pathway, and the binding of a spontaneously activated complement component, in the absence of a specific antibody, initiates the alternative pathway.

The complement system may influence this experimental system, because macrophages, likely AAM, were observed surrounding degenerated *D. immitis* larvae in the peritoneal wall of the Mongolian jird (*Meriones unguiculatus*) at 1 dpi. The aggregation of macrophages around the larvae in the tissue is a response to the initiation of a complement pathway. It is likely that the alternative complement pathway initiates the complement cascade in this model, because the classical complement pathway requires the presence of antibodies already generated against the pathogen and deposited on the pathogen surface. Furthermore, when C1q of the classical complement pathway comes into contact with calreticulin (CRT, a calcium-binding protein on the surface of *B. malayi*), the CRT binds to C1q, resulting in the inhibition of the classical complement pathway [54]. No other filarial species are known to possess CRT, but the parasite *Trichinella spiralis* also utilizes its own CRT to interfere with the host's classical complement pathway, ensuring its survival [55]. The complement cascade is most likely initiated by the spontaneous activation of the alternative complement pathway.

Host-parasite interaction with *D. immitis*

There is a trade-off between immunopathology, caused by an over-reactive immune response to *D. immitis*, and an immune response that may be beneficial for the host [56]. Immune activation against pathogens is an investment in energy and resources of the host, so the trade-off, in addition to strategies developed by *D. immitis* to evade and manipulate the canine immune response [56], allow for the establishment of *D. immitis* in the canine host.

Canine immune response to infection with D. immitis

Most research investigating the immune response of *D. immitis* in the canine host surrounds the humoral response, mediated by antibodies [3], to MF. MF is the most available life stage of *D. immitis* and a major target in drug discovery due to its transmission to the mosquito. It has been widely accepted that an immune response in the canine host is only stimulated upon the death of the parasite, when the antigens of endosymbiotic bacteria, *Wolbachia,* are released from the worm [57]. However, there is evidence of *Wolbachia* antigens in cells and organs of dogs infected with *D. immitis* [58, 59]. There is also evidence of higher levels of anti-*Wolbachia* and *D. immitis* IgG1 antibodies in microfilaremic dogs, which decline once the MF are no longer observed [60]. Contrary to humans, dog IgG1 is predominantly a T helper 2 (Th2)-type response, and IgG2 is a Th1-type response [57]. Therefore, active microfilaremic infections of *D. immitis* induce a Th2 response, and occult infections (no microfilaremia) trigger a Th1 response [57].

Canine infection with *D. immitis* is characterized by both innate and acquired immune responses. Important pro-inflammatory mediators that are always present are TNF-α and iNOS [57]. However, the presence of anti-inflammatory T helper 3 and T regulatory cells, which

secrete TGF-β and IL-10, respectively, was suggested as the reason for the absence of cell-mediated immune responses against helminths [61]. Thus, dogs with patent infections have circulating IL-10, whereas IL-10 in amicrofilaremic dogs is below detectable limits [57]. Additionally, it has been suggested that *D. immitis* is able to secrete molecules that mimic the host, stimulating the production of IL-10 [62].

Dirofilaria immitis larvae and adults are able to evade the canine immune system for the entirety of the parasite's life, but the cellular immune response of the canine host during early stages of infection (L3 and L4) are not well-known due to the challenge of locating and collecting *D. immitis* L3 and L4 from the canine host. Drs. Seiji Kume and Shiro Itagaki (1955) published the first studies of the life cycle of *D. immitis* in the dog. It was determined that after infection of the host, the L3 and L4 penetrate through the tissue and remain in the submuscular membranes, subcutaneous tissue, fat tissue, and muscles until they develop into IA [63]. It was also suggested that the IA travel to the pulmonary artery and right ventricle of the heart via the veins between 85 and 120 dpi [63]. Dr. Thomas Orihel (1961) expanded on Kume and Itagaki's work by documenting the morphology of all larval stages of *D. immitis* development in the dog. Orihel examined worms recovered from dogs between 5 to 278 days after infection with 15 to 450 L3 [34]. Recovery of *D. immitis* varied (6% to 75%) throughout the study. There was no evidence of host immune response to L3 and L4 in the tissues during the third molt, which was suggested to occur at 9 – 12 dpi. However, there were several findings of small inflammatory nodules containing dead L4 in subcutaneous tissue for up to 70 dpi [34].

Perhaps the most informative study documenting the developmental stages of *D. immitis* in the dog was published by Drs. Takao Kotani and Kendall Powers (1982). The authors documented the time of larval molts, the time required for larval development, and the location

of the larvae throughout the *D. immitis* life cycle in the dog. Kotani and Powers was the first study to provide detailed descriptions of the larval stages and location of the L3 and L4. Subcutaneous inoculations with 50-500 L3 were administered to 36 dogs at 2, 5, 6, and 20 weeks of age. Necropsies and worm recovery occurred as early as 3 dpi and at various timepoints until 196 dpi. The third molt from L3 to L4 occurred at the site of inoculation in the subcutaneous tissues, and no host immune response was observed in the tissues. At 3 dpi, 93% of larvae were recovered at the site of inoculation and by 21 dpi, 87% of larvae were L4 and recovered from the abdomen. Although the first larval recovery was 3 dpi, 29% of worms recovered that day were already L4, contrary to Orihel's finding of the third molt occurring 9-12 dpi [34, 43]. In fact, earlier research observed that the third *D. immitis* molt occurs as soon as 1 dpi [64]. Eighty-seven% of larvae were recovered from the abdomen, with 8% found in the thorax. Immature adults were found in the pulmonary arteries and heart as early as 70 dpi, and over 97% of adults were found in the same location at 120 dpi [34, 43, 64]. The only host immune response observed in the Kotani and Powers study was in a littermate with 40% *D. immitis* recovery at 84 dpi, less than its sibling with 84% recovery with no signs of an immune response. There were several nodules in the subcutaneous tissues of the dog in which fewer larvae were recovered. similar in description to the nodules observed by Kume and Itagaki [43, 63]. There is no evidence of a host immune response to *D. immitis* L3 and the third molt in these studies, but the two studies describing a host immune response to subcutaneous nodules surrounding dead L4 suggests further investigation is worthwhile.

Immunomodulatory mechanisms of D. immitis

There are a variety of strategies that *D. immitis* employs to evade the canine immune response [38]; L3 release surface antigens, and juvenile adults and adults express different host molecules and cells on their surfaces [65, 66]. The evasion of canine immunity at initial infection with *D. immitis* is possible due to several factors: proteins secreted from the saliva of the mosquito during the blood meal [67], release of surface antigens from *D. immitis* [68, 69], and an increase in *Wolbachia* [70, 71].

Although there are excretory-secretory products from MF and adult worms that aid in the evasion of the immune response, there is a predominant release of immunomodulatory products from infectious L3 compared to other stages of larval development [72]. A study examining *B. malayi* exosome-like vesicle secretions determined that the L3 excretory-secretory proteins are different than the secreted proteins identified from pre- and post-molt L3, and the results of this study suggest that there is an active and regulated mechanism of exosome-like vesicle secretions for immunomodulation from healthy L3 [72, 73].

An example of the roles that excretory-secretory proteins play in immunoregulation includes a cysteine protease, Bm-CPL-1, which is expressed in abundance with every developmental stage of *B. malayi* and is important for establishing infection and maintaining parasitemia [74]. Another cysteine protein inhibitor, Di-CPI, is expressed by *D. immitis* adult worms and is important in immunomodulation of inflammatory responses by inhibiting canine T-cell proliferation [75]. Identifying the immune cells affected by the excretion-secretion molecules of *D. immitis* L3 is as equally important as understanding the molecules themselves. It remains difficult to characterize all immunoregulatory molecules [72] of filarial parasites, and until identification of these molecules becomes more accessible, understanding the host immune

response may provide the needed information to assess how the L3 is evading the immune system.

It is well known that although antifilarial therapeutics, like ivermectin, inhibit functional components of the worm, it is the host immune response that assists in the removal of the parasite once it can no longer function [28]. Understanding the immune cells that are susceptible to modulation by *D. immitis* L3 will provide deeper insight into the process of parasite establishment and host specificity. Canine peripheral blood mononuclear cells (PBMCs) and isolated neutrophils assist ivermectin in the removal of *D. immitis* MF from circulation [28]. The authors suggest that ivermectin inhibits the secretion of *D. immitis* MF immunomodulatory products, leading to the adherence of PBMCs and neutrophils to the worms, resulting in their removal. Proteins and small RNA [72] excreted by the worm support a role in the ability of a filarial nematode to modulate and evade the host immune response [76, 77].

As a result of the Filarial Genome Project [78], we know *B. malayi* contains two macrophage migration inhibitory factor (MIF) homologues that encode proteins secreted by the parasite [79]. Secretion of MIF homologues have been thought to amplify the complement pathway, but some researchers hypothesize that the continuous secretion of MIF may desensitize the inflammatory response of the host. It is also hypothesized that the duration of MIF exposure to resident macrophages initiates the generation of AAMs, which can have a counter-inflammatory effect [79]. Constant secretion of *B. malayi* MIF may explain the difference in the cellular immune response between *B. malayi* and *D. immitis*. As of today, the whole genome of *D. immitis* is still being investigated. There are *de novo* assemblies of the genome published, but nothing complete. *Dirofilaria immitis* may or may not have their own version of the *B. malayi* MIF homologues. Another theory for immune evasion by *D. immitis* L3 in the jird peritoneal

wall is the release of *D. immitis* cysteine protease inhibitor (Di-CPI), which inhibits the recruitment of monocytes and macrophages in the canine host [75]. It is possible that Di-CPI also inhibits these cells in the jird.

Dirofilaria immitis **SLO-1 channel**

There is a loss of efficacy (LOE) concern with ML-resistant *D. immitis* cases increasing in the United States. The first report of LOE occurred in 1998 [80] and has greatly increased since, primarily in the highly endemic areas of heartworm in the southern United States [81]. It was widely believed that most LOEs were due to compliance failure, but Bourguinat *et al*. (2011) reported that heartworm preventives IVM and MO did not meet expectations regarding microfilaricidal efficacy *in vivo* due to their repeated use and high dose rates [82]. Another clinical study reported preventive LOE with IVM (23.8 - 71.3% efficacy; n = 2) and MOX (21.2%; n = 1) [83], and it was confirmed in later studies that resistance is inherited between generations [84].

As the threat of ML-resistant *D. immitis* rises in the United States, there is a need for either a new class of drugs that is effective in killing *D. immitis*, or another target of host immunity to explore to work in tandem with MLs [37]. The classic targets of MLs in parasitic gastrointestinal nematodes and the free-living model organism, *Caenorhabditis elegans*, are the glutamate-gated chloride channels (GluCls), through which these drugs cause flaccid paralysis in nematodes of somatic muscle, and most importantly the pharynx [81], by opening these channels to the inflow of chloride [85]. preventing nutrient absorption, and allowing the nematodes to be removed by the host's immune system. However, MLs are less effective in filarial nematodes

due to the ability of these parasites to also absorb nutrients through their cuticles and paralysis of somatic muscle at relevant ML concentration in filariae has not been observed [81].

Only one study has been conducted exploring variable immobilizing effects of emodepside on filarial nematodes. Kashyap *et al*. discovered that emodepside has sex-dependent immobilizing effects on adult *B. malayi* due to a differentially spliced binding pocket in the RCK1 region of the SLO-1 K channel [86]. The authors used whole-parasite measurement of single muscle cells to support the hypothesis that adult male *B. malayi* are more sensitive than females to inhibition of motility by emodepside. cDNA from dsRNA-treated worms was amplified to identify SLO-1 splice variants in *B. malayi,* revealing sex-dependent differences in SLO-1 expression in two of the five predicted splice variants, SLO-1a and SLO-1f; both variants are expressed in female *B. malayi*, but only SLO-1f is expressed in male *B. malayi*. It was also determined that SLO-1f is more sensitive to emodepside than SLO-1a, and that the difference in the two variants lies in the cytoplasmic RCK1 domain [86]. Kashyap *et al*. investigated the SLO-1 RCK1 region of two other filarial species, *Onchocerca volvulus* and *D. immitis*. Similar to *B. malayi*, there are five predicted SLO-1 splice variants in *O. volvulus*, and only two are expressed in females: Ovo-SLO-1a and Ovo-SLO-1d. Emodepside was found to bind to the same RCK-1 regions in *O. volvulus* and *B. malayi in silico*. A model of the *in-silico* binding of emodepside to SLO-1 in *D. immitis*, using Parasite Wormbase sequences, suggested that emodepside binds to the same RCK-1 regions, although the Wormbase sequences lack information about splice variants [86].

Investigating *D. immitis* in a nonpermissive immunocompetent rodent model

A comprehensive understanding of filarial parasites requires thorough investigation into each life stage to understand not only the mechanisms of worm establishment within the host, but also their interaction with the host during establishment. Due to the limited availability of *D. immitis* in research settings, the majority of *in vitro* studies has focused on the MF and L3 life stages of the parasite. Although *in vitro* experiments are beneficial for determining the mechanisms of parasite invasion and establishment by the worms, there is a lack of knowledge in the field regarding the host-parasite interaction, specifically the mechanisms of the host that determine the ultimate establishment of the parasite.

Current *in vivo D. immitis* research relies on an established infection in a permissive host, and the best animal models for these studies are dogs and ferrets. Rodent animal models are generally preferred by researchers for *in vivo* work due to the nature of the research and economics; however, previous studies have attempted to establish infection in immunocompetent mice, rats, and jirds without success [38]. The studies in this dissertation are innovative for three reasons: Chapter 2 describes the first study to characterize the initial cellular immune response of a nonpermissive host, the Mongolian gerbil, to *D. immitis* IP infection. Chapter 3 describes the first study to explore the role of gerbil peritoneal cells using flow cytometry and the first to deplete jird peritoneal macrophages. Chapter 4 describes differential splicing of SLO-1 that could underlie differences in emodepside activity against relevant *D. immitis* life stages.

In the studies of this dissertation, we hypothesized that the establishment of *D. immitis* in the definitive host is determined by that host's immune response to the presence of larvae. The results of these proposed studies will fill in a gap of knowledge regarding the determinants of filarial host specificity. The results also provide insight into the anti-filarial mechanisms of the

host, which may be used to discover a preventive and/or therapeutic in the future. These studies will impact canine heartworm research and lead to more targeted eradication efforts of other types of human and animal infectious filarial diseases.

References

1. van Seventer, J.M. and N.S. Hochberg, *Principles of Infectious Diseases: Transmission, Diagnosis, Prevention, and Control*, in *International Encyclopedia of Public Health (Second Edition)*, S.R. Quah, Editor. 2017, Academic Press: Oxford. p. 22-39.

2. Snieszko, S., *The effects of environmental stress on outbreaks of infectious diseases of fishes.* Journal of Fish Biology, 1974. 6(2): p. 197-208.

3. Janeway CA Jr, T.P., Walport M, et al., *Immunobiology: The Immune System in Health and Disease*. 5 ed. 2001, New York: Garland Science.

4. Alberts B, J.A., Lewis J, et al., *Introduction to Pathogens*, in *Molecular Biology of the Cell*. 2002, Garland Science: New York.

5. Peterson JW, *Bacterial Pathogenesis*, in *Medical Microbiology*, B. S, Editor. 1996, University of Texas Medical Branch at Galveston: Galveston (TX).

6. Bowman, D.D., *Georgis' Parasitology for Veterinarians*. 11th ed. 2021: Elsevier, Inc.

7. Sheehan, K.B., *Seen and Unseen: Discovering the Microbes of Yellowstone*. 2005: Falcon.

8. Diaz, J.H., *293 - Introduction to Ectoparasitic Diseases*, in *Mandell, Douglas, and Bennett's Principles and Practice of Infectious Diseases (Eighth Edition)*, J.E. Bennett, R. Dolin, and M.J. Blaser, Editors. 2015, W.B. Saunders: Philadelphia. p. 3243-3245.e1.

9. Castro, G., *Helminths: Structure, Classification, Growth, and Development*, in *Medical Microbiology*, B. S, Editor. 1996, University of Texas Medical Branch at Galveston: Galveston (TX).

10. Tritten, L., et al., *Mining nematode protein secretomes to explain lifestyle and host specificity.* PLOS Neglected Tropical Diseases, 2021. 15(9): p. e0009828.

11. Maizels, R.M. and H.J. McSorley, *Regulation of the host immune system by helminth parasites.* J Allergy Clin Immunol, 2016. 138(3): p. 666-675.

12. Allen, J.E. and R.M. Maizels, *Diversity and dialogue in immunity to helminths.* Nat Rev Immunol, 2011. 11(6): p. 375-88.

13. McSorley, H.J., J.P. Hewitson, and R.M. Maizels, *Immunomodulation by helminth parasites: defining mechanisms and mediators.* Int J Parasitol, 2013. 43(3-4): p. 301-10.

14. Poulin, R., B.R. Krasnov, and D. Mouillot, *Host specificity in phylogenetic and geographic space.* Trends in Parasitology, 2011. 27(8): p. 355-361.

15. Esser, H.J., et al., *Host specificity in a diverse Neotropical tick community: an assessment using quantitative network analysis and host phylogeny.* Parasites & Vectors, 2016. 9(1): p. 372.

16. Casadevall, A. and L.A. Pirofski, *What Is a Host? Attributes of Individual Susceptibility.* Infect Immun, 2018. 86(2).

17. (WHO), W.H.O. *Soil-transmitted helminthiases*. 2024; Available from: https://www.who.int/health-topics/soil-transmitted-helminthiases#tab=tab_1.

18. Cross, J., *Filarial Nematodes*, in *Medical Microbiology*, B. S, Editor. 1996, University of Texas Medical Branch at Galveston: Galveston, TX.

19. Anvari, D., et al., *The global status of Dirofilaria immitis in dogs: a systematic review and meta-analysis based on published articles.* Research in Veterinary Science, 2020. 131: p. 104-116.

20. Jorge, L.R., et al., *An integrated framework to improve the concept of resource specialisation.* Ecol Lett, 2014. 17(11): p. 1341-50.

21. Law, C.J., G.J. Slater, and R.S. Mehta, *Lineage Diversity and Size Disparity in Musteloidea: Testing Patterns of Adaptive Radiation Using Molecular and Fossil-Based Methods.* Systematic Biology, 2017. 67(1): p. 127-144.

22. Flynn, J.J., et al., *Molecular Phylogeny of the Carnivora (Mammalia): Assessing the Impact of Increased Sampling on Resolving Enigmatic Relationships.* Systematic Biology, 2005. 54(2): p. 317-337.

23. Mäser, P., *Filariae as Organisms*, in *Human and Animal Filariases*. 2022. p. 17-32.

24. Duguet, T.B. and L. Tritten, *The Host–Helminth Interface as a Rich Resource for Novel Drug Targets*, in *Human and Animal Filariases*. 2022. p. 493-515.

25. Kozek, W.J., *Transovarially-transmitted intracellular microorganisms in adult and larval stages of Brugia malayi.* J Parasitol, 1977. 63(6): p. 992-1000.

26. Hansen, R.D., et al., *A worm's best friend: recruitment of neutrophils by Wolbachia confounds eosinophil degranulation against the filarial nematode Onchocerca ochengi.* Proc Biol Sci, 2011. 278(1716): p. 2293-302.

27. Schorderet-Weber, S. and S. Specht, *In Vivo Models for the Discovery of New Antifilarial Drugs*, in *Human and Animal Filariases*. 2022. p. 391-458.

28. Vatta, A.F., et al., *Ivermectin-dependent attachment of neutrophils and peripheral blood mononuclear cells to Dirofilaria immitis microfilariae in vitro.* Vet Parasitol, 2014. 206(1-2): p. 38-42.

29. McCall, J.W., *Dirofilariasis in the domestic ferret.* Clinical Techniques in Small Animal Practice, 1998. 13(2): p. 109-112.

30. (FR3), F.R.R.R.C. *Experimental Infection of Dogs, Cats, Ferrets, and Rodents with Dirofilaria immitis, Brugia malayi, B. pahangi, or Dipetalonema reconditum*. Available from: http://www.filariasiscenter.org/protocols/Protocols/experimental-infection-of-dogs-cats-ferrets-and-rodents-with-dirofilaria-immitis-brugia-malayi-b.-pahangi-or-dipetalonema-reconditum.

31. Hess, J.A., et al., *A rodent model for Dirofilaria immitis, canine heartworm: parasite growth, development, and drug sensitivity in NSG mice.* Scientific Reports, 2023. 13(1): p. 976.

32. (CAPC), C.A.P.C. *Canine Heartworm Prevalence Map*. 2023; Available from: https://capcvet.org/maps/#/2023/all-year/heartworm-canine/dog/united-states.

33. (CAPC), C.A.P.C. *Heartworm Guidelines*. 2020; Available from: https://capcvet.org/guidelines/heartworm/.

34. Orihel, T.C., *Morphology of the larval stages of Dirofilaria immitis in the dog.* J Parasitol, 1961. 47: p. 251-62.

35. Bowman, D.D. and C.E. Atkins, *Heartworm Biology, Treatment, and Control.* Veterinary Clinics of North America: Small Animal Practice, 2009. 39(6): p. 1127-1158.

36. Wood, C.L. and P.T. Johnson, *A world without parasites: exploring the hidden ecology of infection.* Frontiers in Ecology and the Environment, 2015. 13(8): p. 425-434.

37. (AHS), A.H.S. *American Heartworm Society Canine Guidelines for the Prevention, Diagnosis, and Management of Heartworm (Dirofilaria immitis) Infection in Dogs*. Macrocyclic Lactones 2024.

38. McCall, J.W., et al., *Chapter 4 Heartworm Disease in Animals and Humans*. 2008, Elsevier. p. 193-285.

39. Bowman, D.D. and J. Drake, *Examination of the "susceptibility gap" in the treatment of canine heartworm infection.* Parasites & Vectors, 2017. 10(S2).

40. Mills, B.J., McTier, T.L., Knauer, C.S., Woods, D.J., *Anthelmintic Laboratory Animal Model for Heartworm*, Z.S. LLC, Editor. 2020.

41. Shultz, L.D., F. Ishikawa, and D.L. Greiner, *Humanized mice in translational biomedical research.* Nat Rev Immunol, 2007. 7(2): p. 118-30.

42. Ishikawa, F. and S. Miyazaki, *New biodefense strategies by neutrophils.* Arch Immunol Ther Exp (Warsz), 2005. 53(3): p. 226-33.

43. Kotani, T.a.P., Kendall G., *Developmental stages of Dirofilaria immitis in the dog.* American Journal of Veterinary Research, 1982. 43: p. 2199-2206.

44. Callahan, G.a.Y., Robin, *Basic Veterinary Immunology*. 2014, Boulder, CO: University Press of Colorado.

45. Cohn, Z.A., *Activation of mononuclear phagocytes: fact, fancy, and future.* J Immunol, 1978. 121(3): p. 813-6.

46. Mosser, D.M. and X. Zhang, *Activation of murine macrophages.* Curr Protoc Immunol, 2008. Chapter 14: p. 14.2.1-14.2.8.

47. Rolot, M. and B.G. Dewals, *Macrophage Activation and Functions during Helminth Infection: Recent Advances from the Laboratory Mouse.* Journal of Immunology Research, 2018. 2018: p. 2790627.

48. Rosowski, E.E., et al., *Toxoplasma gondii Inhibits gamma interferon (IFN-γ)- and IFN-β-induced host cell STAT1 transcriptional activity by increasing the association of STAT1 with DNA.* Infect Immun, 2014. 82(2): p. 706-19.

49. Medzhitov, R., *Toll-like receptors and innate immunity.* Nature Reviews Immunology, 2001. 1(2): p. 135-145.

50. Gordon, S., *Alternative activation of macrophages.* Nat Rev Immunol, 2003. 3(1): p. 23-35.

51. Hölscher, C., et al., *Impairment of alternative macrophage activation delays cutaneous leishmaniasis in nonhealing BALB/c mice.* J Immunol, 2006. 176(2): p. 1115-21.

52. Hesse, M., et al., *Differential regulation of nitric oxide synthase-2 and arginase-1 by type 1/type 2 cytokines in vivo: granulomatous pathology is shaped by the pattern of L-arginine metabolism.* J Immunol, 2001. 167(11): p. 6533-44.

53. Esser-von Bieren, J., et al., *Antibodies trap tissue migrating helminth larvae and prevent tissue damage by driving IL-4Rα-independent alternative differentiation of macrophages.* PLoS Pathog, 2013. 9(11): p. e1003771.

54. Yadav, S., et al., *In silico and in vitro studies on the protein-protein interactions between Brugia malayi immunomodulatory protein calreticulin and human C1q.* PLoS One, 2014. 9(9): p. e106413.

55. Mohammed, M.M.D., et al., *Comprehensive chemical profiling of Bassia indica Wight. aerial parts extract using UPLC-ESI–MS/MS, and its antiparasitic activity in Trichinella spiralis infected mice: in silico supported in vivo study.* BMC Complementary Medicine and Therapies, 2023. 23(1): p. 161.

56. Sorci, G., S. Cornet, and B. Faivre, *Immune evasion, immunopathology and the regulation of the immune system.* Pathogens, 2013. 2(1): p. 71-91.

57. Simón, F., et al., *Immunopathology of Dirofilaria immitis infection.* Vet Res Commun, 2007. 31(2): p. 161-71.

58. Kramer, L.H., et al., *Immunohistochemical/immunogold detection and distribution of the endosymbiont Wolbachia of Dirofilaria immitis and Brugia pahangi using a polyclonal antiserum raised against WSP (Wolbachia surface protein).* Parasitol Res, 2003. 89(5): p. 381-6.

59. Kramer, L.H., et al., *Immune response to and tissue localization of the Wolbachia surface protein (WSP) in dogs with natural heartworm (Dirofilaria immitis) infection.* Vet Immunol Immunopathol, 2005. 106(3-4): p. 303-8.

60. Grieve, R.B., B.M. Gebhardt, and R.E. Bradley, Sr., *Dirofilaria immitis: cell-mediated and humoral immune responses in experimentally-infected dogs.* Int J Parasitol, 1979. 9(4): p. 275-9.

61. Doetze, A., et al., *Antigen-specific cellular hyporesponsiveness in a chronic human helminth infection is mediated by T(h)3/T(r)1-type cytokines IL-10 and transforming growth factor-beta but not by a T(h)1 to T(h)2 shift.* Int Immunol, 2000. 12(5): p. 623-30.

62. Tezuka, H., et al., *Various types of Dirofilaria immitis polyproteins selectively induce a Th2-Type immune response.* Infect Immun, 2003. 71(7): p. 3802-11.

63. Kume, S. and S. Itagaki, *On the Life-Cycle of Dirofilaria Immitis in the Dog as the Final Host.* British Veterinary Journal, 1955. 111(1): p. 16-24.

64. Sawyer, T.W., PP, *Third molt of Dirofilaria immitis in vitro and in vivo.* The Journal of Parasitology, 1965. 51(2): p. 48.

65. Bilge, F.H., et al., *Surface characterization of the cuticle of Dirofilaria immitis.* J Biomed Mater Res, 1989. 23(9): p. 1027-47.

66. Kadipasaoglu, A.K. and F.H. Bilge, *Partial characterization of the adsorbed protein layer on Dirofilaria immitis (Nematoda) cuticle.* Parasitol Res, 1989. 75(7): p. 554-8.

67. Fong, S.W., R.M. Kini, and L.F.P. Ng, *Mosquito Saliva Reshapes Alphavirus Infection and Immunopathogenesis.* J Virol, 2018. 92(12).

68. Ibrahim, M.S., et al., *Antigen shedding from the surface of the infective stage larvae of Dirofilaria immitis.* Parasitology, 1989. 99 Pt 1: p. 89-97.

69. Simón, F., et al., *Human and animal dirofilariasis: the emergence of a zoonotic mosaic.* Clin Microbiol Rev, 2012. 25(3): p. 507-44.

70. Fenn, K. and M. Blaxter, *Quantification of Wolbachia bacteria in Brugia malayi through the nematode lifecycle.* Mol Biochem Parasitol, 2004. 137(2): p. 361-4.

71. Morchón, R., et al., *Specific IgG antibody response against antigens of Dirofilaria immitis and its Wolbachia endosymbiont bacterium in cats with natural and experimental infections.* Vet Parasitol, 2004. 125(3-4): p. 313-21.

72. Zamanian, M., et al., *Release of Small RNA-containing Exosome-like Vesicles from the Human Filarial Parasite Brugia malayi.* PLoS Negl Trop Dis, 2015. 9(9): p. e0004069.

73. Bennuru, S., et al., *Brugia malayi excreted/secreted proteins at the host/parasite interface: stage- and gender-specific proteomic profiling.* PLoS Negl Trop Dis, 2009. 3(4): p. e410.

74. Song, C., et al., *Development of an in vivo RNAi protocol to investigate gene function in the filarial nematode, Brugia malayi.* PLoS Pathog, 2010. 6(12): p. e1001239.

75. Dong, X., et al., *Molecular Characterization of a Dirofilaria immitis Cysteine Protease Inhibitor (Cystatin) and Its Possible Role in Filarial Immune Evasion.* Genes (Basel), 2019. 10(4).

76. Moreno, Y., et al., *Proteomic analysis of excretory-secretory products of Heligmosomoides polygyrus assessed with next-generation sequencing transcriptomic information.* PLoS Negl Trop Dis, 2011. 5(10): p. e1370.

77. Moreno, Y., et al., *Ivermectin disrupts the function of the excretory-secretory apparatus in microfilariae of Brugia malayi.* Proc Natl Acad Sci U S A, 2010. 107(46): p. 20120-5.

78. Williams, S.A., et al., *The filarial genome project: analysis of the nuclear, mitochondrial and endosymbiont genomes of Brugia malayi.* Int J Parasitol, 2000. 30(4): p. 411-9.

79. Maizels, R.M., et al., *Immune evasion genes from filarial nematodes.* Int J Parasitol, 2001. 31(9): p. 889-98.

80. Hampshire, V.A., *Evaluation of efficacy of heartworm preventive products at the FDA.* Veterinary Parasitology, 2005. 133(2): p. 191-195.

81. Prichard, R.K., *Macrocyclic lactone resistance in Dirofilaria immitis: risks for prevention of heartworm disease.* International Journal for Parasitology, 2021. 51(13): p. 1121-1132.

82. Bourguinat, C., et al., *Macrocyclic lactone resistance in Dirofilaria immitis.* Veterinary Parasitology, 2011. 181(2): p. 388-392.

83. Bourguinat, C., et al., *Macrocyclic lactone resistance in Dirofilaria immitis: Failure of heartworm preventives and investigation of genetic markers for resistance.* Veterinary Parasitology, 2015. 210(3): p. 167-178.

84. Pulaski, C.N., et al., *Establishment of macrocyclic lactone resistant Dirofilaria immitis isolates in experimentally infected laboratory dogs.* Parasites & Vectors, 2014. 7(1): p. 494.

85. Wolstenholme, A.J., *Glutamate-gated Chloride Channels*.* Journal of Biological Chemistry, 2012. 287(48): p. 40232-40238.

86. Kashyap, S.S., et al., *Emodepside has sex-dependent immobilizing effects on adult Brugia malayi due to a differentially spliced binding pocket in the RCK1 region of the SLO-1 K channel.* PLOS Pathogens, 2019. 15(9): p. e1008041.

CHAPTER 2

THE BRIEF RESIDENCY OF *DIROFILARIA IMMITIS* IN THE PERITONEAL CAVITY OF THE MONGOLIAN GERBIL (*MERIONES UNGUICULATUS*)

Campbell, E.J. To be submitted to a peer-reviewed journal (Parasites & Vectors).

Abstract

There is much to learn regarding host specificity of canine heartworm (*Dirofilaria immitis*), and we can explore the determinants of *D. immitis* host specificity using a nonpermissive rodent model, the Mongolian gerbil (*Meriones unguiculates*), commonly known as a jird. We hypothesized that the establishment of *D. immitis* is determined by host immunity after the third larval molt. In this study, jirds were infected by intraperitoneal injection with either 100 *Brugia malayi* (n = 20) or *D. immitis* (n = 20) third-stage larvae (L3), for which the jird is permissive or nonpermissive to parasitic establishment, respectively. Necropsies were performed at 1-, 3-, 10-, and 36-days post infection (dpi) (n = 5/timepoint/group). Larvae were recovered by peritoneal lavage at each timepoint, quantified, and stored in formalin for larval-stage morphologic identification. The peritoneal wall and diaphragm were recovered from each jird and stored in ethanol for absolute quantification of larvae using droplet digital PCR (ddPCR). A mean of 37.4% (SEM = 5.8%) *B. malayi* L3 and 0.4% (SEM = 0.2%) *D. immitis* L3 were recovered at 1 dpi ($p<0.0001$). *Brugia malayi* L3 recovery remained the same (mean = 32.8%; SEM = 3.1%) and a mix of *D. immitis* L3 and fourth-stage larvae (L4) were recovered (23.6%; SEM = 1.8%) at 3 dpi, a significant increase for the latter from 1 dpi ($p<0.001$). Both *B. malayi* (25%; SEM = 5.3%) and *D. immitis* L4 recovery (7.8%; SEM = 1.1%) steadily decreased by 10 dpi ($p<0.0001$). By 36 dpi, a mean of 15.2% (SEM = 2.5%) *B. malayi* immature adults (IA) and no viable *D. immitis* larvae were recovered ($p<0.0001$). The absence and reappearance of *D. immitis* larvae at 1 and 3 dpi, respectively, suggests that *D. immitis* larvae are in the tissues of the peritoneum during the 3rd molt and are cleared by the host by 36 dpi, supporting the hypothesis. Identifying the *D. immitis* larval stage at which establishment is prevented by the jird nonpermissive host will provide more insight into host specificity of filarial infections.

Introduction

Canine heartworm disease, caused by the filarial nematode *Dirofilaria immitis*, was diagnosed in almost 200,000 dogs in the United States in 2023 (Figure 2.1) [1]. These parasites are transmitted by mosquito vectors that ingest blood containing microfilariae (MF) from a heartworm-infected dog. The MF undergo two molts in the mosquito, developing to third-stage larvae (L3). These L3 are infectious, as they have made their way to the head, specifically the proboscis of the mosquito. During the mosquito's next blood meal, the L3 are deposited on the dog's skin and enter the bite wound to migrate through the cutaneous tissue and molt into fourth-stage larvae (L4). The L4 travels through the tissues and molts one last time into immature adults (IA) between 50- and 58-days post infection [2]. As early as 68 days post infection [3], the IA establish in the heart and pulmonary arteries, becoming sexually mature adults around 4.5 months post infection and producing MF six months post infection [3]. Adult *D. immitis* worms can live between 5-7 years in dogs [2] and cause irreparable clinical and pathological changes to the heart and pulmonary artery, including inflammation, pulmonary hypertension, disruption of vascular integrity, and fibrosis [4].

Figure 2.1

Canine heartworm disease prevalence in the United States in 2023

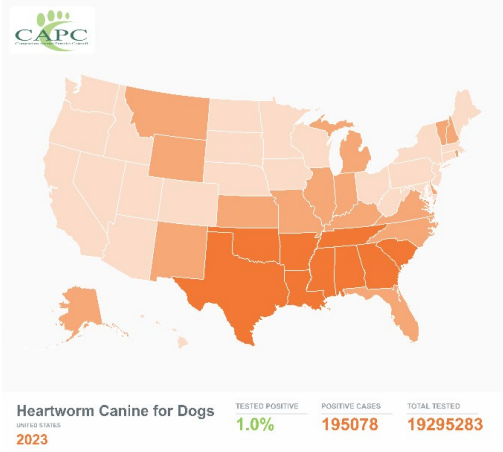

Note: Clinics in the United States reported 195,078 positive cases for canine heartworm disease to the Companion Animal Parasite Council in 2023 [1].

Elimination attempts of vector-transmitted helminthic diseases have proven unsuccessful to date [5]. The challenges in eradicating *D. immitis* include controlling mosquito transmission, ensuring compliance with preventive measures among pet owners, and the emergence of resistance to macrocyclic lactones. Currently, all available Federal Drug Administration (FDA)-approved heartworm preventives belong to the drug class macrocyclic lactone (ML), which includes ivermectin, selamectin, moxidectin, and milbemycin oxime [6]. Alternatively, an organic arsenical compound, melarsomine dihydrochloride, is the only available therapeutic approved by the FDA in dogs for the killing of adult heartworms and can result in pulmonary thromboembolism when the worms die [7]. Macrocyclic lactones are effective against L3 and L4 stages of *D. immitis* and dogs are susceptible to infection without regular administration of MLs [8]. There is a loss of efficacy concern with ML-resistant *D. immitis* cases increasing in the United States, and since most of the MLs require some aspect of host immunity to succeed at killing the L3 and L4, there is a need for either a new class of drugs that is effective in killing *D. immitis* [6].

A comprehensive understanding of filarial parasites requires thorough investigation into each life stage to understand not only the mechanisms of worm establishment within the host, but also their interaction with the host during establishment. Due to the limited availability of *D. immitis* in research settings, the majority of *in vitro* studies focus on the MF and L3/L4 life stages of the parasite. Although *in vitro* experiments are beneficial for determining the mechanisms of parasite invasion and establishment by the worms, there is a lack of knowledge in the field regarding the host-parasite interaction, specifically the mechanisms of the host that determine the ultimate establishment of the parasite.

In addition to domestic dogs, *D. immitis* can establish in wild canids, cats, ferrets, marine mammals, and even infect humans [2]. Current *in vivo D. immitis* research relies on an established infection in a permissive host, and the best animal models for these studies are dogs and ferrets. Rodent animal models are preferred by researchers for *in vivo* work due to the nature of the research and economics; however, previous studies have attempted to establish infection in immunocompetent mice, rats, and jirds with variable success [7].

The Mongolian gerbil, *Meriones unguiculatus,* (jird) serves as an immunocompetent rodent model for another filarial parasite, *Brugia malayi*, a causative agent of lymphatic filariasis [9]. Jirds develop a patent infection after subcutaneous (SC) and intraperitoneal (IP) inoculation of *B. malayi* L3 and developed adult worms are later found in the testes, heart, and lungs with SC infections and the peritoneal cavity in IP infections [9, 10]. Additionally, microfilariae are found circulating in the peripheral blood of SC infections and peritoneal cavity of IP infections [9, 10]. The IP-infected jird model is the ideal control for this study because of the ability to recover all developmental stages of the parasite from a single location [10].

This study is innovative, because it is the first to observe the initial immune response of a nonpermissive host, the jird [11], to *D. immitis* IP infection. The objective of this study was to investigate the cellular immune response to infection with *B. malayi* and *D. immitis* larvae in the peritoneal cavity of the jird. We hypothesized that the establishment of *D. immitis* is determined by host immunity after the third larval molt (Figure 2.2). Identifying the *D. immitis* larval stage for which establishment is prevented by the jird nonpermissive host will provide more insight into host specificity of filarial infections.

Figure 2.2
Hypothesis of when in the life cycle of D. immitis that host specificity occurs

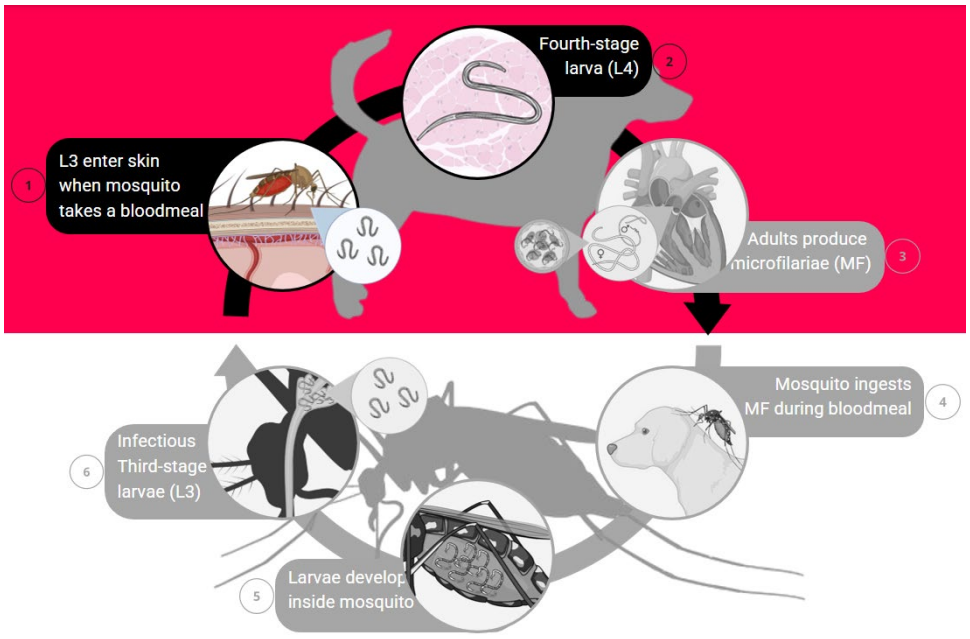

Note: We hypothesized that the establishment of *D. immitis* is determined by host immunity after the third larval molt (L3 to L4). Created with BioRender.com.

Materials and Methods

Animals

All experiments with adult male jirds *(Meriones unguiculatus;* Charles River Laboratories, Kingston, New York) and purpose-bred cats and dogs were performed in accordance to the University of Georgia Institutional Animal Care and Use Committee guidelines and approved Animal Use Protocol A2022 04-009.

Parasites

Brugia malayi and *D. immitis* L3 were collected [12] from laboratory-raised *Aedes aegypti* black-eyed Liverpool mosquitoes [13] 15 days after feeding [14] on microfilaremic cat

(Filariasis Research Reagent Resource Center, University of Georgia, Athens, GA) and dog (University of Georgia, Athens, GA) blood, respectively. Third-stage larvae were isolated into groups of 100 in Hanks' balanced salt solution (HBSS; MP Biomedicals, Santa Ana, California) supplemented with 2% ciprofloxacin (Sigma-Aldrich, St. Louis, MO).

Infection of jirds

Adult male jirds were infected by intraperitoneal injection according to standard procedures [15] with either 100 *B. malayi* (n = 20) or *D. immitis* L3 (n = 20) for which the jird is permissive and nonpermissive to parasitic establishment, respectively. The jirds were separated into one of four timepoint groups: 1, 3, 10, and 36 dpi (Figure 2.3).

Figure 2.3
Experimental design

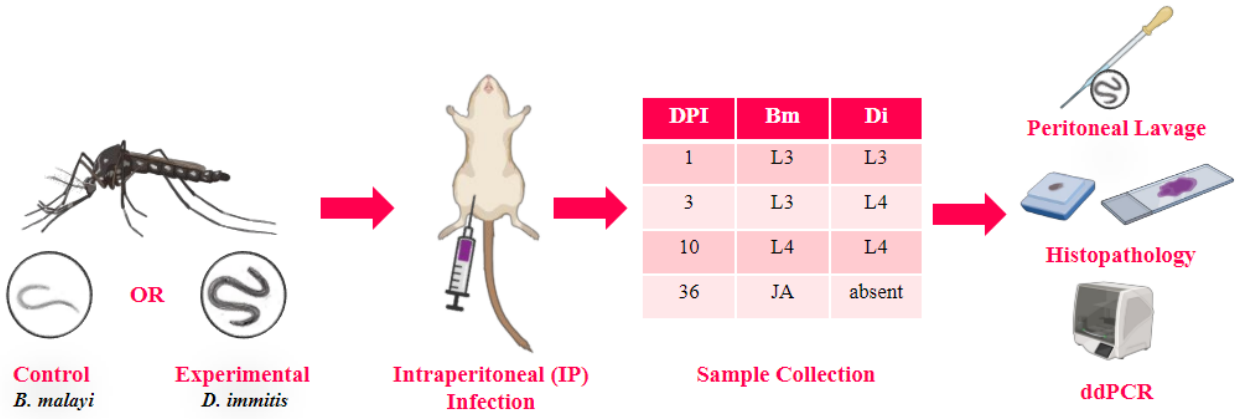

Note: *Aedes aegypti* mosquitos were fed *B. malayi* and *D. immitis* microfilaremic blood, respectively. L3 were harvested from the mosquitos 15 days post blood feeding, and jirds were infected by IP injection with 100 *B. malayi* (n = 20) or *D. immitis* (n = 20) L3. Necropsies were performed at 1-, 3-, 10-, and 36-days post infection (dpi) (n = 5/timepoint/group) according to the larval stage of the parasite. Larvae were recovered by peritoneal lavage at each timepoint, quantified, and stored in formalin for larval-stage morphologic identification. The peritoneal wall and diaphragm were recovered from each jird and stored in ethanol for absolute quantification of larvae with ddPCR. Histopathology was performed on the peritoneal wall and diaphragm of jirds infected by IP injection with either 500 *B. malayi* (n=6) or *D. immitis* (n=6) L3. H&E stains were used on the tissue slides for larval detection, and immunohistochemistry was also performed using anti-Iba1 antibody for detection of macrophages.

Peritoneal recovery of larvae

Jirds were humanely euthanized by carbon dioxide asphyxiation followed by cervical dislocation at 1, 3, 10, or 36 dpi [10]. Larvae were collected by peritoneal lavage via a 5-mm abdominal incision with approximately 32 ml of 0.9% isotonic saline solution (Sigma-Aldrich, St. Louis, MO) to maintain the shape and size of the peritoneal exudate cells (PECs) [10]. Recovered larvae were quantified and transferred from the cell suspension to 10% neutral-buffered formalin (Epredia, Kalamazoo, MI) for identification of the larval stage. All remarkable observations were documented, including PEC attachment to larvae and degenerated larvae. The peritoneal wall (separated into the subject-oriented right and left side) and diaphragm of each jird were excised and stored in 70% ethanol (Sigma-Aldrich, St. Louis, MO) for further analysis with ddPCR.

Histopathology

Adult male jirds were infected by IP injection according to standard procedures [15] with either 500 *B. malayi* (n = 6) or *D. immitis* (n = 6) L3. A naïve jird (n = 1) served as a negative control for infection and was inoculated with parasite-free HBSS (MP Biomedicals, Santa Ana, California) supplemented with 2% ciprofloxacin (Sigma-Aldrich, St. Louis, MO) for which the same procedures were performed using mosquitoes that had been fed uninfected dog blood 15 days prior. All jirds were humanely euthanized by carbon dioxide asphyxiation followed by cervical dislocation at 1 dpi. Following euthanasia, a peritoneal lavage was performed as previously described, larvae were recovered, quantified, and the developmental stages of the larvae were identified. The peritoneal wall (separated into the subject-oriented right and left side) and diaphragm of each jird were excised and stored in 10% neutral-buffered formalin (Epredia,

Kalamazoo, MI) and submitted to the University of Georgia Histology Laboratory (Athens, GA) for processing, step sectioning at 5-µm thickness, 10-µm apart, and staining with hematoxylin and eosin (H&E) stains for larval detection. Immunohistochemistry was also performed by the University of Georgia Histology Laboratory with 1:8000 dilution of anti-ionized calcium binding adaptor molecule, rabbit (Iba1; FUJIFULM Wako Chemicals, Richmond, VA) for detection of macrophages [16]. Light microscopic evaluation (Olympus BX41; Olympus America Inc., Center Valley, PA) was performed on the slides and images were captured using Olympus CellSens software, version 1.16 (Olympus America Inc., Center Valley, PA).

DNA extraction for conventional PCR validation of primers

Genomic DNA was extracted from the diaphragms of naïve jirds (n = 3) combined with 1, 50, and 100 *D. immitis* L3, respectively, using the REDExtract-N-Amp™ Tissue PCR Kit (Sigma-Aldrich, St. Louis, MO) as per the manufacturer's instructions. DNA was stored at 4°C until PCR was performed the following day.

Conventional PCR validation of primers

A conventional PCR assay, followed by gel electrophoresis, was performed to detect 1, 50, and 100 *D. immitis* L3 homogenized with naïve jird diaphragm, respectively. The mitochondrial cytochrome oxidase c subunit I (cox1) gene of *D. immitis* was amplified using forward (5′- CAT CCT GAG GTT TAT GTT ATT TT -3′) and reverse (5′- CWG TAT ACA TAT GAT GRC CYC A -3′) primers (Integrated Data Technologies, Coralville, IA) [17-19]. Cycling conditions included an initial denaturation at 94°C for 3 minutes, followed by 35 cycles for 1 minute of denaturation at 94°C and annealing at 45°C, extension at 72°C for 30 seconds,

and a final extension at 72°C for 1 minute. The jird highly expressed reference gene, glyceraldehyde-3-phosphate dehydrogenase (GAPDH) (Forward: 5′- CAT GGC CTT CCG AGT TCC T -3′; Reverse: 5′- TTC TGC AGT CGG CAT GTC A -3′) (Integrated Data Technologies, Coralville, IA), served as a positive control [20-22]. Cycling conditions included an initial denaturation at 94°C for 3 minutes, followed by 35 cycles for 1 minute of denaturation at 94°C and annealing at 51°C, extension at 72°C for 30 seconds, and a final extension at 72°C for 1 minute. All reaction samples were performed in 50 µL volumes using 0.4 µM of each primer, 25 µL REDExtract-N-Amp™ PCR Reaction Mix (Sigma-Aldrich, St. Louis, MO), and 200 pg/µL DNA template. Electrophoresis (Fisherbrand Mini-Horizontal Electrophoresis Systems, Fisher Scientific, Hampton, NH) was performed in a 2% agarose 1x TAE gel stained with ethidium bromide (Sigma-Aldrich, St. Louis, MO), and the PCR products were visualized under a UV light.

DNA extraction for droplet digital PCR

Genomic DNA was extracted from the peritoneal wall (separated into the subject-oriented right and left side) and diaphragm of each jird (n = 10), collected only at the 1 dpi timepoint, using the QIAGEN Blood & Cell Culture DNA Maxi Kit and QIAGEN Genomic-tips (QIAGEN Sciences Inc, Germantown, MD) as per manufacturer's instructions. Precipitation of DNA was performed to concentrate each sample as recommended by QIAGEN Sciences, Inc. A 1/10 volume of 3 M sodium acetate (pH 5.2) and 2 volumes of ice-cold 100% ethanol was added to the DNA sample. The sample was mixed and stored at –20 °C for 1 hour to precipitate the DNA. The precipitated DNA was recovered by centrifugation at 21,000 x *g* in a microcentrifuge for 20 minutes. The ethanol was discarded by rapid decantation and the pellet washed twice with

room-temperature 70% ethanol. The DNA pellet was air-dried prior to resuspension in 100 µL distilled water. Quality control of DNA samples was performed on a NanoDrop™ 2000 Spectrophotometer (Thermo Fisher Scientific, Waltham, MA). DNA was stored at -80°C until ddPCR was performed.

Droplet digital PCR (ddPCR)

The absolute quantification of *B. malayi* and *D. immitis* L3 DNA in the jird peritoneal wall and diaphragm was performed on a Bio-Rad QX200 w/ADG ddPCR System (Bio-Rad Laboratories, Hercules, CA) by the Emory Integrated Genomics Core. This system of digital PCR uses water-oil emulsion droplet technology combined with fluidics [23]. A DNA sample, along with primers, probes, and reaction mix (2x ddPCR™ Supermix for Probes (no dUTP); (Bio-Rad Laboratories, Hercules, CA) was divided into 20,000 nanoliter-sized droplets in which the DNA was randomly distributed, followed by PCR amplification of the DNA in each individual droplet [23].

The mitochondrial cytochrome oxidase c subunit I (cox1) gene of *D. immitis* was amplified using forward (5′-CAT CCT GAG GTT TAT GTT ATT TT-3′) and reverse (5′-CWG TAT ACA TAT GAT GRC CYC A- 3′) primers with a FAM-fluorescent probe (5’-/56-FAM/CGG TGT TTG /ZEN/GGA TTG TTA GTG /3IABkFQ/ -3’) (Integrated Data Technologies, Coralville, IA) [17-19]. Cycling conditions included an initial denaturation at 94°C for 3 minutes, followed by 35 cycles for 1 minute of denaturation at 94°C and annealing at 45°C, extension at 72°C for 30 seconds, and a final extension at 72°C for 1 minute. *Brugia malayi* HhaI, the most repeated gene in the genome, was amplified using forward (5′- GCA ATA TAC GAC CAG CAC -3’) and reverse (5′-ACA TTA GAC AAG GAA ATT GGT T -3′)

primers with a FAM-fluorescent probe (5'- /56-FAM/TTA GTA GTT /ZEN/TTG GCA CTT /3IABkFQ/ -3') (Integrated Data Technologies, Coralville, IA) [24, 25]. Cycling conditions included an initial denaturation at 94°C for 3 minutes, followed by 35 cycles for 1 minute of denaturation at 94°C and annealing at 45°C, extension at 72°C for 30 seconds, and a final extension at 72°C for 1 minute.

Completing the ddPCR process, each droplet was read by a droplet reader to determine the fraction of positive droplets in the total DNA sample, using Poisson statistical formulas to determine absolute quantification without the need for a standard curve [23].

Data analysis

The sample size for this study was based on a study power of 0.8 and significance level of 0.05 with G*Power 3.1.9.7 software for Windows (Heinrich Heine Universität Düsseldorf, Düsseldorf, GER). A contingency analysis was performed on recovered *D. immitis* and *B. malayi* larvae at each timepoint, respectively, from the total amount of L3 administered to the jirds. Descriptive observational analyses of the histopathology slides were performed by a boarded veterinary pathologist blinded to the samples' infection status and parasite. A Chi-square two-sided test followed the contingency analysis. Larval recovery analyses were performed with GraphPad Prism version 10 (GraphPad Software, San Diego, CA). Copy numbers of *D. immitis* cox1 gene and *B. malayi* HhaI gene will be determined by ddPCR and analyzed with Poisson correction and equation on QuantaSoft™ Analysis Pro software (Bio-Rad Laboratories, Hercules, CA).

Results

Larval recovery and cell attachment

A mean of 37.4% (SEM = 5.8%) *B. malayi* L3 and 0.4% (SEM = 0.2%) *D. immitis* L3 were recovered at 1 dpi ($p<0.0001$). *Brugia malayi* L3 recovery remained the same (mean = 32.8%; SEM = 3.1%) and a mix of *D. immitis* L3 and L4 were recovered (23.6%; SEM = 1.8%) at 3 dpi, a significant increase from 1 dpi for *D. immitis* ($p<0.001$). Both *B. malayi* (mean = 25%; SEM = 5.3%) and *D. immitis* L4 recovery (mean = 7.8%; SEM = 1.1%) steadily decreased at 10 dpi ($p<0.0001$). By 36 dpi, a mean of 15.2% (SEM = 2.5%) *B. malayi* immature adults (IA) and no viable *D. immitis* larvae were recovered ($p<0.0001$) (Figures 2.4 and 2.5). In summary, *D. immitis* larvae are not recovered by peritoneal lavage at 1 dpi infection, reappear in the peritoneal cavity at 3 dpi, all viable larvae are L4 by 10 dpi, and larvae are no longer recovered in the peritoneal cavity by 36 dpi.

Figure 2.4

The relative presence of D. immitis in the peritoneal cavity of the Mongolian gerbil

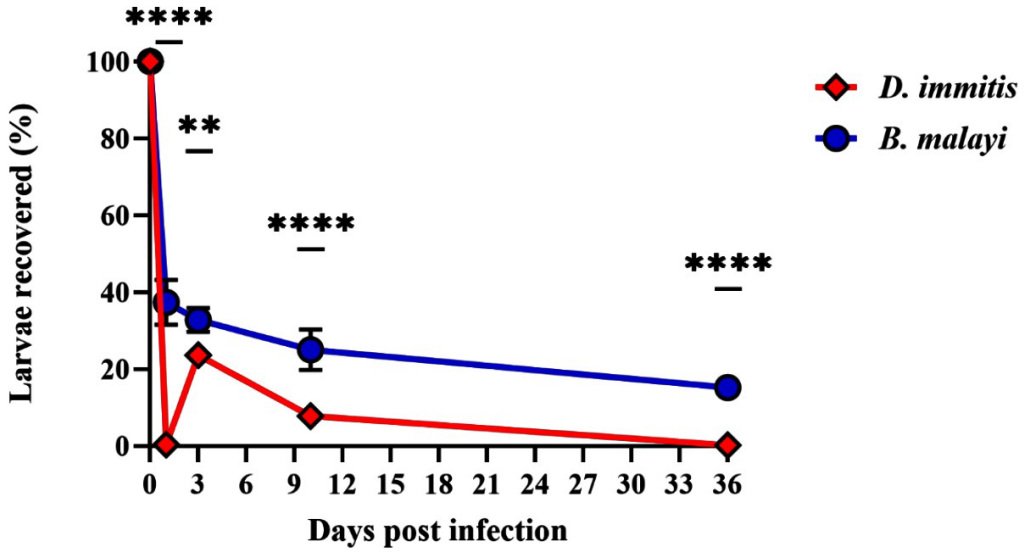

Note: The percentage of larvae recovered from *B. malayi*-infected jirds (mean: 37.4%) after 1 day was significantly greater ($p < 0.0001$) than larvae recovered from *D. immitis*-infected jirds (0.4%). There was a reappearance of *D. immitis* larvae recovered at 3 dpi (23.6%; $p<0.001$).

Figure 2.5

D. immitis and B. malayi larvae recovered from the peritoneal cavity of the Mongolian gerbil

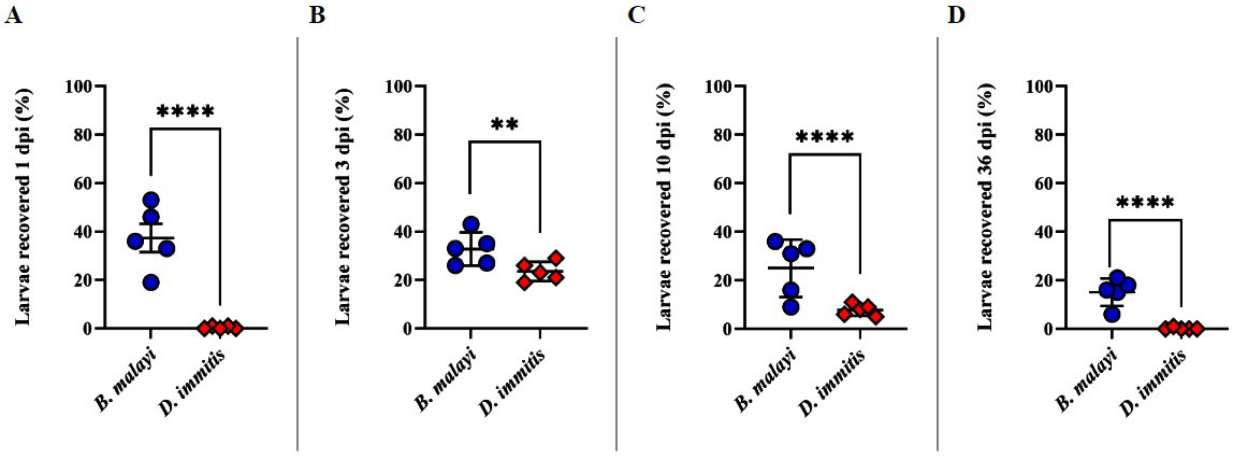

Note: A-D) *D. immitis* larvae recovered from the peritoneal cavity on days 1, 3, 10, and 36 dpi were significantly fewer than *B. malayi* larvae ($p < 0.001$ 3 dpi; $p < 0.0001$ 1, 10, and 36 dpi).

The authors observed jird PEC attachment to *D. immitis* larvae recovered in peritoneal lavage fluid at 3- and 10-dpi and observed only 1 degenerated larva at 36 dpi (Figure 2.6). The observed cell attachment to *D. immitis* larvae *in vivo* complements the results previously seen *in vitro* [16].

Figure 2.6

Peritoneal exudate cells attach to D. immitis L3

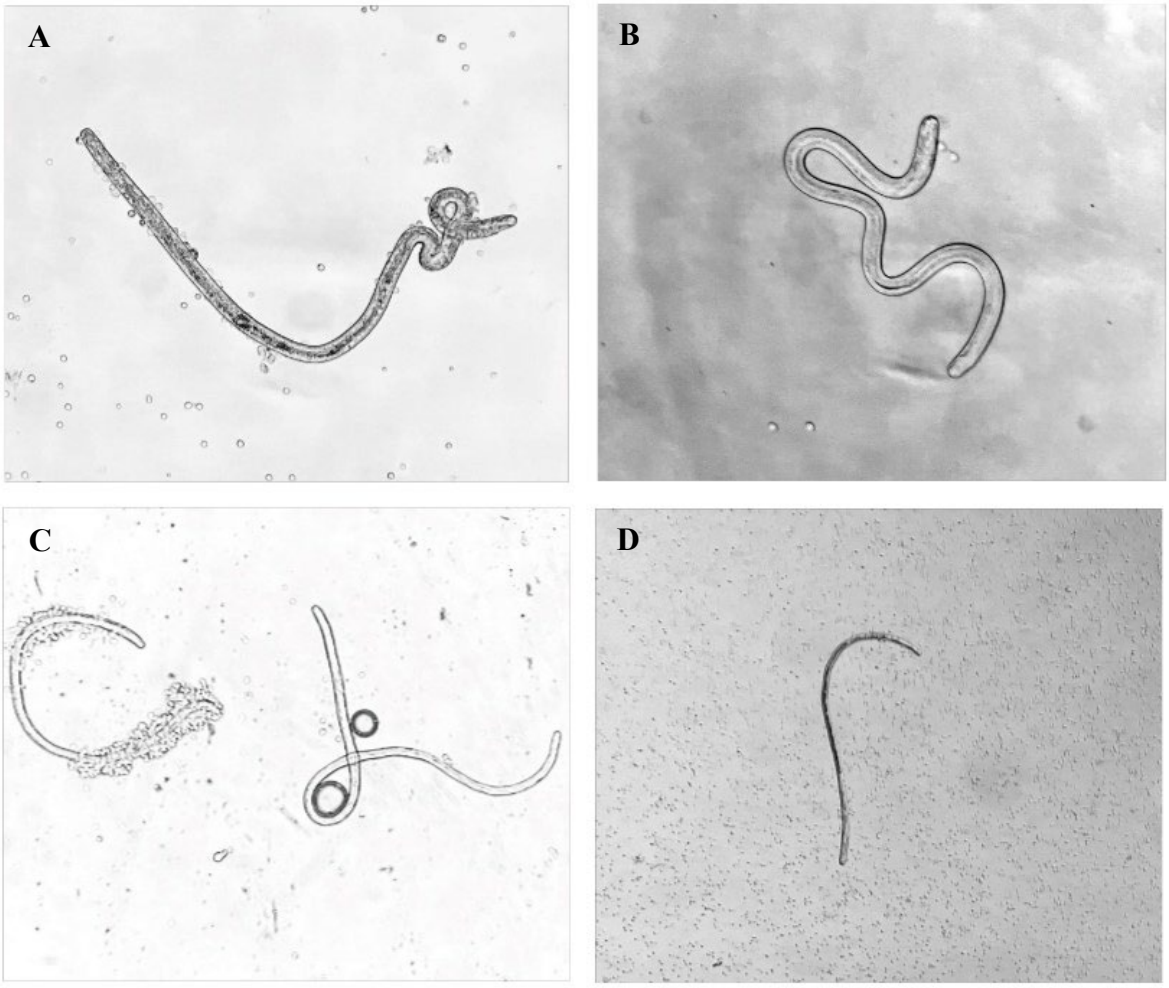

Note: D. immitis larvae were recovered from the peritoneal cavity at 1, 3, 10, and 36 dpi. PECs were attached to *D. immitis* L3 at 3 and 10 dpi. A) Some *D. immitis* L3 had PEC attachment at 3 dpi. B) A shed cuticle from a *D. immitis* L3 was observed 3 dpi after its third molt. C) At 10 dpi, a *D. immitis* L3 with PEC attachment and an L4 with no cell attachment was observed. D) The only *D. immitis* larvae recovered 36 dpi was degenerated.

Histopathology

The peritoneal wall, separated into subject-oriented right and left sides, and the diaphragm of a naïve jird, Jird A, served as a negative control for the cellular response to infection with *B. malayi* and *D. immitis* L3 at 1 dpi. The jird A right and left peritoneal wall contained focal, mild satellite cell proliferation, suggesting muscle regeneration. The left peritoneal wall contained locally extensive infiltration of the perimysium, which surrounds bundles of muscle fibers, by moderate numbers of neutrophils and macrophages (Table 2.1), extending into the muscle, effacing a few myofibers, and dissecting between others. A thin strip of dense, diaphragm connective tissue was multifocally infiltrated by moderate numbers of neutrophils, lymphocytes, and macrophages, particularly surrounding vessels, with another focal aggregate of inflammatory cells adhered to the skeletal muscle surface.

The most notable results in *B. malayi*-infected jirds came from two jirds, Jird B and Jird C (Table 2.1). The right and left peritoneal wall and diaphragm of Jird B contained locally extensive aggregates of neutrophils, macrophages, and lymphocytes with fibrin, necrotic debris, and entrapped, variably sized, degenerated nematodes. Degenerated nematodes (Figure 2.7) were also found lining the surface of the diaphragm and along a strip of associated connective tissue. Both the right and left peritoneal wall had perimysium and interstitium that were multifocally expanded by edema and small numbers of neutrophils, lymphocytes, and macrophages.

Similarly, the right peritoneal wall of Jird C contained multifocal mats of fibrin, mixed with neutrophils, lymphocytes, and macrophages, along the surface of the epimysium, a connective tissue sheath surrounding muscle. The perimysium and epimysium of the right and left peritoneal wall and diaphragm were multifocally expanded by edema and low (right peritoneal wall) to moderate numbers (left peritoneal wall and diaphragm) of neutrophils,

lymphocytes, and macrophages with scattered degenerated and regenerative myofibers. The left peritoneal wall had a focal fibrin mat on the loose connective tissue layer, and the epimysium contained mixed degenerate neutrophils, lymphocytes, and macrophages. The diaphragm of Jird C had multifocal mats of neutrophils, macrophages, and lymphocytes, with fibrin and necrotic debris, lining the surface of the muscle and the connective tissue layer with a viable larva entrapped in exudate.

Notably, the right and left peritoneal wall and diaphragm of Jird D (Table 2.1), infected with *D. immitis*, were multifocally lined by of neutrophils, macrophages, and lymphocytes, with fibrin and necrotic debris, on the muscle surface. The perimysium and endomysium (connective tissue surrounding individual muscle fibers) were multifocally expanded by edema and low (right and left peritoneal wall) to moderate numbers (diaphragm) of neutrophils, lymphocytes, and macrophages with scattered degenerated and regenerative myofibers. A few degenerate and viable larvae were observed in the left peritoneal wall, and a single, entrapped, larval nematode lining the muscle surface and connective tissue layer was observed in the diaphragm (Figure 2.7).

Table 2.1
Cells observed surrounding larvae in the peritoneal wall and diaphragm of the jird

Jird	Parasite	Viable L3	Degenerated L3	Neutrophils	Lymphocytes	Macrophages	Fibrin
A	*Naive*	n/a	n/a	++[bc]	++[c]	++[bc]	-
B	*B. malayi*	-	++[abc]	+[abc]	+[abc]	+[abc]	+[abc]
C	*B. malayi*	+[c]	-	++[abc]	++[abc]	++[abc]	++[abc]
D	*D. immitis*	++[b]	++[abc]	++[abc]	++[abc]	++[abc]	++[abc]

Note: A naïve jird served as a control for the cells seen in infected tissues. *B. malayi* L3 was observed in only 2 of the 5 infected jirds. *D. immitis* L3 was observed in only 1 of the 5 infected jirds.
+: Represents a single nematode regarding L3 observation and small number of cells regarding the cell types.
++: Represents a few nematodes regarding L3 observation and moderate number of cells regarding the cell types.
[a]: Observed in the right peritoneal wall
[b]: Observed in the left peritoneal wall
[c]: Observed in the diaphragm

Figure 2.7

Larvae sequestered in the peritoneal wall and diaphragm of the jird

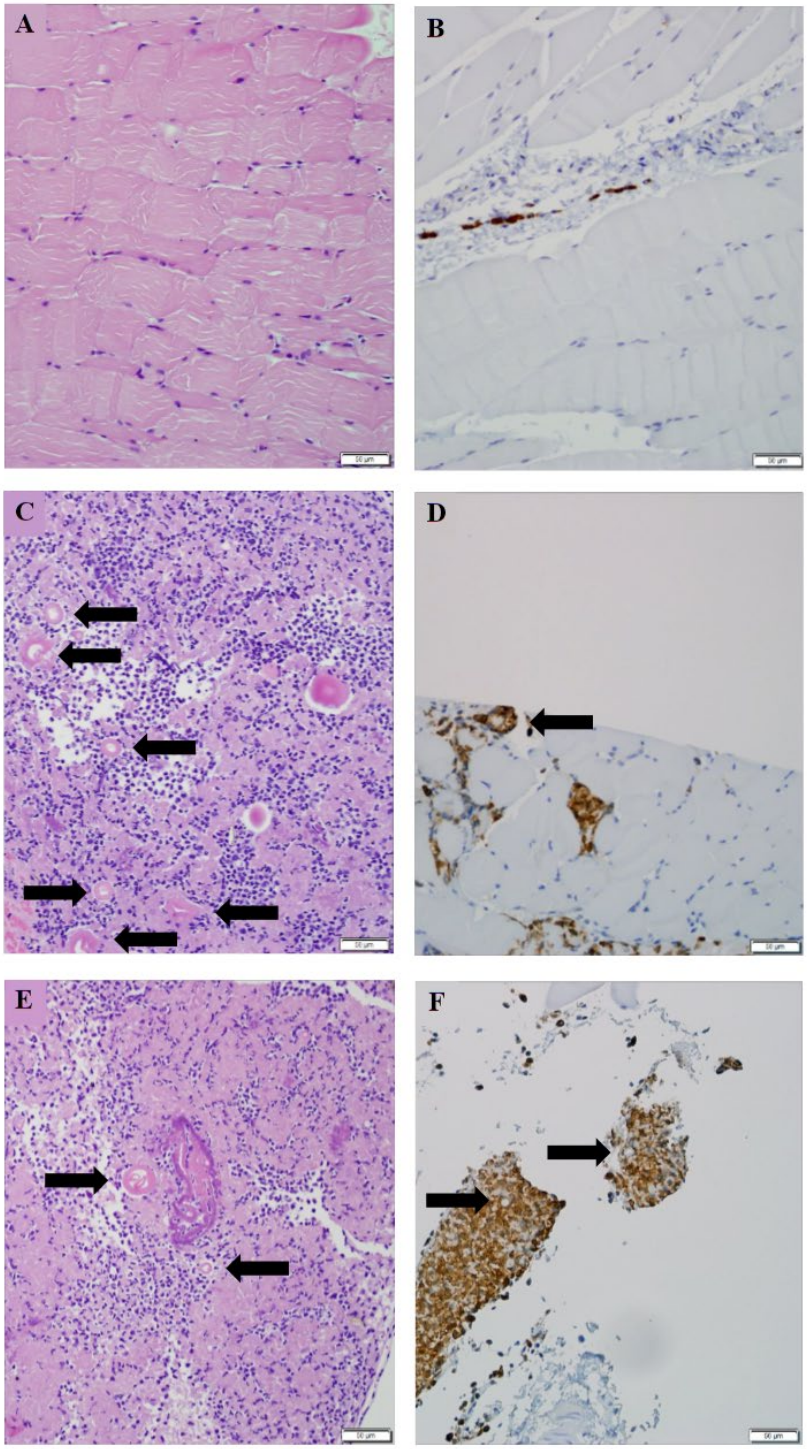

Note: All images are of jird peritoneal wall. Panels A, C, and E tissues were stained with H&E, staining the leukocytes dark purple. Panels B, D, and F tissues were stained for Iba1 using immunohistochemistry, showing macrophages as brown (immunopositive). Arrows direct attention to larvae embedded in tissue.

Discussion

There is a lack of knowledge regarding the host-parasite interaction during *D. immitis* infection, specifically the mechanisms of the canine host that determine the ultimate establishment of the parasite. As the threat of ML-resistant *D. immitis* rises in the United States, there is a need for either a new class of drugs that is effective in killing *D. immitis*, or another target of host immunity to explore to work in tandem with MLs [6]. In this study, the authors explored the determinants of *D. immitis* host-specificity using a nonpermissive rodent model, the Mongolian jird (*Meriones unguiculates*). We hypothesized that host immunity determines the establishment of *D. immitis* after the third larval molt. The data presented here partially support this hypothesis, specifically indicating that establishment occurs following the third larval molt. However, the specific host immunity factor responsible for determining the establishment of *D. immitis* remains unknown, though it may involve the cell attachment observed to the larvae.

Only one publication exists that details the development of intraperitoneal infection of *D. immitis* in the jird [11]. Wong and Lim inoculated jirds with large numbers of L3 IP (400-600), and worms were recovered between 16 and 132 dpi, the earliest timepoints yielding minimal recovery: 0.5% L4 at 16 dpi, 3.5% L4 at 23 dpi, and 0.75% L4 at 44 dpi. This current study infected jirds with fewer (n = 100) L3 than in that study, but the results were similar: *D. immitis* larvae did not develop past the L4 stage except for one mating pair of adult worms that was recovered (n = 1 or 5 jirds) alive from the pulmonary artery and right heart [11]. We did not maintain our gerbils for a sufficient amount of time required to determine whether there was development into adults.

Dirofilaria immitis L3 were found in the peritoneal wall and diaphragm of jirds, which were examined for their cellular response to infection with *B. malayi* and *D. immitis* L3. A naïve

jird served as a negative control for the cellular response; the peritoneal wall had focal, mild satellite cell proliferation, suggesting muscle regeneration, and only the left peritoneal wall had extensive infiltration of perimysium by a moderate number of neutrophils and macrophages. Although the naïve jird was not infected with larvae, the peritoneal cavity was inoculated with parasite-free HBSS for which the same L3 harvest procedures were performed using mosquitoes that had been fed on blood from an uninfected dog. The HBSS was not sterile and most likely contained microscopic mosquito debris, eliciting inflammation within the peritoneal cavity.

The most notably affected *B. malayi* jirds contained extensive aggregates of neutrophils, macrophages, and lymphocytes with fibrin, necrotic debris, and degenerated nematodes. Compared to the naïve jird, there was an increase in the number of areas with immune cells and these areas were focused around the degenerated larvae. The cellular immune response observed in the jird to *B. malayi* aligned with the cell types observed in previous studies with subcutaneously infected jirds. These studies observed a moderate number of macrophages, a few lymphocytes and neutrophils, and a few eosinophils as early as 1- and 7- dpi, respectively [26, 27].

Observing a cellular immune response in the naïve jird negative control and *B. malayi* positive control serves as a baseline for evaluation of the jird cellular response to *D. immitis* L3. Jirds infected with *D. immitis* had multifocal mats of neutrophils, macrophages, and lymphocytes, with fibrin and necrotic debris on the muscle surface in contrast with the loose aggregates of cells observed in *B. malayi* tissues. The perimysium and endomysium were expanded by edema, with low to moderate numbers of similar inflammatory cells. Although the negative control displayed perimysial infiltration by macrophages and neutrophils, the *D. immitis* tissue additionally contained lymphocytes and edema of the perimysium. Overall, there was an

increase in inflammation localized around *D. immitis* L3 compared to *B. malayi*-infected peritoneal wall and naïve tissue.

Peritoneal recovery of *D. immitis* larvae in the jird was as expected, with a gradual decline, but the absence and reappearance of *D. immitis* larvae at 1 and 3 dpi, respectively, was of the utmost interest to the authors. Although the recovery of *B. malayi* larvae was slightly lower at 10% than the expected 23%, this could be due to the overall variability of jird infectivity [28]. Previous studies demonstrated that subcutaneously inoculated *D. immitis* L3 and L4 are found in the skin and muscle of dogs and ferrets up to 58 dpi [29, 30], so the peritoneal wall and diaphragm were excised and submitted for histopathology to potentially locate L3 in the tissues at 1 dpi. Although *D. immitis* L3, along with a few *B. malayi* L3, were observed in the step sections of these tissues, it was highly likely that larvae were overlooked through the process. Notably, there was a clear increase in the presence of inflammatory cells and macrophages that appeared in the tissues with *D. immitis* L3 as compared to the tissues with *B. malayi* L3. These results demonstrate that there is a cellular immune response to *D. immitis* L3 and *B. malayi* L3.

In 2021, Evans *et al*. reported jird peritoneal exudate cell attachment *in vitro* to *D. immitis* L3 after 20 hours of culture [16]. The cells attaching to *D. immitis* L3 were identified primarily as macrophages. Similarly, this study observed cell attachment to viable *D. immitis* L3 at 3 dpi (Figure 2.7). It is likely that the PECs attached to L3 in the peritoneal cavity are primarily macrophages, considering that the primary cell type surrounding larvae in the tissues is the macrophage as seen in the Iba1 IHC slides (Figure 2.7).

A major limitation of this research is the jird model. There are almost no immunochemistry markers known to work with gerbils, and characterization of jird peritoneal cells has yet to be published. There are more unknowns than knowns regarding gerbil immunity,

requiring researchers to gain a more basic understanding of jirds before dedicating their efforts to using them as a model. However, the jird was an ideal model for this study, because it is permissive to the establishment of a *B. malayi* intraperitoneal infection, allowing for an easier method of worm recovery than a subcutaneous inoculation method.

The histopathology results were useful in describing the cellular immune response in the peritoneal wall and diaphragm to the parasites. However, through the process of sectioning samples, the probability of overlooking larvae is high. Droplet digital PCR is a more sensitive test for the absolute quantification of DNA than other PCR methods. By quantifying the copy numbers of parasite DNA within each tissue sample, the issue of potentially missing L3 with light microscopy is resolved.

Performing ddPCR on the rest of the peritoneal tissue (e.g., liver, spleen, kidneys, adipose fat, etc.) that was collected and stored in 70% ethanol after necropsy at each timepoint is a natural progression to continue this work. It is important to further investigate *D. immitis* actions while sequestering in peritoneal tissue at 1 dpi in order to determine whether the tissue aids in the *D. immitis* molt to L4 or assists the parasites in evading the innate immune response of the jird.

It is well known that macrophages target extracellular parasites by alternative activation, so investigation into the specific role macrophages play in preventing the establishment of *D. immitis* in the jird is necessary to better understand host specificity from the perspective of host-parasite interaction. This is the first study to document the initial immune response of the Mongolian jird to intraperitoneal inoculation with *D. immitis* L3. The majority of *D. immitis* research is performed *in vitro* due to the limited availability of resources and the current social and political climate surrounding animal research [31-34]. It is essential to shift perspectives and

explore new avenues to understand the host-parasite interaction in the initial stages of infection. This study demonstrates that the nonpermissive host has an increased cellular immune response *to D. immitis* compared to *B. malayi*, for which the jird is susceptible to infection. Since MLs work with the host immune system to prevent establishment and eliminate *D. immitis*, the jird cellular immune response to *D. immitis* should be explored.

Conclusion

Current *D. immitis in vivo* research depends on an established infection in a permissive host, with dogs and ferrets being preferred animal models. This study is the first to investigate the initial immune response of a nonpermissive host, the Mongolian jird, to *D. immitis* intraperitoneal infection. The results of the study suggest the hypothesis that the establishment of *D. immitis* is determined by host immunity after the third larval molt. However, interpretation of the reported data should take into consideration that all of the inoculated larvae were not located. The cellular immune response of the jird was examined at 1 dpi infection with *B. malayi* and *D. immitis*, respectively. The absence and reappearance of *D. immitis* larvae at 1 and 3 days were the most significant differences in recovery from the peritoneal cavity. Absent from peritoneal lavage fluid at 1dpi, *D. immitis* L3 were found in the peritoneal wall and diaphragm of jirds, surrounded primarily by macrophages, followed by neutrophils and lymphocytes.

Understanding filarial parasites requires thorough investigation into each life stage, including the mechanisms of worm establishment within the host and their interaction with the host during establishment. Identifying the larval stage at which *D. immitis* establishment is prevented by the jird nonpermissive host will provide more insight into host specificity of filarial

infections and encourage the potential development of new drugs or host immunity targets to combat the increasing threat of ML-resistant *D. immitis* in the United States.

Acknowledgements

The authors thank Chris Evans, Angela Tolbert, Tanya Cooper, Catherine Pope, Nicole Davis, and Yi Chu for their technical assistance. *Brugia* life cycle stages were obtained through the NIH/NIAID Filarial Research Reagent Resource Center (FR3); morphological voucher specimens are stored at the Harold W. Manter Museum at University of Nebraska, accession numbers P2021-2032. This study was supported in part by the Emory Integrated Genomics Core (EIGC) (RRID:SCR_023529), which is subsidized by the Emory University School of Medicine and is one of the Emory Integrated Core Facilities. Additional support was provided by the Georgia Clinical & Translational Science Alliance of the National Institutes of Health under Award Number UL1TR002378. The content is solely the responsibility of the authors and does not necessarily reflect the official views of the National Institutes of Health.

Disclosures

The authors have no financial conflict of interest. Funding for this study is from various revenue streams of the Moorhead laboratory at the University of Georgia.

References

1. (CAPC), C.A.P.C. *Canine Heartworm Prevalence Map*. 2023; Available from: https://capcvet.org/maps/#/2023/all-year/heartworm-canine/dog/united-states.

2. (CAPC), C.A.P.C. *Heartworm Guidelines*. 2020; Available from: https://capcvet.org/guidelines/heartworm/.

3. Orihel, T.C., *Morphology of the larval stages of Dirofilaria immitis in the dog.* J Parasitol, 1961. 47: p. 251-62.

4. Bowman, D.D. and C.E. Atkins, *Heartworm Biology, Treatment, and Control.* Veterinary Clinics of North America: Small Animal Practice, 2009. 39(6): p. 1127-1158.

5. Wood, C.L. and P.T. Johnson, *A world without parasites: exploring the hidden ecology of infection.* Frontiers in Ecology and the Environment, 2015. 13(8): p. 425-434.

6. (AHS), A.H.S. *American Heartworm Society Canine Guidelines for the Prevention, Diagnosis, and Management of Heartworm (Dirofilaria immitis) Infection in Dogs*. Macrocyclic Lactones 2024.

7. McCall, J.W., et al., *Chapter 4 Heartworm Disease in Animals and Humans*. 2008, Elsevier. p. 193-285.

8. Bowman, D.D. and J. Drake, *Examination of the "susceptibility gap" in the treatment of canine heartworm infection.* Parasites & Vectors, 2017. 10(S2).

9. Ash, L.R. and J.M. Riley, *Development of subperiodic Brugia malayi in the jird, Meriones unguiculatus, with notes on infections in other rodents.* J Parasitol, 1970. 56(5): p. 969-73.

10. Mutafchiev, Y., et al., *Intraperitoneal development of the filarial nematode Brugia malayi in the Mongolian jird (Meriones unguiculatus).* Parasitology Research, 2014. 113(5): p. 1827-1835.

11. Wong, M.M., Lim, K. C., *Development of Intraperitoneally Inoculated Dirofilaria immitis in the Laboratory Mongolian Jird (Meriones unguiculates).* The Journal of Parasitology, 1975. 61(3): p. 573-574.

12. (FR3), F.R.R.R.C. *Collecting Infective Larvae of Brugia pahangi, B. malayi, Dirofilaria immitis, and Dirofilaria repens From Infected Mosquitoes*. Available from: http://www.filariasiscenter.org/protocols/Protocols/collecting-infective-larvae-of-brugia-pahangi-b.-malayi-dirofilaria-immitis-and-dirofilaria-repens-from-infected-mosquitoes.

13. (FR3), F.R.R.R.C. *Mosquito Rearing Techniques*. Available from: http://www.filariasiscenter.org/protocols/Protocols/mosquito-rearing-techniques.

14. (FR3), F.R.R.R.C. *Infecting Aedes aegypti with Brugia pahangi, B. malayi, and Dirofilaria immitis*. Available from: http://www.filariasiscenter.org/protocols/Protocols/infecting-aedes-aegypti-with-brugia-pahangi-b.-malayi-and-dirofilaria-immitis.

15. (FR3), F.R.R.R.C. *Experimental Infection of Dogs, Cats, Ferrets, and Rodents with Dirofilaria immitis, Brugia malayi, B. pahangi, or Dipetalonema reconditum*. Available from: http://www.filariasiscenter.org/protocols/Protocols/experimental-infection-of-dogs-cats-ferrets-and-rodents-with-dirofilaria-immitis-brugia-malayi-b.-pahangi-or-dipetalonema-reconditum.

16. Evans, C.C., et al., *A rapid, parasite-dependent cellular response to Dirofilaria immitis in the Mongolian jird (Meriones unguiculatus).* Parasit Vectors, 2021. 14(1): p. 25.

17. Sobotyk, C., et al., *Detection of Dirofilaria immitis via integrated serological and molecular analyses in coyotes from Texas, United States.* Int J Parasitol Parasites Wildl, 2022. 18: p. 20-24.

18. Negron, V., et al., *Probe-based qPCR as an alternative to modified Knott's test when screening dogs for heartworm (Dirofilaria immitis) infection in combination with antigen detection tests.* Parasites & Vectors, 2022. 15(1): p. 306.

19. Laidoudi, Y., et al., *Development of a multiplex qPCR-based approach for the diagnosis of Dirofilaria immitis, D. repens and Acanthocheilonema reconditum.* Parasit Vectors, 2020. 13(1): p. 319.

20. Saito, H., et al., *Roles of virD4 and cagG genes in the cag pathogenicity island of Helicobacter pylori using a Mongolian gerbil model.* Gut, 2005. 54(5): p. 584-90.

21. Guo, Y.Y., et al., *Brown adipose tissue plays thermoregulatory role within the thermoneutral zone in Mongolian gerbils (Meriones unguiculatus).* J Therm Biol, 2019. 81: p. 137-145.

22. Lewczuk, A., A. Boratyńska-Jasińska, and B. Zabłocka, *Validation of the Reference Genes for Expression Analysis in the Hippocampus after Transient Ischemia/Reperfusion Injury in Gerbil Brain.* Int J Mol Sci, 2023. 24(3).

23. Bio-Rad Laboratories, I., *QX200TM Droplet Reader and QX Manager Software Standard Edition*. 2023.

24. Rao, R.U., et al., *Detection of Brugia parasite DNA in human blood by real-time PCR.* J Clin Microbiol, 2006. 44(11): p. 3887-93.

25. Pilotte, N., et al., *A TaqMan-based multiplex real-time PCR assay for the simultaneous detection of Wuchereria bancrofti and Brugia malayi.* Mol Biochem Parasitol, 2013. 189(1-2): p. 33-7.

26. Vincent, A.L., S.P. Frommes, and L.R. Ash, *Brugia malayi, Brugia pahangi, and Brugia patei: Pulmonary pathology in jirds, Meriones unguiculatus.* Experimental Parasitology, 1976. 40(3): p. 330-354.

27. Chirgwin, S.R., et al., *Profiling the cellular immune response to multiple Brugia pahangi infections in a susceptible host.* J Parasitol, 2005. 91(4): p. 822-9.

28. Eberhard, M.L. and R.C. Lowrie, *Variable infectivity of third-stage larvae of Brugia malayi.* Journal of Helminthology, 1985. 59(3): p. 283-285.

29. Supakorndej, P., J.W. McCall, and J.J. Jun, *Early Migration and Development of Dirofilaria immitis in the Ferret, Mustela putorius furo.* The Journal of Parasitology, 1994. 80(2): p. 237-244.

30. Kotani, T. and K.G. Powers, *Developmental stages of Dirofilaria immitis in the dog.* Am J Vet Res, 1982. 43(12): p. 2199-206.

31. H.R.4757. *Cease Animal Research Grants Overseas Act of 2023*. 118th Congress (2023-2024) 2023 2023, July 21; Available from: https://www.congress.gov/bill/118th-congress/house-bill/4757.

32. MI-SB0149. *Animals: research facilities; certain research facilities to offer certain laboratory animals for adoption before euthanization; require. Amends title & secs. 1 & 7 of 1969 PA 224 (MCL 287.381 & 287.387) & adds sec. 8a. TIE BAR WITH: SB 0148'23*. State of Michigan, 102nd Legislature - Regular Session of 2023 2023 02/13/2024; Available from: https://legiscan.com/MI/text/SB0149/id/2864838.

33. S.4288. *Reducing Animal Testing Act*. 117th Congress (2021-2022) 2022 2022, May 19; Available from: https://www.congress.gov/bill/117th-congress/senate-bill/4288.

34. S.1378. *Animal Freedom from Testing, Experiments, and Research Act of 2021*. 117th Congress (2021-2022) 2021 2021, April 27; Available from: https://www.congress.gov/bill/117th-congress/senate-bill/1378/all-info.

CHAPTER 3

THE ROLE OF MACROPHAGES IN THE IMMUNE RESPONSE TO PERITONEAL INFECTION WITH *DIROFILARIA IMMITIS* LARVAE IN THE MONGOLIAN GERBIL (*MERIONES UNGUICULATUS*)

Campbell, E.J. To be submitted to a peer-reviewed journal (Frontiers in Cellular and Infection Microbiology)

Abstract

There is a lack of knowledge in canine heartworm research regarding the mechanisms of the host that determine the ultimate establishment of the parasite. In a previous study, we found that there is a cellular immune response by the Mongolian jird (*Meriones unguiculatus*) host to *Dirofilaria immitis* third-stage larvae (L3) that prevents establishment in the jird. The objective of this study was to determine the role of macrophages in the immune response to peritoneal infection with *D. immitis* larvae in the Mongolian jird. We hypothesized that the absence of jird macrophages in the peritoneal cavity would allow L3 to remain in the peritoneal cavity instead of evading the immune response by migrating into tissues. In this study, jirds (n = 6) were administered clodronate liposomes (100 µl/10 g body weight) by intraperitoneal injection for the depletion of peritoneal macrophages prior to intraperitoneal inoculation with 100 *D. immitis* L3. Another group of jirds (n = 6) were administered phosphate-buffered saline liposomes (100 µl/10 g body weight) by intraperitoneal injection to serve as a control vehicle prior to *D. immitis* infection. Necropsies were performed 1 day post infection (dpi), and L3 were recovered and quantified by peritoneal lavage. Flow cytometry was performed on peritoneal exudative cells (PECs), recovered from the peritoneal lavage fluid, to confirm the absence (or presence in the control group) of macrophages. Significantly ($p < 0.03$) more *D. immitis* L3 (mean = 17.7%; SEM = 6.0%) were recovered from peritoneal macrophage-depleted jirds than from the control group (mean = 3.8%; SEM = 1.9%) at 1 dpi. The significant recovery of L3 from peritoneal macrophage-depleted jirds and lack of recovered L3 from control jirds suggests that macrophages play a key role in the cellular immune response of jirds to determine the establishment of *D. immitis* in this model.

Introduction

In addition to domestic dogs, *Dirofilaria immitis* can establish in wild canids, cats, ferrets, marine mammals, and even infect humans [1]. Current *in vivo D. immitis* research relies on an established infection in a permissive host, and the best animal models for these studies are dogs and ferrets due to the ability of the parasite to become patent in the hosts. The limited availability of *D. immitis* in research settings results in mostly *in vitro* study of the parasite. There is a lack of knowledge in dirofilarial research regarding the host-parasite interaction and the mechanisms of the host that determine the ultimate establishment of the parasite due to the challenges of studying the parasite *in situ* [2].

Host specificity refers to the different host species a parasite can infect and is largely dependent on structural, phylogenetic, and geographic specificity [3, 4]. Although host susceptibility factors, such as microbiome, inoculum, sex, temperature, environment, age, chance, history, immunity, nutrition, and genetics [5], can affect the establishment of a parasite, host susceptibility and specificity are distinct from one another, because the former pertains to an individual host and the latter includes the species. One factor of host specificity is the relative ecological importance [4] of both the *D. immitis* mosquito intermediate host and the canine definitive host, known as structural specificity.

Dirofilaria immitis is generally found in the warmer regions of North and South America, Europe, Asia, and Australia, where transmission of the parasite by the mosquito can occur for most of the year [6]. Phylogenetic specificity, another factor of host specificity, is the evolutionary commonality of the different host species [4]. Hosts susceptible to patent *D. immitis* infection, such as dogs, wild canids, ferrets, and seals, belong to the suborder Caniformia within

the order Carnivora [7, 8]. A third factor of host specificity is geography, where the parasite, intermediate host, and definitive host are able to interact [4].

The Companion Animal Parasite Council 2023 heartworm prevalence map calculates that roughly 1 in every 100 dogs were reported as positive for *D. immitis* in the United States of America [9]. Canine heartworm disease is found in every region of the country but is most prevalent in the southeastern states, where there were positive reports in every 1 in 50 dogs. Elimination attempts of vector-transmitted helminthic diseases have proven unsuccessful to date [10]. Elimination of vector-transmitted parasites like *D. immitis* faces several challenges due to the parasites' various life stages. Complete elimination of mosquitoes, the vector, is impractical and could have unpredictable environmental consequences. Additionally, wildlife reservoir hosts contribute to ongoing disease transmission, further complicating elimination efforts. Furthermore, it is not possible at this time to locate and intervene in the larval development of all parasite-transmitting mosquitoes.

There is a loss of efficacy concern with ML-resistant *D. immitis* cases increasing in the United States, and since most of the MLs require some aspect of host immunity to succeed at killing the L3 and L4, there is a need for a new class of drugs that is effective in killing *D. immitis* [11]. Since most of the MLs require some aspect of host immunity to interfere with the development of third- and fourth- stage *D. immitis* larvae (L3 and L4, respectively), an investigation into the initial days of infection during the L3 and L4 developmental stages will offer more insight into the host-parasite interaction.

As discussed in Chapter 2, the Mongolian gerbil, *Meriones unguiculatus* (jird), is nonpermissive to the establishment of *D. immitis*, which can be explained from the perspective of host phylogenetic and geographic specificity. The jird shares the taxonomic class Mammalia

with the domestic dog, but is under a different order, Rodentia. Mongolian jirds are also native to semi-arid and desert geographical areas including Mongolia, northeastern China, and central Asia [12, 13]. The phylogenic distance between the jird and the domestic dog, and the lack of jird interaction with the mosquito vector, suggests reasons for the failure of *D. immitis* establishment in the jird. Although the jird is not susceptible to *D. immitis* establishment, investigating the jird immune response to the initial infection of *D. immitis* can provide better insight into the cross talk between the parasite and the host, specifically the mechanism of the host cellular response that prevents the establishment of the parasite.

A versatile cell type that plays an essential role in host immunity is the macrophage. Helminth infections trigger type 2 immune responses that prompt the macrophage to undergo alternative activation [14, 15]. Macrophages are known to be directly involved in the elimination of filariae, such as *Litomosoides sigmodontis*, *Acanthocheilonema viteae*, *Brugia malayi*, and *Brugia pahangi* [16, 17]. As discussed in Chapter 2, *D. immitis* L3 were found in the peritoneal wall and diaphragm of jirds 1 dpi, surrounded primarily by macrophages.

The objective of this study was to determine the role of macrophages in the immune response to peritoneal infection of *D. immitis* larvae in the Mongolian jird. We hypothesized that the absence of jird macrophages in the peritoneal cavity would allow L3 to remain in the peritoneal cavity instead of evading the immune response by migrating into tissues. This study was the first to use flow cytometry with jird peritoneal exudate cells and the first to deplete jird peritoneal macrophages.

Materials and Methods

Animals

All experiments with adult male jirds *(Meriones unguiculatus;* Charles River Laboratories, Kingston, New York) and purpose-bred dogs were performed in accordance with the University of Georgia Institutional Animal Care and Use Committee guidelines and approved Animal Use Protocol A2022 04-006.

Immunocytochemistry macrophage marker validation for flow cytometry application

Naïve jirds were humanely euthanized by carbon dioxide asphyxiation followed by cervical dislocation, and peritoneal exudate cells (PECs) were collected by peritoneal lavage via a 5-mm abdominal incision with approximately 32 mL Dulbecco's PBS-modified medium, without $CaCl_2$ and $MgCl_2$, and sterile-filtered for cell culture (DPBS; Sigma-Aldrich, St. Louis, MO). Cells were counted with a TC20 cell counter (Bio-Rad Laboratories, Hercules, CA), and approximately 1 x 10^6 PECs were transferred to 12 x 75-mm test tubes in 1 mL DPBS. Cells were split into several control groups: heat-shocked cells (65°C for 5 minutes) and viable cells (on ice) for viability control, respectively, cells with primary antibody, cells with secondary antibody, cells alone, and cells with viability stain, and primary and secondary antibodies. LIVE/DEAD™ Fixable Violet Dead Cell Stain, for 405 nm excitation (Invitrogen, Waltham, MA), was dissolved per manufacturer instructions, and 1 µL was added to the appropriate samples, followed by incubation at room temperature, protected from light, for 30 minutes. Two mL of 1.0% (w/v) bovine serum albumin (BSA; Sigma-Aldrich, St. Louis, MO) in HBSS with no phenol red (Thermo Fisher Scientific, Waltham, MA) was added to the cells and centrifuged at 350 x *g* for 5 minutes at 4°C. Cells were fixed with 1 mL 4% methanol-free formaldehyde

(Cell Signaling Technology, Danvers, MA) at 4°C for 1 hour. After centrifuging the cell suspension at 350 x *g* for 5 minutes at 4°C, the supernatant was removed by rapid decantation, and 1 mL 0.1% (w/v) saponin (Thermo Fisher Scientific, Waltham, MA) was added to the cell pellet to permeabilize for 15 minutes at room temperature. One mL of DPBS with saponin was added to the cells and spun at 4°C 350 x *g* for 5 minutes, followed by rapid decantation of the supernatant and the addition of the blocking step with heat-inactivated normal mouse serum (50 µL; Sigma-Aldrich, St. Louis, MO) for 1 minute to reduce nonspecific binding of the antibodies to follow. Another 1 mL of DPBS with saponin was added to the cells and centrifuged at 4°C 350 x *g* for 5 minutes, followed by rapid decantation of the supernatant. One hundred µL of the primary antibody [1 µg/mL rabbit anti-ionized calcium binding adaptor molecule 1 antibody (Iba1); Fujifilm Wako Pure Chemical Corporation, Osaka, JP] [18, 19] was added to the cell pellet and incubated for 30 minutes at room temperature, protected from light. Washing buffer (1 mL of 0.1% (w/v) Saponin + 0.5% (w/v) BSA) was added prior to centrifugation at 4°C 350 x *g* for 5 minutes and rapid decantation of the supernatant; the wash step was performed a total of three times. One hundred µL of the secondary antibody (4 µg/mL Alexa Fluor™ 647-conjugated chicken anti-rabbit antibody; Invitrogen, Waltham MA) [19] was added to the cell pellet and incubated for 30 minutes at room temperature, protected from light. A wash step was performed for a total of three times as described with the primary antibody. The cells were resuspended at a concentration of 1 x 10^6 cells in 1 mL DPBS (without saponin). Flow cytometry was performed immediately after preparation of the cells using a NovoCyte Quanteon Flow Cytometer (Agilent Technologies Inc., USA).

F4/80 macrophage marker validation for flow cytometry

Peritoneal exudate cells were collected from naïve jirds, counted and incubated with viability stain as previously described. The PECs were incubated with a blocking buffer of 2% BSA in HBSS (100 µL). The cells were washed with 1 mL DPBS and centrifuged 350 x *g at* 4°C for 5 minutes, followed by rapid decantation of the supernatant. Next, the cells were incubated with 5 µL of 0.2 mg/mL Alexa Fluor™ 647-conjugated anti-F4/80 monoclonal antibody (Invitrogen, Waltham, MA) [20] for 20 minutes on ice, protected from light. Two mL of staining buffer [0.1 (w/v) sodium azide and 1% (w/v) BSA in HBSS] was added to the cells for centrifugation at 350 x *g* 4°C for 5 minutes, followed by rapid decantation of the supernatant; this wash step was repeated once more. The cells were resuspended at a concentration of 1 x 10^6 cells in 1 mL DPBS, and flow cytometry was performed immediately after preparation of the cells using a NovoCyte Quanteon Flow Cytometer (Agilent Technologies Inc., USA).

Clodronate and PBS liposome validation

A validation study was performed with 8 jirds to establish a dose and administration regimen of the CL (100 µL/10 g BW) and PBS (100 µL/10 g BW) liposomes. Jirds (n = 3 CL, n = 1 PBS) were administered either one or two doses that were three days apart via intraperitoneal injection to insure the depletion of peritoneal macrophages [21]. Jirds were humanely euthanized by carbon dioxide asphyxiation followed by cervical dislocation 24 hours after the first or second administration of liposomes, respectively. PECs were prepared with viability stain and F4/80 as previously described. Imaging flow cytometry was performed with a Cytek® Amnis® ImageStream®X Mk II Imaging Flow Cytometer (Luminex Corporation, Seattle, Washington) [20] to assess the effect of the administered liposome dose(s) on peritoneal macrophages.

Parasites

D. immitis L3 were collected [22] from laboratory-raised *Aedes aegypti* black-eyed Liverpool mosquitoes [23] 15 days after feeding [24] on a microfilaremic dog (University of Georgia, Athens, GA) blood. Third-stage larvae were isolated into groups of 100 in Hanks' balanced salt solution (HBSS; MP Biomedicals, Santa Ana, California) supplemented with 2% ciprofloxacin (Sigma-Aldrich, St. Louis, MO).

Peritoneal macrophage depletion and infection with D. immitis

Adult male jirds were separated into one of two groups: macrophage-depleted (n = 6) and control (n = 6). Jirds were administered CL (100 µL/10 g BW) or PBS (100 µL/10 g BW) liposomes via intraperitoneal injection for the depletion of macrophages and control, respectively. The initial administration of liposomes occurred 4- and 1-day(s) prior to infection with *D. immitis*. Jirds were then infected with 100 *D. immitis* L3 by intraperitoneal injection 24 hours after the second administration of liposomes (Figure 3.1).

Figure 3.1
Experimental design

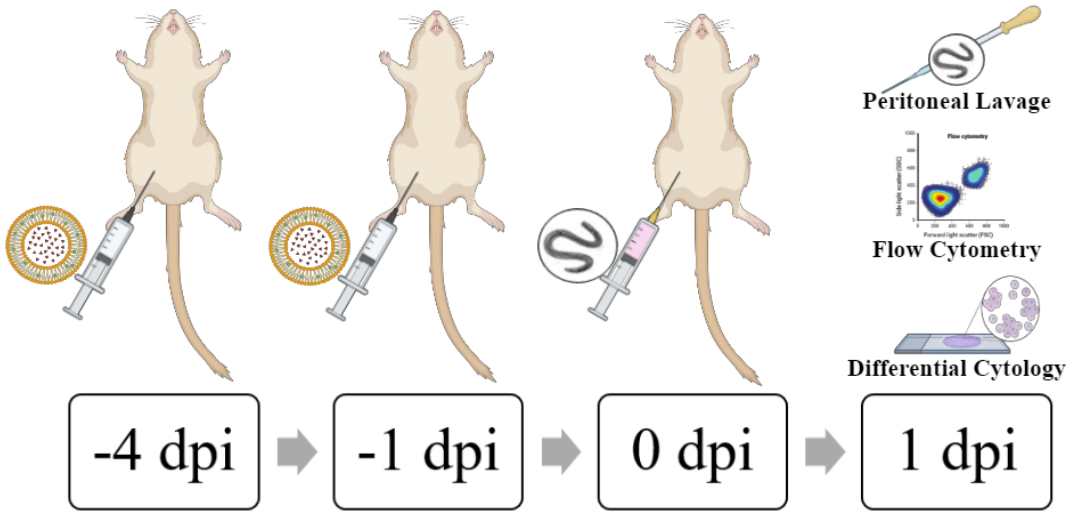

Note: Jirds were administered CL (100 µL/10 g BW; n = 6) or PBS (100 µL/10 g BW; n = 6) liposomes via intraperitoneal injection for the depletion of macrophages and control, respectively, 4- and 1-day(s) prior to infection with 100 *D. immitis* L3. Larvae and PECs were recovered by peritoneal lavage 1 dpi. The larvae were observed for cell attachment and quantified. The PECs were used to determine the depletion of macrophages via flow cytometry and differential cytology. Made with BioRender.

Recovery of L3 and peritoneal exudate cells

Jirds were humanely euthanized by carbon dioxide asphyxiation followed by cervical dislocation at 1 dpi. PECs and L3 were collected by peritoneal lavage via a 5-mm abdominal incision with approximately 32 mL of DPBS (Sigma-Aldrich, St. Louis, MO). Recovered larvae were quantified and removed from the cell suspension with all remarkable observations documented, including cell attachment to larvae and degenerated larvae. The cell suspension without L3 was used for differential cytology and flow cytometry.

Differential cytology

A cyto-centrifuge cell smear was performed using 0.5 mL of cell suspension from each jird in a Thermo Scientific™ EZ Cytofunnel™ and centrifuged at 1,000 rpm for 5 minutes in a Thermo Scientific™ Cytospin 4 Centrifuge (Thermo Fisher Scientific, Waltham, MA) [25]. All cell smears were air-dried and stained with Wright's stain by the University of Georgia Veterinary Diagnostic Clinical Pathology and Cytology Laboratory (Athens, GA). Light microscopic evaluation (Olympus BX41; Olympus America Inc., Center Valley, PA) was performed on the smears, and a total of 200 cells consisting of identified macrophages, neutrophils, lymphocytes, large mononuclear cells, and mast cells (Figure 3.2) were quantified. Images were captured using Olympus CellSens software, version 1.16 (Olympus America Inc., Center Valley, PA).

Figure 3.2
Jird peritoneal exudate cells at 1 dpi

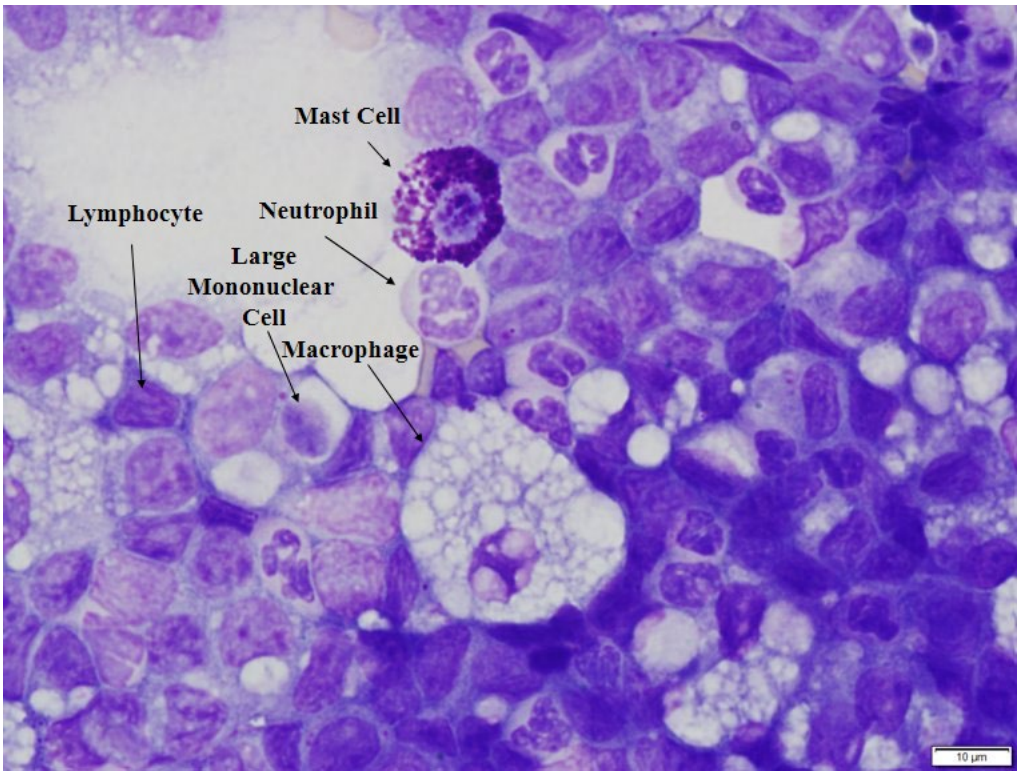

Note: Lymphocytes, large mononuclear cells, macrophages, neutrophils, and mast cells were identified and quantified for the differential cytology analysis.

Flow cytometry

Cells from an individual jird were equally distributed to four, 12 x 75-mm test tubes in 1 mL of DPBS for a negative control of only cells, cells with viability stain, cells with antibody, and cells with both viability and antibody, respectively. PECs were prepared with viability stain and anti-F4/80 antibody as previously described, and flow cytometry was performed immediately after preparation of the cells with a NovoCyte Quanteon Flow Cytometer (Agilent Technologies Inc., USA).

Data Analysis

Larval recovery data were normally distributed, and a one-tailed, unpaired *t* test with Welch's correction was performed for comparison of L3 recovery in macrophage-depleted and control jirds. Differential cytology data were normally distributed, and a two-way analysis of variance (ANOVA) was performed for each comparison of cell-type prevalence per group, applying Bonferroni correction. Flow cytometry analysis was performed with FlowJo software (Version 10.2. Ashland, OR: Becton, Dickinson and Company; 2019). The flow cytometry data were normally distributed, and a one-tailed, unpaired *t* test with Welch's correction was performed for comparison of macrophage prevalence in macrophage-depleted and control jirds. Statistical analyses were performed using GraphPad Prism version 10 (GraphPad Software, San Diego, CA).

Results

Cross-reactive macrophage marker

The rat anti-mouse Alexa Fluor™ 647-conjugated, anti-F4/80 monoclonal antibody used in this study was observed to be cross-reactive with jird PECs as was the LIVE/DEAD™ Fixable Violet Dead Cell Stain, as shown in Figure 3.3.

Figure 3.3

Gating strategy for the validation of cell viability stain and macrophage marker

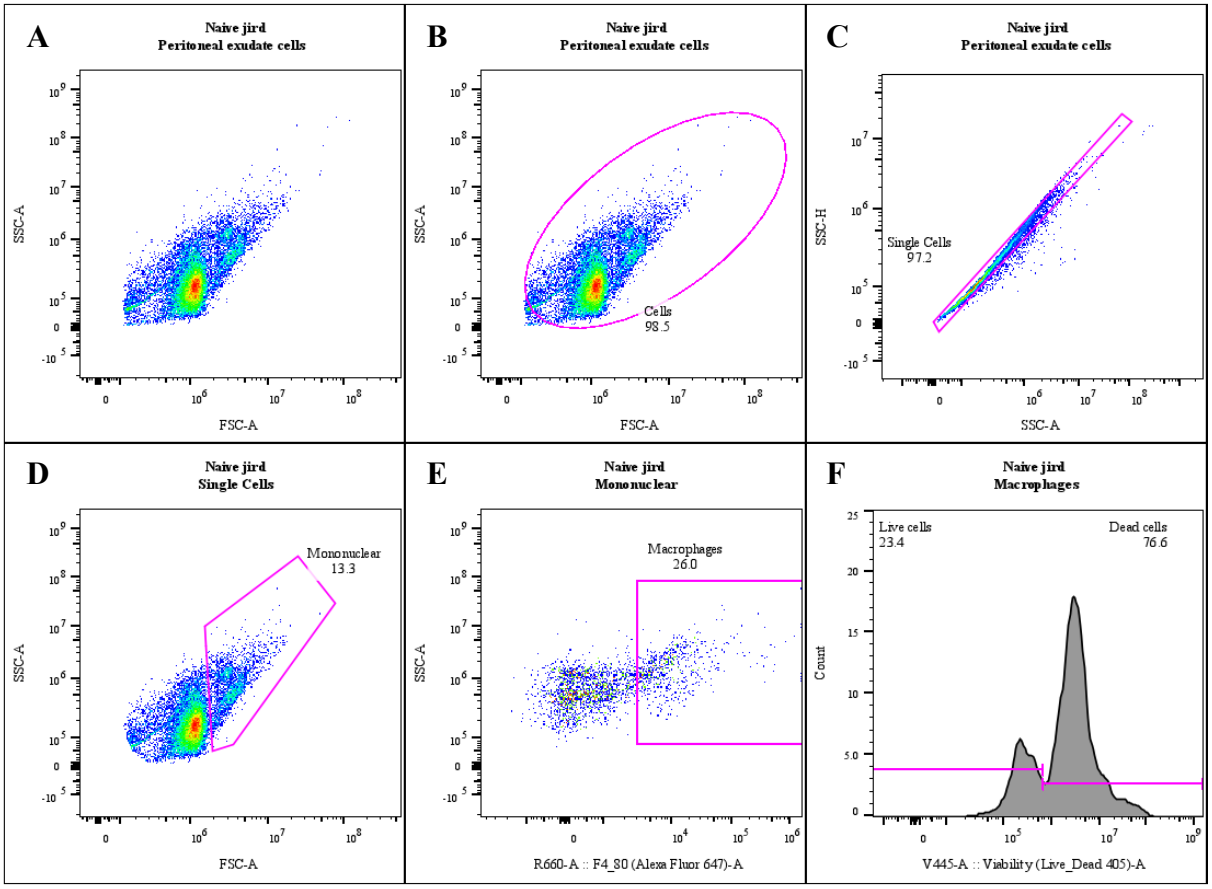

Note: A) PECs are displayed as a dot plot. B) A gate for cells was created to exclude debris. C) A gate for single cells was created to exclude doublets. D) A gate for mononuclear cells was created from single cells. E) A gate for macrophages was created within the mononuclear cell population according to the F4/80 fluorescent emission. F) A histogram displayed live and dead cells, gated according to the fluorescent emission of the viability stain.

Clodronate and PBS liposome validation

Imaging flow cytometry and standard flow cytometry validated the dose and administration regimen of the CL (100 µL/10 g BW) and PBS (100 µL/10 g BW) liposomes. Jirds (n = 3 CL, n = 1 PBS) were administered with either one or two doses that were given three days apart via intraperitoneal injection, and the depletion of peritoneal macrophages was successful as shown in Figures 3.4 and 3.5.

Figure 3.4

Imaging flow cytometry confirmed F4/80 cross-reactivity with jird macrophages

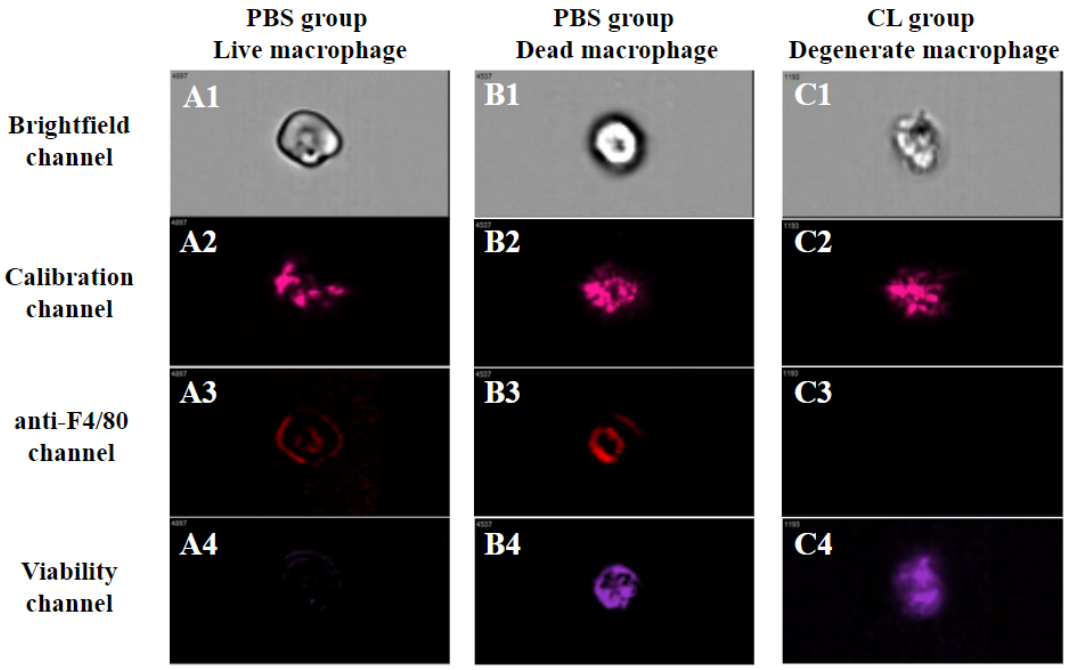

Note: Column A is a live (A4) $F480^{+}$ (A3) macrophage from a jird administered PBS liposomes that displays a clear cell wall. Column B is a dead (B4) $F4/80^{+}$ (B3) macrophage from a jird administered PBS liposomes that displays early degradation of the cell wall. Column C is a dead (C4) $F4/80^{-}$ (C3) macrophage from a jird administered CL liposomes that displays signs of cell death (C1). Row 1 displays images of the cell (white) in the brightfield channel to assess the cell and exclude doubles and debris from analysis. Row 2 is calibration channel, where speed beads (pink) help internal calibration of the camera and flow rate. Row 3 displays $F480^{+}$ macrophages (red) and row 4 displays dead cells (purple).

Figure 3.5

Gating strategy for the validation of macrophage depletion

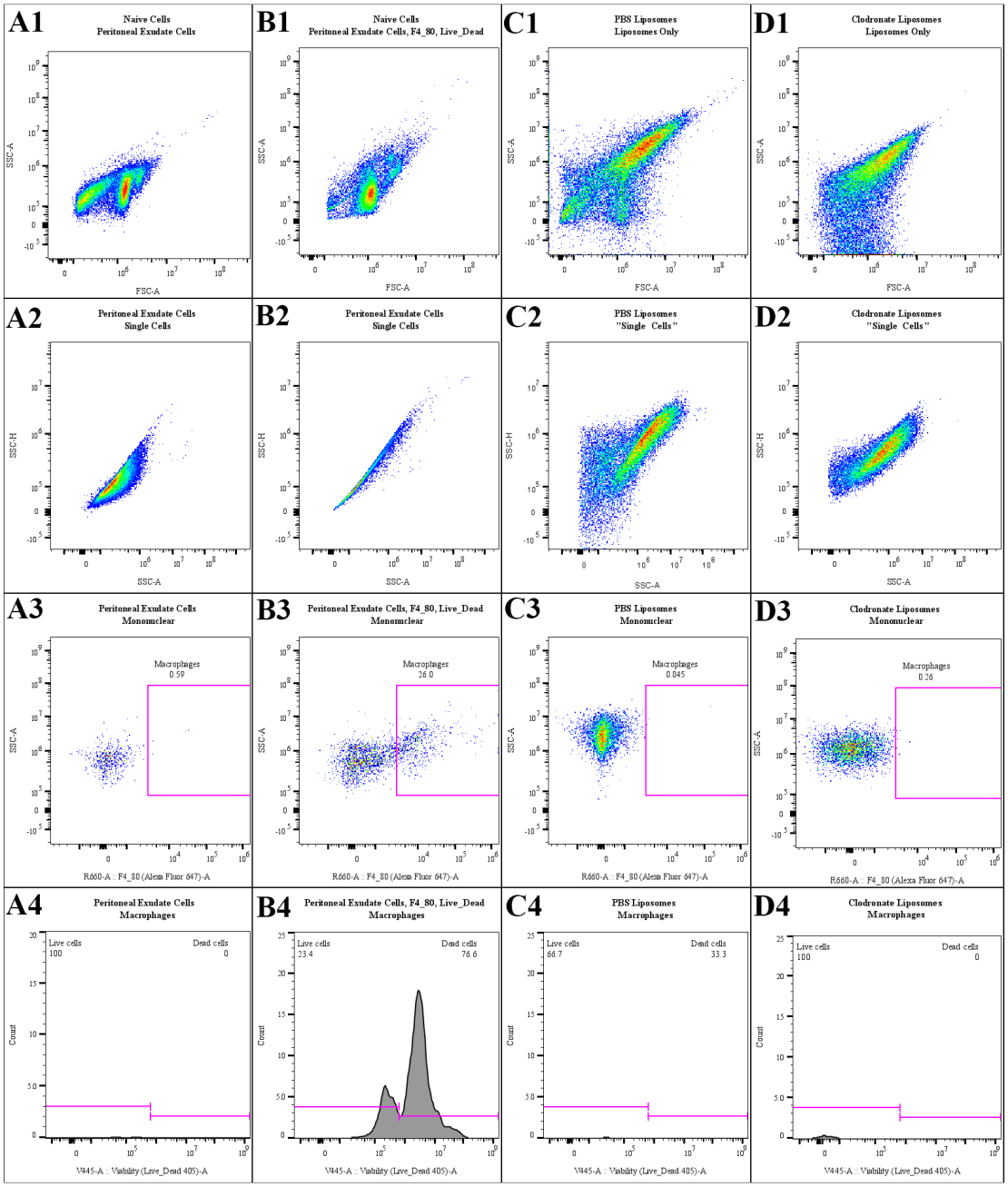

Note: Row 1) PECs were displayed as a dot plot, and debris was excluded. Row 2) A gate for single cells was created to exclude doublets. Row 3) A gate for macrophages was created within the mononuclear cell population according to the F4/80 fluorescent emission. Row 4) A histogram displayed live and dead cells, gated according to the fluorescent emission of the viability stain. Column A) Naïve PECs without F4/80 or viability stain. Column B) Naïve PECs with F4/80 and viability stain. Column C) PBS liposomes. Column D) CL liposomes.

Larval recovery

Significantly ($p < 0.03$) more *D. immitis* L3 (mean = 17.7%; SEM = 6.0%) were recovered from peritoneal macrophage-depleted jirds than from the control group (mean = 3.8%; SEM = 1.9%) at 1 dpi as shown in Figure 3.6 A. Cell attachment was observed in 2 of the 6 control jirds (Figure 3.7) and 1 of the 6 macrophage-depleted jirds (Figure 3.8).

Figure 3.6
Macrophage presence in all jirds (n = 6/group) infected with D. immitis

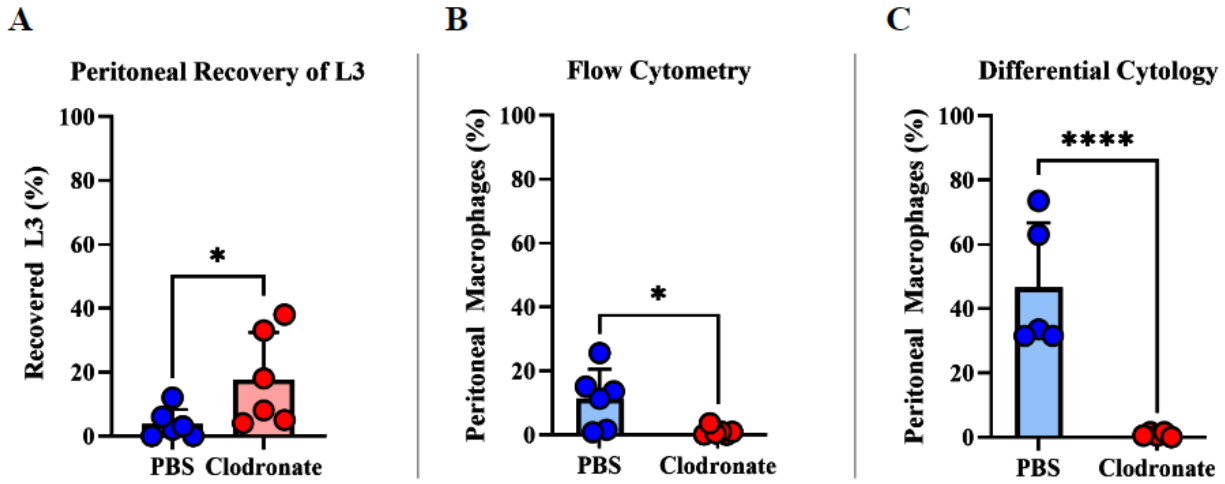

Note: A) Significantly ($p < 0.03$) more *D. immitis* L3 were recovered from peritoneal macrophage-depleted jirds than from the control group 1 dpi. B) Flow cytometry analysis determined there were significantly fewer ($p < 0.02$) peritoneal macrophages in jirds administered CL than from jirds administered control PBS liposomes 1 dpi with *D. immitis*. C) Differential cytology analysis determined there were significantly fewer ($p < 0.0001$) macrophages in jirds administered CL liposomes than from jirds administered PBS liposomes 1 dpi with *D. immitis*.

Figure 3.7
Cell attachment to D. immitis L3 in a control jird

Note: PECs encapsulate 1 *D. immitis* L3 (top) and 2 L3 are encapsulated together (bottom) in a control jird after recovery from the peritoneal cavity.

Figure 3.8
Cell attachment to D. immitis L3 in a macrophage-depleted jird

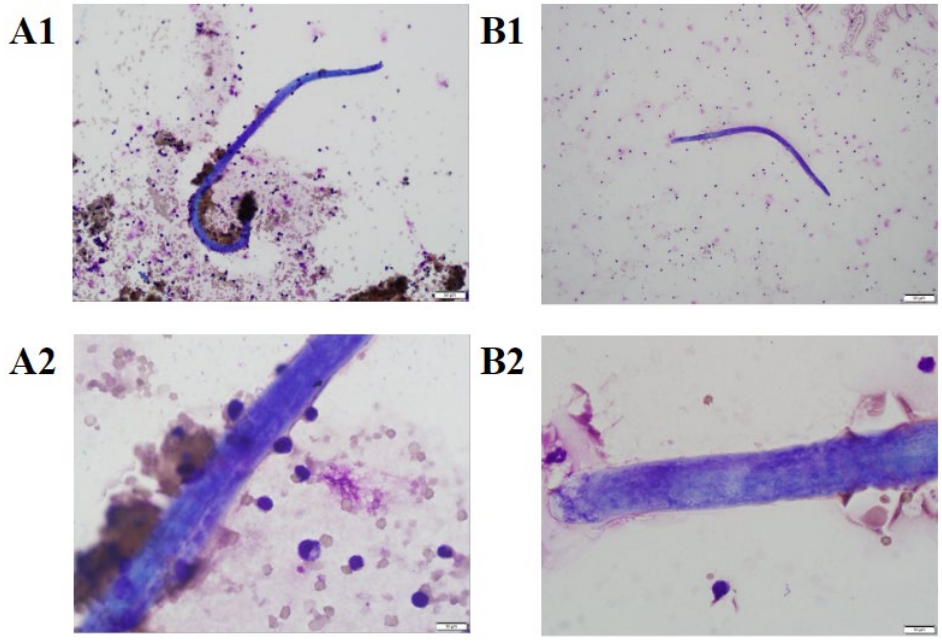

Note: *D. immitis* L3 (n = 2) were observed in a Wright's-stained, cytocentrifuged smear of a macrophage-depleted jird. A1) PECs attached to a *D. immitis* L3. A2) The PECs attached to the L3 in A1 are not activated macrophages due to their small size. B1) No PEC attachment to *D. immitis* L3. B2) The PECs near the L3 are not macrophages.

Flow cytometry

There were significantly fewer ($p < 0.02$) peritoneal macrophages in jirds administered CL liposomes (mean = 1.1% of all PECs; SEM = 0.5%) than from jirds administered control PBS liposomes (mean = 11.4% of all PECs; SEM = 3.8%) 1 dpi with *D. immitis* (Figure 3.6 B). A visual representation of the differences in CL and control groups are as shown in Figures 3.9 and 3.10.

Figure 3.9

Macrophage presence in jirds infected with D. immitis

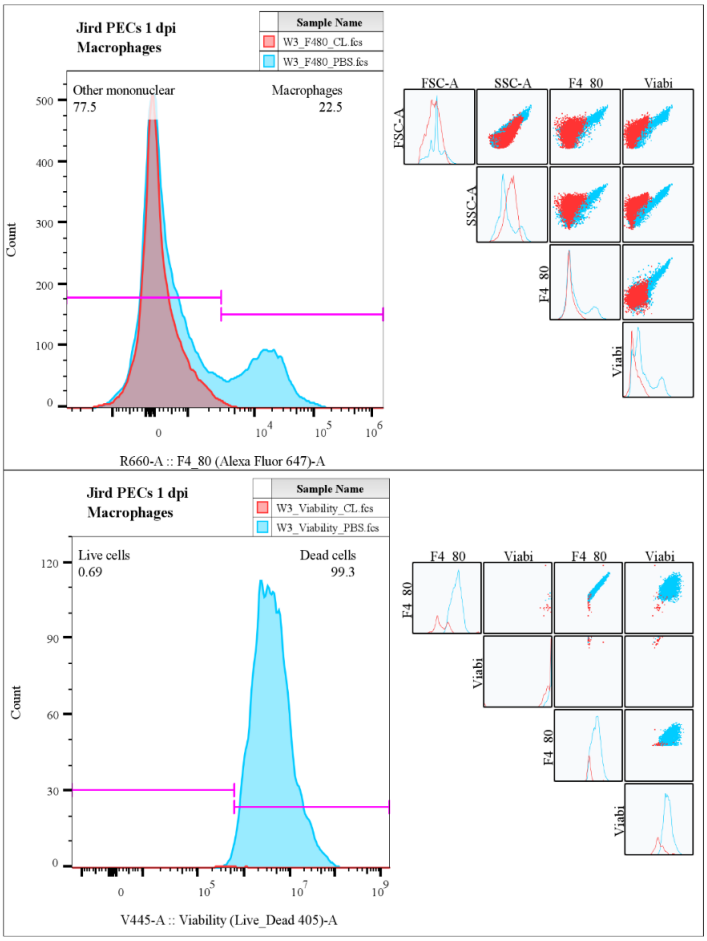

Note: Top) A histogram for macrophages was created within the mononuclear cell population according to the F4/80 fluorescent emission. There were no macrophages detected in this particular sample that received CL liposomes (red). There were a few macrophages in the sample that received PBS liposomes (blue). Bottom) A histogram displayed live and dead macrophages, gated according to the fluorescent emission of the viability stain. There were very low numbers of macrophages in the CL PEC sample compared with the control sample.

Figure 3.10

Macrophage presence in all jirds (n = 6/group) infected with D. immitis

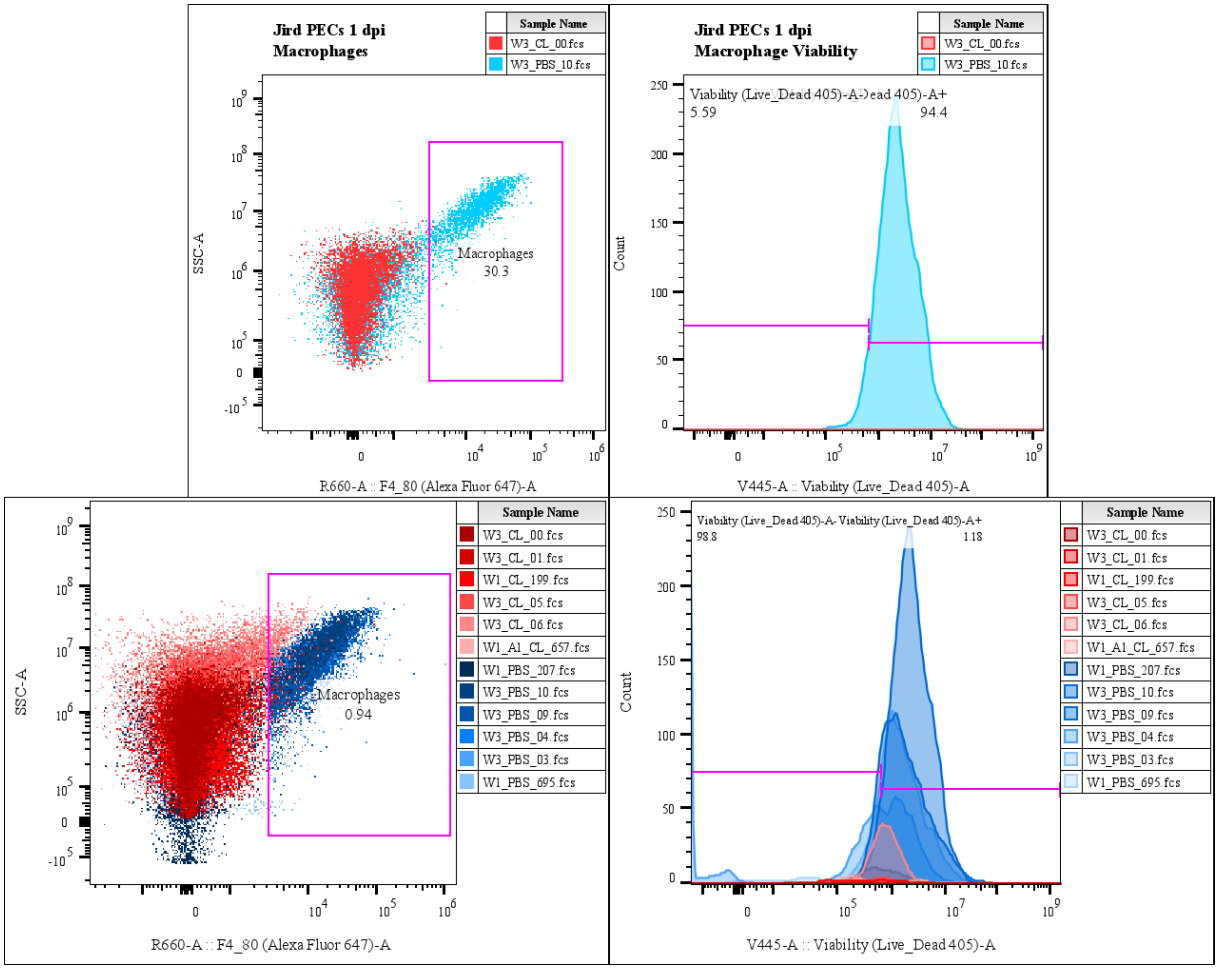

Note: Top left) A dot plot for macrophages was created within the mononuclear cell population according to the F4/80 fluorescent emission. Macrophages detected in this particular sample that received CL liposomes (red) were below detectable limits. Top right) A histogram displayed live and dead macrophages, gated according to the fluorescent emission of the viability stain. There were very low numbers of macrophages in the CL PEC sample compared with the control sample. Bottom left) A dot plot for macrophages across all samples (red: CL group, blue: PBS group). Bottom right) A histogram for the viability of macrophages across all samples (red: CL group, blue: PBS group).

Differential cytology

There were significantly fewer ($p < 0.0001$) macrophages in jirds administered CL liposomes (mean = 0.8% of all PECs; SEM = 0.3%) than from jirds administered PBS liposomes (mean = 46.6% of all PECs; SEM = 9.0%) at 1 dpi with *D. immitis* (Figure 3.6 C). There was no significant difference in large mononuclear cells between jirds administered CL liposomes (mean = 23.5% of all PECs; SEM = 4.9%) or control PBS liposomes (mean = 26.9% of all PECs; SEM = 7.8%) at 1 dpi with *D. immitis*. There were significantly more ($p < 0.0001$) neutrophils in jirds administered CL liposomes (mean = 64.5% of all PECs; SEM = 6.1%) than in jirds administered PBS liposomes (mean = 19.6% of all PECs; SEM = 4.6%) at 1 dpi with *D. immitis*. There was no significant difference in lymphocytes in jirds administered CL liposomes (mean = 11.0% of all PECs; SEM = 4.0%) and PBS liposomes (mean = 6.7% of all PECs; SEM = 3.5%) at 1 dpi with *D. immitis*. Mast cell numbers observed in jirds administered CL liposomes and PBS liposomes were the same (mean = 0.2% of all PECs; CL SEM = 0.1%; PBS SEM = 0.2%) at 1 dpi with *D. immitis*. A visual representation of the differences in CL and control groups are shown in Figures 3.11 and 3.12.

Figure 3.11

Percentage of different peritoneal exudate cell types observed by differential cytology

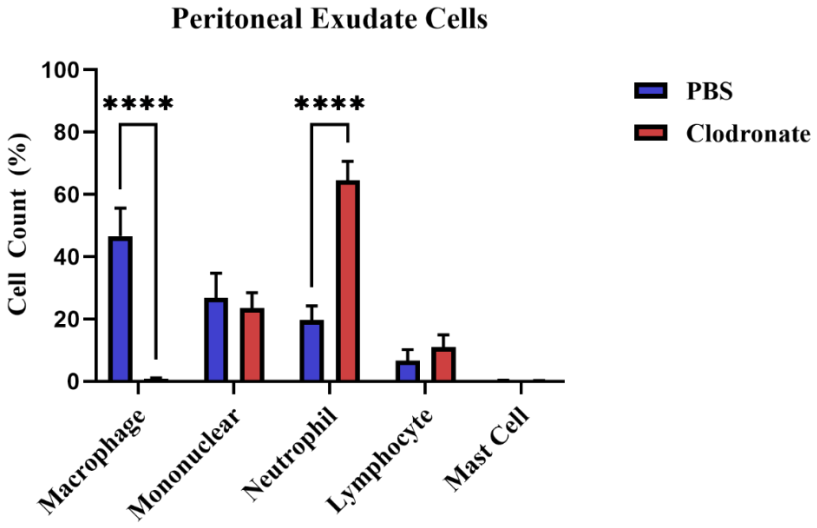

Note: There were significantly ($p < 0.0001$) fewer macrophages recovered from jirds administered CL liposomes than jirds administered PBS liposomes. Alternatively, there was a significant ($p < 0.0001$) increase of neutrophils in macrophage-depleted jirds compared to control jirds. There were no significant differences between the two groups for large mononuclear cells, lymphocytes, and mast cells.

Figure 3.12

The differences in macrophages and neutrophils observed with differential cytology

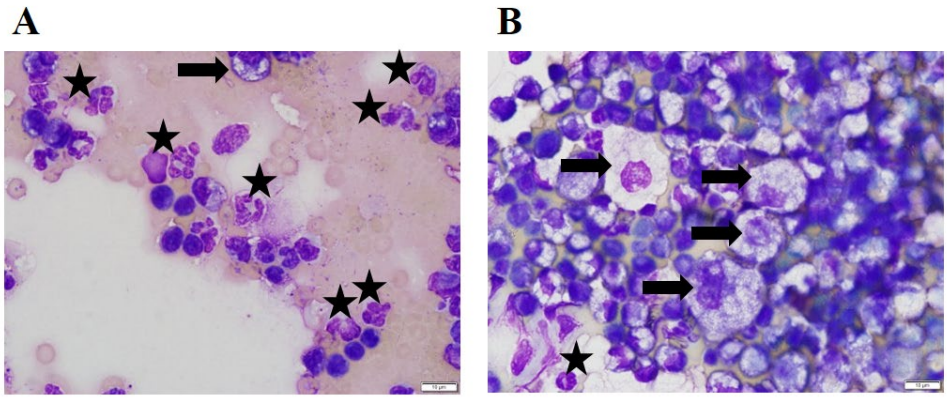

Note: There were significantly ($p < 0.0001$) fewer macrophages recovered from jirds administered CL liposomes (A) than jirds administered PBS liposomes (B). Alternatively, there was a significant ($p < 0.0001$) increase of neutrophils in macrophage-depleted jirds (A) compared to control jirds (B). *Arrow*: macrophage; *Star*: neutrophil

Discussion

The phospholipid bilayers of the control PBS liposomes are composed of phosphatidylcholine and cholesterol, 10 mM disodium hydrogen phosphate, 10 mM sodium dihydrogen phosphate, and 140 mM sodium chloride suspended in sterile PBS. The CL liposomes have the same phospholipid bilayers as the PBS liposomes with an addition of 5 mg/mL CL in the form of $CH_2Na_2Cl_2O_6P_2 \cdot 4\ H_2O$ [26]. The PBS and CL liposomes are negatively charged to serve as an anticoagulant, and the liposomes are variably sized, up to 3 microns in diameter with a median of 1.7 micron [26]. The use of liposomes to encapsulate CL is necessary, because free CL is unable to cross cell membranes, leading to its rapid removal by the kidneys [27, 28]. Once the CL liposomes are ingested by a macrophage, the accumulation of the CL will exceed the intracellular concentration and signal the macrophage to initiate apoptosis [27, 28].

The liposome manufacturer [Liposoma, the Netherlands (clodronateliposomes.com)] provides recommendations for the dose and frequency of administration, but this can be variable across species, age, and size of the animal. There is not an established protocol for CL liposome administration in jirds, so the following protocol recommended by the manufacturer was used: for intraperitoneal administration, the recommended injection dose is 100 µL of suspension/10 grams of animal weight) and can be increased considerably. According to the manufacturer, this route depletes peritoneal macrophages, but will take longer (roughly 3 days) to deplete macrophages in the liver and spleen. Biewenga *et al.* (2010) published a study depleting peritoneal macrophages in Wistar rats [21]. Rats were administered 10 mg/mL CL liposomes at days 0 and 3, respectively, and the authors observed the presence of peritoneal macrophages on days 4-7. Macrophages were 80-90% depleted at 4 days and repopulated by 7 days. The authors concluded that 3-5 days after two administrations of CL, 3 days apart, was ideal for complete

depletion of peritoneal macrophages. There is only one publication with use of CL liposomes in Mongolian gerbils [29]. However, there is a discrepancy in the manuscript regarding the route of CL liposome administration; the majority of the manuscript states that liposomes were administered intravenously at a dose of 4 mL/kg either every 2 days or 3 times a week, but in one section, there is mention of an intraperitoneal liposome administration with no dose or frequency of administration.

Validation of the dose and administration regimen of the CL (100 µL/10 g BW) for the depletion of macrophages, and PBS (100 µL/10 g BW) liposomes as the control, was performed using imaging flow cytometry and standard flow cytometry. To perform flow cytometry, the cell of interest, macrophages, must be tagged with a fluorescent antibody to be identified from other cell types when sorting through a mixed cell population. Antibodies for jird peritoneal exudate cells are not commercially available, hence, the validation for cross-reactivity of an antibody was required. The first cross-reactive macrophage marker validated was the rabbit anti-Iba1 antibody [18], which was used as an immunohistochemistry macrophage marker in Chapter 2 and in Evans, *et al*. (2021). Although the Iba1 was not intended for flow cytometry application, it was validated for flow cytometry by Koh, *et al*. using the secondary conjugated antibody, Alexa Fluor™ 647 chicken anti-rabbit [19]. Initial trials with naïve jird PECs using the intracellular Iba1 macrophage marker were successful, but due to workflow, using a cell surface marker was preferred. The cross-reactive macrophage marker validated for use with jird PECs in this study was rat anti-mouse Alexa Fluor™ 647-conjugated anti-F4/80 monoclonal antibody. F4/80 is a standard murine macrophage marker [30], and the Alexa Fluor 647 conjugate was selected to insure no spectral overlap with the LIVE/DEAD viability fluorescence.

Jird PECs have yet to be characterized at the time of writing this dissertation, and the identification of cells and gating strategies were heavily influenced by the success of F4/80 as a jird peritoneal macrophage marker. Imaging flow cytometry was performed, not only to validate the liposome dose and frequency of administration, but to visualize the fluorescence of macrophages tagged with the Alex Fluor 647 F4/80 antibody to confirm its cross-reactivity with jird macrophages. The success of the F4/80 antibody after the imaging flow cytometry allowed the authors to confidently gate for F4/80^{+} cells by standard flow cytometry, allowing for quantification of the depletion of macrophages from the total PECs recovered from the jird peritoneal cavity.

Macrophages were immunopositive for LIVE/DEAD viability fluorescence, which indicates that the macrophages were dead prior to flow cytology analysis. It is highly probable that due to the workflow of this study, the macrophages died after extraction from the gerbil and prior to fixation while preparing for flow cytometry. Ideally, recovered PECs are kept on ice and immediately stained for viability, followed by fixation. In this study, larvae were recovered from the peritoneal cavity along with the PECs. Although PEC samples were kept on ice to slow down degradation of the cells, separation of the larvae from the PEC samples under a dissecting scope was a time-consuming process that required the PEC samples to be at room temperature for longer than preferred.

Another confirmation of the depletion of macrophages was deemed necessary, because there was no protocol for the depletion of jird peritoneal macrophages or standard flow cytometry on jird PECs prior to this study. A reliable method of quantifying a population of cells is differential cytology. Differential cytology is typically performed with a cell count, cytocentrifugation of cells on a slide, a direct smear slide, and fixing and staining the cells with a

Wright's stain. A cell count was not performed prior to cytocentrifugation in this study, because the CL and PBS liposomes interfered with the cell counter. Previous experiments (unpublished) have calculated 5 x 10^5 – 1 x 10^6 PECs/mL suspension, with the lower range occurring in naïve jirds and the upper range occurring in infected jirds. The differential cytology was performed on the cytocentrifuged slides, because the cells were sparse on the direct smear with the CL-treated PECs. A benefit of differential cytology is the ability to morphologically identify and assess the health of multiple cell types without a cell marker. This method is also quite cost effective. Alternatively, differential cytology is more prone to human error and requires that observation and quantification of cells be performed by the same person to reduce bias.

Significantly ($p < 0.03$) more *D. immitis* L3 (mean = 17.7%) were recovered from peritoneal macrophage-depleted jirds than from the control group (mean = 3.8%) at 1 dpi (Figure 3.6A), supporting the hypothesis that the absence of jird macrophages in the peritoneal cavity would allow L3 to remain in the peritoneal cavity instead of evading the immune response by migrating into tissues. Although there was a significant difference of in L3 recovered from macrophage-depleted and control jirds, this study recovered more *D. immitis* L3 1 dpi (mean = 3.8%; 0%-12%) than the study in Chapter 2 (mean = 0.4%; 0%-1%) as shown in Table 3.1. Each jird's immune response is specific to that individual, so biological variability in the susceptibility to infection with *D. immitis* L3 must be taken into consideration. Each L3 is also a biological variable in its own regard, because one larva may be more fit to survive the initial invasion events than another. Another variable to consider is the effect of liposomes, specifically PBS liposomes on *D. immitis* L3. The CL liposomes are immediately phagocytosed by the macrophages, but the PBS liposomes remain in the peritoneal cavity. PBS liposomes can block phagocytosis for periods of time by saturation of the peritoneal cavity [27, 28] and do not

represent a control experiment with normal, healthy, non-activated macrophages. The benefit of using PBS liposomes in this study is that the *D. immitis* L3 activate macrophages upon infection, so the PBS becomes an appropriate control for the CL liposomes. It is likely that the PBS liposomes administered 4- and 1-day(s) prior to *D. immitis* infection illicit a cellular inflammatory response due to the action of intraperitoneal injection, drawing the attention of the innate cellular immune response, allowing the *D. immitis* to better evade jird immunity compared to jirds without previous administration of liposomes into the peritoneal cavity.

Table 3.1
Percentage of D. immitis L3 recovered from individual jirds

No Liposomes (Chapter 2)	PBS Liposomes (control)	CL Liposomes (macrophage-depleted)
1%	0%	8%
0%	0%	18%
1%	2%	4%
0%	3%	5%
0%	12%	38%
n/a	6%	33%

Notes: The numbers displayed in each cell represent the total number of L3 recovered from the peritoneal cavity of an individual jird. Each number represents an individual jird, and each column represents a different variable introduced to the peritoneal cavity prior to infection with *D. immitis* L3. Five jirds were infected with *D. immitis* in Chapter 2, and 12 (n = 6/group) jirds were infected in this current study.

The cell attachment to L3 observed in 2 of the 6 control jirds (Figure 3.7) aligns with the cell attachment to L3 observed in Chapter 2 and Evans, *et al.* (2021). Although cell attachment was observed in one L3 of one of the macrophage-depleted jirds (Figure 3.8), the cells attached were not activated macrophages due to their morphology. Previous studies, including Chapter 2, observed jird macrophages and neutrophils either attached directly to *D. immitis* L3 or surrounding the L3 while sequestered in the peritoneal wall and diaphragm [18]. Once the L3 penetrate the peritoneal wall, there is an inflammatory response.

Neutrophils are the first cell type to be recruited to the site of infection, aligning with the results observed in macrophage-depleted jirds. Recruitment of non-resident macrophages follow the neutrophils. Neutrophils are the immune system's first line of defense when alerted of infection and inflammation. It is believed that neutrophils are attracted to filarial worms because of the endosymbiotic bacteria, *Wolbachia* [31]. In a study containing *Wolbachia*-deficient and *Wolbachia*-containing *Onchocerca*, neutrophils were only found in nodules with the *Wolbachia*-containing *Onchocerca* and not the *Wolbachia*-deficient worms [32]. Once neutrophils detect the *Wolbachia* lipopeptides from the worms, they form neutrophil extracellular traps (NETs) to trap the larvae until assistance from macrophages can arrive. The NETs and neutrophils alone are enough to kill the larvae [31].

While the neutrophils are forming NETs to trap the larvae in the peritoneal wall tissue of the jird, tissue-specific resident macrophages (residing in all tissues of the host and often characterized by homeostatic proliferation) and recruited macrophages are undergoing molecular changes, known as activation of macrophages [15]. The activation of macrophages refers to the ability of these cells to change their form and physiology in response to environmental stimuli [33, 34]. These innate cells clear apoptotic cell bodies, regulate the host immune response, and can destroy pathogens [15].

There are currently three known types of activated macrophages: classically activated macrophages (CAMs), alternatively activated (AAMs), and regulatory macrophages. CAMs are important to host defense and can propagate inflammatory responses [34]. Macrophages that have been exposed to the cytokines interleukin-4 (IL-4) and/or Il-13 and upregulate expression of mannose receptor CD206 are referred to as AAMs [15, 35]. AAMs are no better at killing microbes than CAMs and have been suggested to be more susceptible to intracellular infections

[36], possibly due to their reduced iNOS production compared to CAMs [15]. They do, however, assist in the process of tissue repair; Il-4 induces arginase activity by converting arginine to ornithine, which is a precursor of collagen and polyamides that are essential for wound healing [15, 37]. Extracellular pathogens, such as helminths, may colonize in host tissues, inducing the release of Il-4 and Il-13, and recruiting eosinophils, neutrophils, basophils, and/or natural killer T cells, which then signal the alternative activation of macrophages [35]. However, IL-4 may not be necessary for inducing AAMs, because helminth-specific antibodies in the presence of helminth antigens have been found to alternatively activate macrophages in the absence of IL-4 [38]. Arginase, expressed by AAMs, attempts to inhibit larval motility whilst the larvae are trapped by the NETs. However, the role of AAMs is primarily to control inflammation and tissue repair, and because their efforts are pulled in that direction, the AAMs in the peritoneal wall are ineffective at destroying the L3 [38].

The next step to understanding the role of macrophages in the establishment *of D. immitis* is to determine the activation of macrophages in the immune response to peritoneal infection of *D. immitis* larvae in the Mongolian jird. An arginase assay can be performed on naive jird PECs treated with alternative activation cytokines, IL-4 and IL-13, and compared with naïve PECs cultured with *D. immitis* L3. The presence of urea, a product of arginase, suggests that naïve jird PECs contain macrophages that are alternatively activated, and that *D. immitis* L3 trigger alternative activation in macrophages. These experiments provide insight into the mechanisms of the jird macrophages in response to the presence of *D. immitis*.

Conclusion

Current *D. immitis* research relies on *in vivo* infection in permissive hosts, with dogs and ferrets being the best animal models. However, limited availability of *D. immitis* in research settings results in mostly *in vitro* study of the parasite, and there is a lack of knowledge about the host-parasite interaction, the mechanisms of the host that determine the establishment of the parasite, and host specificity of *D. immitis*. This study aimed to determine the role of macrophages in the immune response to peritoneal infection of *D. immitis* larvae in the Mongolian jird. The study hypothesized that the absence of jird macrophages in the peritoneal cavity would allow L3 to remain in the peritoneal cavity instead of evading the immune response. This is the first study to use flow cytometry with jird PECs, and the first to deplete jird peritoneal macrophages using clodronate liposomes and confirmation of macrophage depletion with a cross-reactive macrophage marker, F4/80.

More *D. immitis* L3 were recovered from peritoneal macrophage-depleted jirds than from the control group at 1 dpi, supporting the hypothesis that the absence of jird macrophages in the peritoneal cavity would allow L3 to remain in the peritoneal cavity instead of being sequestered in the diaphragm and peritoneal wall. Cell attachment, presumably macrophages, were observed on *D. immitis* L3 in the control group. In the absence of macrophages, there is a significant increase in the presence of neutrophils. Neutrophils are the first cell type to be recruited to the site of infection, followed by non-resident macrophages, so in PECs with macrophage depletion, an increase of neutrophils is to be expected. A future direction to explore the role of macrophages in the establishment of *D. immitis* in Mongolian jirds is to perform an arginase assay to compare naïve jird PECs with naïve PECs cultured with *D. immitis* L3. Understanding the activation of macrophages is the first step to investigating the jird immune response to the

initial infection with *D. immitis*. These efforts may provide better insight into the cross talk between the parasite and the host, specifically the mechanism of the host cellular response that prevents the establishment of *D. immitis*.

Acknowledgments

The authors thank Samantha Hogan for their technical assistance and Dr. Juan Bustamente, Dr. Kristina Meichner, Dr. Christine Henderson, and Jamie Barber for their guidance with flow cytometry. This study was supported in part by the Center for Tropical & Emerging Global Diseases Cytometry Shared Resource Laboratory (CTEG CSRL), which is a unit of the University of Georgia Office of Research. The ImageStream X MK II (Luminex Corporation, Seattle, Washington) utilized in this study was purchased with the NIH grant #1S10OD021719-01A1. The content is solely the responsibility of the authors and does not necessarily reflect the official views of the National Institutes of Health.

Disclosures

The authors have no financial conflict of interest. Funding for this study is from various revenue streams of the Moorhead laboratory at the University of Georgia.

References

1. (CAPC), C.A.P.C. *Heartworm Guidelines*. 2020; Available from: https://capcvet.org/guidelines/heartworm/.

2. Kotani, T. and K.G. Powers, *Developmental stages of Dirofilaria immitis in the dog.* Am J Vet Res, 1982. 43(12): p. 2199-206.

3. Poulin, R., B.R. Krasnov, and D. Mouillot, *Host specificity in phylogenetic and geographic space.* Trends in Parasitology, 2011. 27(8): p. 355-361.

4. Esser, H.J., et al., *Host specificity in a diverse Neotropical tick community: an assessment using quantitative network analysis and host phylogeny.* Parasites & Vectors, 2016. 9(1): p. 372.

5. Casadevall, A. and L.A. Pirofski, *What Is a Host? Attributes of Individual Susceptibility.* Infect Immun, 2018. 86(2).

6. Anvari, D., et al., *The global status of Dirofilaria immitis in dogs: a systematic review and meta-analysis based on published articles.* Research in Veterinary Science, 2020. 131: p. 104-116.

7. Law, C.J., G.J. Slater, and R.S. Mehta, *Lineage Diversity and Size Disparity in Musteloidea: Testing Patterns of Adaptive Radiation Using Molecular and Fossil-Based Methods.* Systematic Biology, 2017. 67(1): p. 127-144.

8. Flynn, J.J., et al., *Molecular Phylogeny of the Carnivora (Mammalia): Assessing the Impact of Increased Sampling on Resolving Enigmatic Relationships.* Systematic Biology, 2005. 54(2): p. 317-337.

9. (CAPC), C.A.P.C. *Canine Heartworm Prevalence Map*. 2023; Available from: https://capcvet.org/maps/#/2023/all-year/heartworm-canine/dog/united-states.

10. Bowman, D.D. and C.E. Atkins, *Heartworm Biology, Treatment, and Control.* Veterinary Clinics of North America: Small Animal Practice, 2009. 39(6): p. 1127-1158.

11. (AHS), A.H.S. *American Heartworm Society Canine Guidelines for the Prevention, Diagnosis, and Management of Heartworm (Dirofilaria immitis) Infection in Dogs*. Macrocyclic Lactones 2024.

12. Field, K.J. and A.L. Sibold, *The laboratory hamster and gerbil*. 1998: CRC Press.

13. Fisher, M.F. and G.C. Llewellyn, *The Mongolian Gerbil: Natural History, Care, and Maintenance.* The American Biology Teacher, 1978. 40(9): p. 557-560.

14. Van Dyken, S.J. and R.M. Locksley, *Interleukin-4- and Interleukin-13-Mediated Alternatively Activated Macrophages: Roles in Homeostasis and Disease.* Annual Review of Immunology, 2013. 31(Volume 31, 2013): p. 317-343.

15. Rolot, M. and B.G. Dewals, *Macrophage Activation and Functions during Helminth Infection: Recent Advances from the Laboratory Mouse.* Journal of Immunology Research, 2018. 2018: p. 2790627.

16. Remion, E., et al., *Unbalanced Arginine pathway and altered maturation of pleural macrophages in Th2-deficient mice during Litomosoides sigmodontis filarial infection.* Frontiers in Immunology, 2022. 13.

17. Allen, J.E. and P. Loke, *Divergent roles for macrophages in lymphatic filariasis.* Parasite Immunol, 2001. 23(7): p. 345-52.

18. Evans, C.C., et al., *A rapid, parasite-dependent cellular response to Dirofilaria immitis in the Mongolian jird (Meriones unguiculatus).* Parasit Vectors, 2021. 14(1): p. 25.

19. Koh, H.S., et al., *The HIF-1/glial TIM-3 axis controls inflammation-associated brain damage under hypoxia.* Nature Communications, 2015. 6(1): p. 6340.

20. Pelletier, M.G.H., et al., *Characterization of neutrophils and macrophages from ex vivo-cultured murine bone marrow for morphologic maturation and functional responses by imaging flow cytometry.* Methods, 2017. 112: p. 124-146.

21. Biewenga, J., et al., *Macrophage depletion in the rat after intraperitoneal administration of liposome-encapsulated clodronate: depletion kinetics and accelerated repopulation of peritoneal and omental macrophages by administration of Freund's adjuvant.* Cell Tissue Res, 1995. 280(1): p. 189-96.

22. (FR3), F.R.R.R.C. *Collecting Infective Larvae of Brugia pahangi, B. malayi, Dirofilaria immitis, and Dirofilaria repens From Infected Mosquitoes*. Available from: http://www.filariasiscenter.org/protocols/Protocols/collecting-infective-larvae-of-brugia-pahangi-b.-malayi-dirofilaria-immitis-and-dirofilaria-repens-from-infected-mosquitoes.

23. (FR3), F.R.R.R.C. *Mosquito Rearing Techniques*. Available from: http://www.filariasiscenter.org/protocols/Protocols/mosquito-rearing-techniques.

24. (FR3), F.R.R.R.C. *Infecting Aedes aegypti with Brugia pahangi, B. malayi, and Dirofilaria immitis*. Available from: http://www.filariasiscenter.org/protocols/Protocols/infecting-aedes-aegypti-with-brugia-pahangi-b.-malayi-and-dirofilaria-immitis.

25. Al-Abbadi, M.A., *Basics of cytology.* Avicenna J Med, 2011. 1(1): p. 18-28.

26. Liposoma. *Product Description*. 2019; Available from: https://clodronateliposomes.com/about-clodronate-liposomes/product-information/.

27. van Rooijen, N., A. Sanders, and T.K. van den Berg, *Apoptosis of macrophages induced by liposome-mediated intracellular delivery of clodronate and propamidine.* J Immunol Methods, 1996. 193(1): p. 93-9.

28. Van Rooijen, N. and A. Sanders, *Liposome mediated depletion of macrophages: mechanism of action, preparation of liposomes and applications.* J Immunol Methods, 1994. 174(1-2): p. 83-93.

29. Yanai, A., et al., *Activation of IkappaB kinase and NF-kappaB is essential for Helicobacter pylori-induced chronic gastritis in Mongolian gerbils.* Infect Immun, 2008. 76(2): p. 781-7.

30. Dos Anjos Cassado, A., *F4/80 as a Major Macrophage Marker: The Case of the Peritoneum and Spleen.* Results Probl Cell Differ, 2017. 62: p. 161-179.

31. Ajendra, J. and J.E. Allen, *Neutrophils: Friend or foe in Filariasis?* Parasite Immunology, 2022. 44(6): p. e12918.

32. Brattig, N.W., D.W. Büttner, and A. Hoerauf, *Neutrophil accumulation around Onchocerca worms and chemotaxis of neutrophils are dependent on Wolbachia endobacteria.* Microbes Infect, 2001. 3(6): p. 439-46.

33. Cohn, Z.A., *Activation of mononuclear phagocytes: fact, fancy, and future.* J Immunol, 1978. 121(3): p. 813-6.

34. Mosser, D.M. and X. Zhang, *Activation of murine macrophages.* Curr Protoc Immunol, 2008. Chapter 14: p. 14.2.1-14.2.8.

35. Gordon, S., *Alternative activation of macrophages.* Nat Rev Immunol, 2003. 3(1): p. 23-35.

36. Hölscher, C., et al., *Impairment of alternative macrophage activation delays cutaneous leishmaniasis in nonhealing BALB/c mice.* J Immunol, 2006. 176(2): p. 1115-21.

37. Hesse, M., et al., *Differential regulation of nitric oxide synthase-2 and arginase-1 by type 1/type 2 cytokines in vivo: granulomatous pathology is shaped by the pattern of L-arginine metabolism.* J Immunol, 2001. 167(11): p. 6533-44.

38. Esser-von Bieren, J., et al., *Antibodies trap tissue migrating helminth larvae and prevent tissue damage by driving IL-4Rα-independent alternative differentiation of macrophages.* PLoS Pathog, 2013. 9(11): p. e1003771.

CHAPTER 4

DIROFILARIA IMMITIS STAGE-SPECIFIC VARIATIONS OF SLO-1 CHANNEL EXPRESSION THROUGH RNA SEQUENCING ANALYSIS

Campbell, E.J. To be submitted to a peer-reviewed journal (PLOS Pathogens).

Abstract

Emodepside, a cyclooctadepsipeptide, is effective against both canine gastrointestinal nematodes and *Dirofilaria immitis* (heartworm). The mode of action of cyclooctadepsipeptides is distinct from other anthelmintic classes, and emodepside is effective against *D. immitis* isolates that are resistant to macrocyclic lactones (MLs). Emodepside and related compounds act by selective opening of the calcium activated, voltage-dependent potassium channel, SLO-1, resulting in inhibition of nematode body muscle contraction. There is evidence that the sex-dependent effects of emodepside on the closely related filarial parasite *Brugia malayi* are due to splice variations in the RCK1 region of the SLO-1 channel. We carried out a transcriptomic study to explore the hypothesis that gene expression of the SLO-1 channel vary across *D. immitis* larval stages. RNA-seq was carried out on *D. immitis* microfilariae and L3 and L4 stages of two ML-susceptible isolates (Missouri and Georgia 2) and one ML-resistant isolate (JYD-34). We present whole-transcriptome comparisons across isolates and stages and an there is an ongoing survey of SLO-1 channel isoforms across the different isolates and larval stages with later efforts devoted to isoform analysis.

Introduction

Dirofilaria immitis, also known as canine heartworm, is most commonly found in the warmer regions of North and South America, Europe, Asia, and Australia, where transmission of the parasite by the mosquito intermediate host to the canine definitive host can occur for most of the year [1]. Canine heartworm disease caused by *D. immitis* was diagnosed in almost 200,000 dogs in the United States in 2023 [2]. Adult *D. immitis* worms can live between 5-7 years in dogs [3] and cause irreparable, clinical and pathological changes to the heart and pulmonary artery,

including inflammation, pulmonary hypertension, disruption of vascular integrity, and fibrosis [4].

Attempts at elimination of vector-transmitted helminth diseases have proven unsuccessful [5]. An obstacle to eradication may be the several life stages of a parasite, such as *D. immitis,* in the vector intermediate host. Currently, all available Federal Drug Administration (FDA)-approved heartworm preventives belong to the drug class macrocyclic lactones (ML), which includes ivermectin (IVM), selamectin, moxidectin (MOX), and milbemycin oxime (MO) [6]. MLs kill most L3 and L4 stages younger than 45 days, resulting in susceptibility of dogs to patent *D. immitis* infection if not treated with MLs at regular intervals [7].

Concern about loss of efficacy (LOE) attributed to ML-resistant *D. immitis* cases is increasing in the United States. The first reports of LOE appeared in 1998 [8] and have greatly increased since, primarily in the highly endemic areas of heartworm in the southern United States [9]. It was widely believed that most LOEs were due to compliance failure, but Bourguinat *et al*. (2011) reported that IVM and MO did not meet expectations regarding microfilaricidal efficacy *in vivo* despite repeated use and high dose rates [10]. Another clinical study reported preventive LOE with IVM (23.8 - 71.3% efficacy; n = 2) and MOX (21.2%; n = 1) [11], and it was confirmed in later studies that resistance is inherited between generations [12].

Nematode glutamate-gated chloride channels (GluCls) are the most important targets of the MLs [9]. MLs cause flaccid muscle paralysis by opening these channels to allow inflow of chloride ion [13]. MLs paralyze somatic muscles and the pharynx in parasitic gastrointestinal nematodes and the free-living model organism, *Caenorhabditis elegans*, preventing nutrient absorption, and resulting in the removal of the nematodes from the host by peristalsis. However,

MLs affect filarial nematodes by blocking secretion of immunomodulatory molecules; inhibition of pharyngeal pumping has less effect due to the ability of these parasites to absorb nutrients through the cuticle [9].

Emodepside, a cyclooctadepsipeptide, is effective against both gastrointestinal and filarial nematodes. The mode of action of cyclooctadepsipeptides is distinct from other anthelmintic classes [14], and emodepside is effective against *D. immitis* isolates that are resistant to MLs [15]. Emodepside selectively opens the calcium activated, voltage-dependent, potassium channel, SLO-1, and inhibits nematode body muscle contraction [15, 16].

There is evidence that the sex-dependent potency of emodepside on the closely related filarial parasite *Brugia malayi* is due to splice variations in the RCK1 region of the SLO-1 channel [17]. We carried out a transcriptomic study to explore the hypothesis that gene expression of the SLO-1 channel vary across *D. immitis* larval stages. RNA sequencing was carried out across *D. immitis* microfilariae, and L3 and L4 stages of the ML-susceptible isolates Missouri (MO) and Georgia 2 (GA), and an ML-resistant isolate, JYD-34 (JYD). We present whole-transcriptome comparisons across isolates and stages and an there is an ongoing survey of SLO-1 channel isoforms across the different isolates and larval stages with later efforts devoted to isoform analysis.

Materials and Methods

Animals

All experiments with adult male jirds *(Meriones unguiculatus;* Charles River Laboratories, Kingston, New York) and purpose-bred dogs were performed in accordance with

the University of Georgia Institutional Animal Care and Use Committee guidelines and approved Animal Use Protocol A2022 04-009.

Microfilariae isolation from whole blood

The MO and GA isolates of microfilaremic dog blood were provided from the University of Georgia (Athens, GA) and JYD was provided from TRS Labs, Inc. (Athens, GA). The MO isolate (origin: MO, USA) in this study has been under laboratory conditions since 2005 and has never been in contact with MLs [18]. The GA isolate (origin: Vidalia, GA, USA) used in this study has been under laboratory conditions since 2013, not exposed to MLs. Lastly, the JYD isolate (origin: Keytesville, MI, USA via Pittsfield, IL, USA) has been under laboratory conditions since 2010 with no known exposure to MLs and confirmed to be resistant to MLs [18-20]. Microfilaremic whole blood was mixed by inversion with 1:11 saponin hemolysis solution of 0.85% sodium chloride (Sigma-Aldrich, St. Louis, MO) and 0.2% saponin (Tokyo Chemical Industry, Tokyo, JPN) in distilled water, and incubated at 37°C for 15 minutes to hemolyze. The hemolyzed sample was filtered through a 5-µm filter membrane in a 1:8 solution with PBS (Crystalgen, Inc, Commack, NY). The filter membrane was set microfilariae-side down in a petri dish containing PBS and incubated at 37°C for 1 hour. The filter membrane was removed, and the microfilariae in PBS were transferred to a conical tube and centrifuged (15 minutes at 650 x *g*, 4°C) to concentrate the sample. The supernatant was removed, and the microfilariae pellet was resuspended in 100 µL of nuclease-free water (Thermo Fisher Scientific, Waltham, MA) and 300 µL Trizol LS (Thermo Fisher Scientific, Waltham, MA), flash frozen in liquid nitrogen, and stored at -80°C until RNA extraction was performed.

Collection of L3 from mosquitoes

Dirofilaria immitis L3 were collected [21] from laboratory-raised, black-eyed Liverpool-strain *Aedes aegypti* [22] 15 days after feeding [23] on microfilaremic dog blood provided from previously described sources. L3 were isolated in Hanks' balanced salt solution (HBSS; MP Biomedicals, Santa Ana, California) supplemented with 2% ciprofloxacin (Sigma-Aldrich, St. Louis, MO). The L3 were washed three times in nuclease-free water and resuspended in a cryovial with 100 µL of nuclease-free water and 300 µL Trizol LS, flash frozen in liquid nitrogen, and stored at -80°C until RNA extraction was performed.

L4 derived from in vitro culture

Dirofilaria immitis L3 were collected as previously described. The L3 were washed three times in RPMI-1640 with L-glutamine (Thermo Fisher Scientific, Waltham, MA) and 20 L3 were transferred per well in a 12-well plate with 2 mL culture medium [RPMI-1640 with L-glutamine supplemented with 10% fetal bovine serum (FBS; Thermo Fisher Scientific, Waltham, MA)], 100 U/ml penicillin and 100 µg/mL streptomycin (Penicillin-Streptomycin solution, Thermo Fisher Scientific, Waltham, MA), 100 µg/mL gentamicin (Sigma-Aldrich, St. Louis, MO), 10 µg/mL ciprofloxacin (Sigma-Aldrich, St. Louis, MO), and 10 µg/mL Fungin™ (InvivoGen, San Diego, CA)] per well. The culture plate was covered and incubated at 37ºC and 5% CO_2, with a tray of water for humidity, and the medium was changed to fresh culture medium after 3 days. Viable L4 that completely shed their cuticle 6 days after the culture was initiated were washed in nuclease-free water prior to resuspension in a cryovial with 100 µL nuclease-free water and 300 µL Trizol LS, flash frozen in liquid nitrogen, and stored at -80°C until RNA extraction was performed.

RNA extraction

A designated work area, all supplies, and all equipment were cleaned with Rnase Zap (Sigma-Aldrich, St. Louis, MO). Trizol samples were removed from -80°C and thawed on ice. Two-mL round-bottom tubes were set with one, stainless steel, 3-mm BB bead per tube (autoclaved; uxcell, Hong Kong). Thawed samples were transferred to the 2-ml round-bottom tubes and vortexed on the highest speed for 45 minutes, stopping every 10 minutes to incubate samples on ice for 3 minutes before return to vortex. Homogenized samples were processed for RNA extraction with the Direct-zol RNA MiniPrep kit (Zymo Research Corporation, Irvine, CA) as per manufacturer's instructions. Extracted RNA was eluted in 50 μL nuclease-free water (Zymo Research Corporation, Irvine, CA) twice. Quality control of RNA samples was performed on a NanoDrop™ 2000 Spectrophotometer (Thermo Fisher Scientific, Waltham, MA). RNA was stored at -80°C until submitted for RNA-seq.

RNA sequencing

Extracted RNA was prepared by the University of Wisconsin Biotechnology Center - Gene Expression Center using the QIAseq FastSelect - rRNA Bacteria Kit (QIAGEN Sciences Inc, Germantown, MD) as per manufacturer's instructions, and synthesized cDNA was purified using Illumina-provided AMPure XP beads (Illumina, Inc., San Diego, CA). The resulting cDNA library was sequenced on an Illumina NovaSeq X plus (2 x 150 10B Full Lane). Sequenced reads were trimmed using fastp (v.0.20.1) [24] and aligned to the *D. immitis* reference genome (WBPS19, PRJNA723804) using STAR (v.2.7.6a) [25]. Differential gene expression was completed using the R statistical software (v4.2.1) [26] and software package DESeq2 (v. 1.36.0) [27]. Two of the three Missouri L4 biological replicates were lost prior to sequencing.

Data analysis

Hierarchical clustering was performed on the raw read counts by creating a DESeq object with the experimental design designated as design = ~stage + strain. Genes containing 20 reads across a minimum of three samples were maintained and variance stabilizing transformed (vst) prior to calculating the sample distances (method = "euclidean") and clustering (method = "ward.D2"). Principal component analysis was run on the vst transformed data. Differential gene expression between isolates and stages was completed with DESeq2 by changing the design formula to make comparisons. Data were visualized using the ggplot2 R package (v.3.4.3) [28]. Gene annotation from reference genome PRJEB1797 was carried over from PRJNA723804 using a reciprocal blast approach on the proteomes. Proteins with high amino acid similarity were maintained (percent identify ≥ 80, E-value < $1E^{-4}$, and bit score > 30). All differences compared in the results were deemed significant with a p value < 0.01.

Results

Gene expression across D. immitis MO and GA larval stages

There were 348 genes upregulated and 294 genes downregulated in GA L3 compared with L4 (Table 4.1 and Figure 4.1A). Comparisons between MO L3 and L4 were not conducted due to the loss of two of the three MO L4 biological replicates. There were 267 genes upregulated and 721 genes downregulated in GA MF compared with L4 (Figure 4.1B). Comparisons between MO MF and L4 were not conducted due to the loss of two of the three MO L4 biological replicates. There were 566 genes upregulated and 1,021 genes downregulated in GA MF compared with L3 (Figure 4.1C). There were fewer differences (n = 1,007) in MO MF

to L3 comparisons than GA MF to L3 (n=1,587), with 163 genes upregulated and 844 genes downregulated (Figure 4.1D).

Table 4.1
Differences in gene expression across D. immitis MO and GA larval stages

Larval stage comparisons	*D. immitis* isolate	Genes with different levels of expression (n)	Upregulated genes (n)	Downregulated genes (n)
L3 to L4	GA	642	348	294
L3 to L4	MO[a]	no data	no data	no data
MF to L4	GA	988	267	721
MF to L4	MO[b]	no data	no data	no data
MF to L3	GA	1587	556	1021
MF to L3	MO	1007	163	844

Notes: All differences are significant ($p < 0.01$).
[ab]: Comparisons with MO L4 were not conducted due to the loss of two of the three biological replicates.

Figure 4.1
Differences in gene expression across D. immitis larval stages and isolates

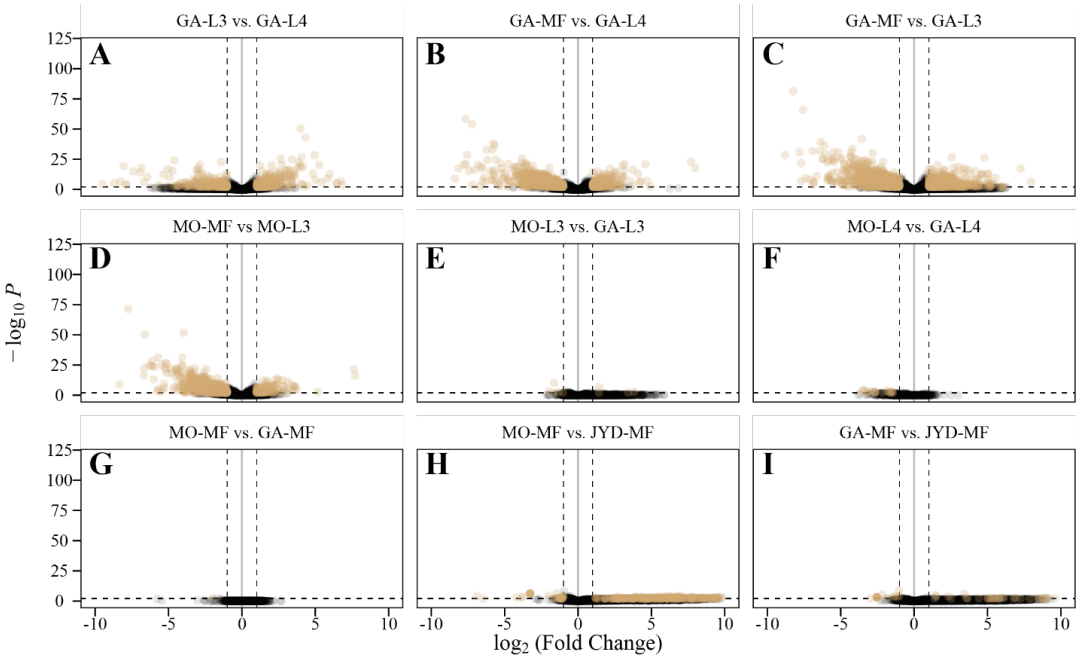

Notes: Volcano plots display the $\log_2$ fold changes in gene expression across *D. immitis* larval stages and isolates. All significant ($p < 0.01$) differences are displayed in brown.

Gene expression across D. immitis MO, GA, and JYD isolates

Four genes were upregulated and 5 genes downregulated in MO L3 compared with GA L3 (Table 4.2 and Figure 4.1E). No genes were upregulated and 18 genes downregulated in MO L4 compared with GA L4 (Figure 4.1F). No genes were upregulated and only 1 gene was downregulated in MO MF compared with GA MF (Figure 4.1G). There were 320 genes upregulated and 37 genes downregulated in MO MF compared with JYD MF (Figure 4.1H). Fewer (n = 66) genes were upregulated and downregulated (n = 17) in GA MF compared with JYD MF than MO MF to JYD MF (Figure 4.1I).

Table 4.2

Differences in gene expression across D. immitis MO, GA, and JYD isolates

***D. immitis* isolate comparisons**	**Larval stage**	**Genes with different levels of expression (n)**	**Upregulated genes (n)**	**Downregulated genes (n)**
MO to GA	L3	9	4	5
MO to GA	L4[a]	18	0	18
MO to GA	MF	1	0	1
MO to JYD	MF	357	320	37
GA to JYD	MF	83	66	17

Notes: All differences are significant ($p < 0.01$).
[a]: Comparison with MO L4 contained only one MO biological replicate.

SLO-1 differences across larval stages and isolates

There was a significant ($p < 0.004$) downregulation of SLO-1 gene-DINM_003377 expression in GA MF to L3 (log_2 fold change: -1.39) and MO MF to L3 (log_2 fold change: -1.44), but no significant differences in expression of this gene across *D. immitis* L3 to L4 comparisons and MF to L4 comparisons (Table 4.3 and Figure 4.2). There were no significant differences in expression of the SLO-1 channel across *D. immitis* MO, GA, and JYD isolates (Table 4.4).

Table 4.3
Differences in SLO-1 expression across D. immitis MO and GA larval stages

Larval stage comparisons	*D. immitis* isolate	SLO-1 with different levels of expression (n)	Upregulated genes (log2FoldChange)	Downregulated genes (log2FoldChange)
L3 to L4	GA	0	0	0
L3 to L4	MO[a]	no data	no data	no data
MF to L4	GA	0	0	0
MF to L4	MO[b]	no data	no data	no data
MF to L3	GA	1	0	-1.39
MF to L3	MO	1	0	-1.44

Notes: The only significant ($p < 0.01$) difference in SLO-1 expression across *D. immitis* MO and GA larval stages was downregulation of SLO-1 gene-DINM_003377 in MF compared with L3. [ab]: Comparisons with MO L4 were not conducted due to the loss of two of the three biological replicates.

Figure 4.2
Differences in SLO-1 expression across D. immitis larval stages and isolates

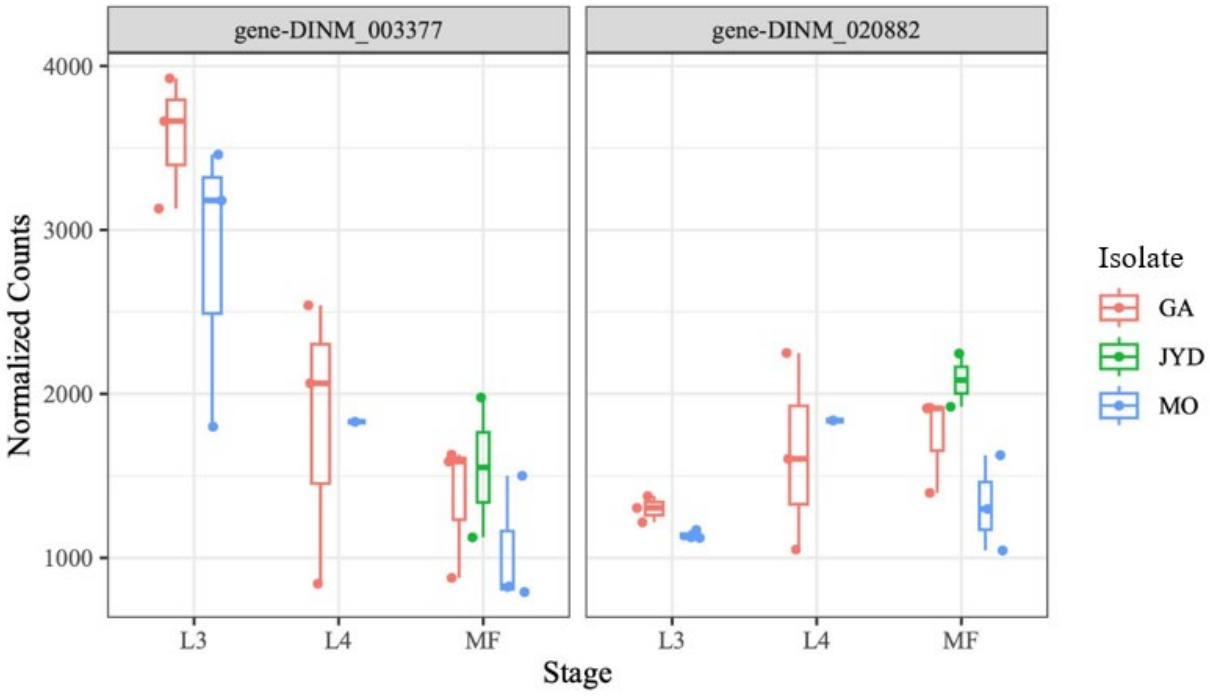

Notes: Dot plots display differences in SLO-1 expression of gene-DINM_003377 and gene-DINM_020882 across *D. immitis* larval stages and isolates. There was significant ($p < 0.004$) downregulation of gene-DINM_003377 expression in GA MF to L3 (log_2 fold change: -1.39) and MO MF to L3 (log_2 fold change: -1.44).

Discussion

As the threat of ML-resistant *D. immitis* rises in the United States, there is a need for either a new class of drugs that is effective in killing *D. immitis*, or another target of host immunity to explore to work in tandem with MLs [6]. The classic targets of MLs in nematodes are the GluCls, through which these drugs cause flaccid paralysis of somatic muscle, and most importantly the pharynx [9], by opening these channels to the inflow of chloride [13]. Paralysis of somatic muscle at relevant ML concentration in filariae is not observed, however. Paralysis of the pharynx prevents nutrient absorption, but *D. immitis* L3 and L4 are removed from the host by the host's immune system. Unlike ML-susceptible gastrointestinal nematodes, ML paralysis of the pharynx is not impactful in *D. immitis* and other filarial nematodes due to the ability of these parasites to absorb nutrients through their cuticles [9].

Only one study has been conducted exploring variable immobilizing effects of emodepside on filarial nematodes. Kashyap *et al*. discovered that emodepside has sex-dependent immobilizing effects on adult *B. malayi* due to a differentially spliced binding pocket in the RCK1 region of the SLO-1 K channel [17]. The authors used whole-parasite measurement of single muscle cells to support the hypothesis that adult male *B. malayi* are more sensitive than females to inhibition of motility by emodepside. cDNA from dsRNA-treated worms was amplified to identify SLO-1 splice variants in *B. malayi,* revealing sex-dependent differences in SLO-1 expression in two of the five predicted splice variants, SLO-1a and SLO-1f. Both variants are expressed in female *B. malayi*, but only SLO-1f is expressed in male *B. malayi*. It was also determined that SLO-1f is more sensitive to emodepside than SLO-1a, and that the difference in the two variants lies in the cytoplasmic RCK1 domain [17]. Kashyap *et al*. investigated the SLO-1 RCK1 region of two other filarial species, *Onchocerca volvulus* and *D. immitis*. Similar to *B.*

malayi, there are five predicted SLO-1 splice variants in *O. volvulus*, and only two are expressed in females: Ovo-SLO-1a and Ovo-SLO-1d. Emodepside was found to bind to the same RCK-1 regions in *O. volvulus* and *B. malayi in silico*. A model of the *in-silico* binding of emodepside to SLO-1 in *D. immitis*, using Parasite Wormbase sequences, suggested that emodepside binds to the same RCK-1 regions, although the Wormbase sequences lack information about splice variants [17].

We carried out a transcriptomic study to explore the hypothesis that gene expression of the SLO-1 channel vary across *D. immitis* larval stages. RNA sequencing was carried out on *D. immitis* microfilariae and L3 and L4 stages of ML-susceptible isolates MO and GA and ML-resistant isolate JYD. Whole-transcriptome comparisons across isolates and stages were conducted, and there is an ongoing survey of SLO-1 channel isoforms across the different isolates and larval stages.

There were significant ($p < 0.01$) differences in gene expression across *D. immitis* - transcriptomes of larval stages (Figure 4.3). Similar numbers of genes were upregulated across L3 to L4 [n = 348 (GA)], MF to L4 [n = 267 (GA)], and MF to L3 [n = 556 (GA); n = 163 (MO)]. Alternatively, fewer genes were downregulated than upregulated from L3 to L4 [n = 294 (GA)], and a greater increase in genes downregulated than upregulated from MF to L4 [n = 721 (GA)] and MF to L3 [n = 1,021 (GA); n = 844 (MO)].

A mosquito ingests blood containing MF from a heartworm-infected dog. The MF then undergo two molts in the mosquito before developing to L3. L3 are deposited on the dog's skin during an infected mosquito’s blood meal and enter the bite wound to migrate through the cutaneous tissue and molt into L4. The L4 molt one last time into immature adults, establish in the heart and pulmonary arteries, becoming sexually mature adults and producing MF 6 months

post infection [30]. The results of the whole-transcriptomic analysis across larval stages suggest that L3 and L4 are more similar in gene expression than MF to L3 or MF to L4, which is likely due to the developmental time and molts in between one stage to the other.

Figure 4.3
D. immitis similarities across larval stages and isolates

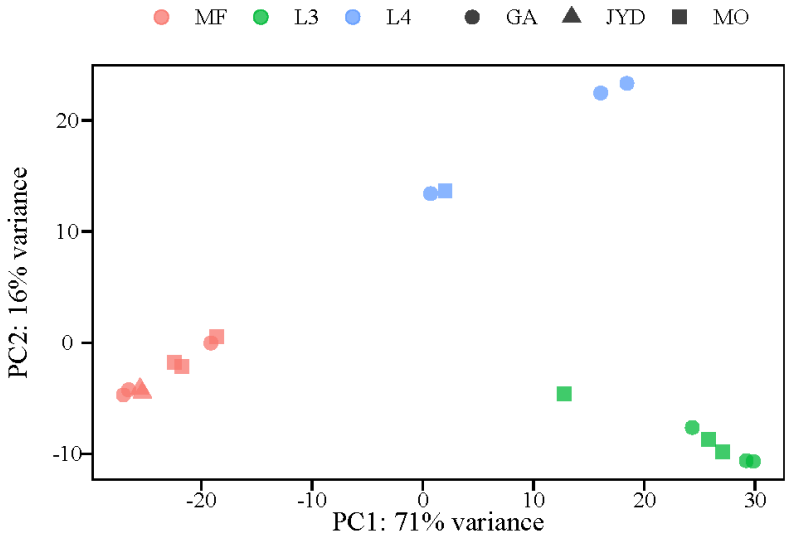

Notes: A principal component analysis (PCA) plot indicates similarities between larval stages and isolates. The samples cluster by larval stage displaying similar transcriptomic profiles.

There were few significant ($p < 0.01$) differences in gene expression across the *D. immitis* ML-susceptible and ML-resistant whole-transcriptomes studied (Figure 4.3). Only four genes were upregulated and five genes downregulated in MO L3 compared with GA L3. No genes were upregulated in MO L4 to GA L4, but 18 genes were downregulated. The gene expression patterns in MF were nearly identical in MO to GA isolates, with no upregulation and only one gene downregulated in MO compared with GA. Overall, gene expression patterns across ML-susceptible isolates MO and GA were very similar in the L3, L4, and MF stages. Notably, there were differences in MF of ML-susceptible and ML-resistant gene expression. More genes were upregulated in the ML-susceptible isolates compared with the ML-resistant isolate [n = 320

(MO); n = 66 (GA)] than downregulated [n = 37 (MO); n = 17 (GA)]. In summary, there were a total of 357 differences in gene expression in MO compared with JYD, and only 83 differences in gene expression in GA compared with JYD, aligning with ML-susceptible and ML-resistant genetic differences observed in a previous study [29].

The only significant ($p < 0.004$) differences in gene expression of the SLO-1 channel (gene-DINM_003377 and gene-DINM_020882) were the downregulation of gene-DINM_003377 expression in GA MF to L3 ($\log_2$ fold change: -1.39) and MO MF to L3 ($\log_2$ fold change: -1.44). There were no significant differences in MF compared to L4, or L3 compared to L4, in MO and GA isolates. There were also no significant differences in gene expression of the SLO-1 channel across *D. immitis* MO, GA, and JYD isolates.

As there were no significant differences in the gene expression of the SLO-1 channel in L3 and L4 of ML-susceptible isolates MO and GA, the effect of emodepside on *D. immitis* L3 and L4 should be equally effective. Since there was downregulation in the expression of one SLO-1 gene (gene-DINM_003377) and not the other (gene-DINM_020882) in the comparison of MF with L3, it is unlikely that there is a decrease in efficacy of emodepside due to this downregulation, knowing that emodepside is effective against all stages of *D. immitis in vitro* [30].

Conclusion

Emodepside is effective against *D. immitis* isolates that are resistant to MLs through selective opening of the calcium activated, voltage-dependent, potassium channel, SLO-1, and inhibition of nematode body muscle contraction. The authors of this study presented significant whole-transcriptome differences across *D. immitis* ML-susceptible and ML-resistant isolates and

larval stages. Although the authors hypothesized that differential splicing of SLO-1 could underlie differences in emodepside activity against relevant *D. immitis* life stages, a survey of SLO-1 channel splice variants across the different isolates and larval stages is still underway.

Acknowledgements

The authors thank Katelin Greenway for technical assistance and Dr. Timothy Geary for contributions in study design. The authors also thank Drs. Douglas Hutchens and Logan Andrews of Animol Discovery, Inc. for the study concept and funding of the RNA sequencing. This work was completed in part with resources provided by the University of Wisconsin Biotechnology Center - Gene Expression Center (RRID: SCR_017757).

Disclosures

The authors have no financial conflict of interest. Funding for larval resources and RNA extraction is from various revenue streams of the Moorhead laboratory at the University of Georgia. Funding for RNA sequencing is from Animol Discovery, Inc.

References

1. Hansen, R.D., et al., *A worm's best friend: recruitment of neutrophils by Wolbachia confounds eosinophil degranulation against the filarial nematode Onchocerca ochengi.* Proc Biol Sci, 2011. 278(1716): p. 2293-302.

2. (CAPC), C.A.P.C. *Canine Heartworm Prevalence Map*. 2023; Available from: https://capcvet.org/maps/#/2023/all-year/heartworm-canine/dog/united-states.

3. (CAPC), C.A.P.C. *Heartworm Guidelines*. 2020; Available from: https://capcvet.org/guidelines/heartworm/.

4. Bowman, D.D. and C.E. Atkins, *Heartworm Biology, Treatment, and Control.* Veterinary Clinics of North America: Small Animal Practice, 2009. 39(6): p. 1127-1158.

5. Wood, C.L. and P.T. Johnson, *A world without parasites: exploring the hidden ecology of infection.* Frontiers in Ecology and the Environment, 2015. 13(8): p. 425-434.

6. (AHS), A.H.S. *American Heartworm Society Canine Guidelines for the Prevention, Diagnosis, and Management of Heartworm (Dirofilaria immitis) Infection in Dogs*. Macrocyclic Lactones 2024.

7. Bowman, D.D. and J. Drake, *Examination of the "susceptibility gap" in the treatment of canine heartworm infection.* Parasites & Vectors, 2017. 10(S2).

8. Hampshire, V.A., *Evaluation of efficacy of heartworm preventive products at the FDA.* Veterinary Parasitology, 2005. 133(2): p. 191-195.

9. Prichard, R.K., *Macrocyclic lactone resistance in Dirofilaria immitis: risks for prevention of heartworm disease.* International Journal for Parasitology, 2021. 51(13): p. 1121-1132.

10. Bourguinat, C., et al., *Macrocyclic lactone resistance in Dirofilaria immitis.* Veterinary Parasitology, 2011. 181(2): p. 388-392.

11. Bourguinat, C., et al., *Macrocyclic lactone resistance in Dirofilaria immitis: Failure of heartworm preventives and investigation of genetic markers for resistance.* Veterinary Parasitology, 2015. 210(3): p. 167-178.

12. Pulaski, C.N., et al., *Establishment of macrocyclic lactone resistant Dirofilaria immitis isolates in experimentally infected laboratory dogs.* Parasites & Vectors, 2014. 7(1): p. 494.

13. Wolstenholme, A.J., *Glutamate-gated Chloride Channels*.* Journal of Biological Chemistry, 2012. 287(48): p. 40232-40238.

14. Harder, A., et al., *Cyclooctadepsipeptides—an anthelmintically active class of compounds exhibiting a novel mode of action.* International Journal of Antimicrobial Agents, 2003. 22(3): p. 318-331.

15. Kulke, D., et al., *Characterization of the Ca2+-gated and voltage-dependent K+-channel Slo-1 of nematodes and its interaction with emodepside.* PLoS Negl Trop Dis, 2014. 8(12): p. e3401.

16. Verma, S., et al., *Recording drug responses from adult Dirofilaria immitis pharyngeal and somatic muscle cells.* Int J Parasitol Drugs Drug Resist, 2021. 15: p. 1-8.

17. Kashyap, S.S., et al., *Emodepside has sex-dependent immobilizing effects on adult Brugia malayi due to a differentially spliced binding pocket in the RCK1 region of the SLO-1 K channel.* PLOS Pathogens, 2019. 15(9): p. e1008041.

18. Maclean, M.J., et al., *Does evaluation of in vitro microfilarial motility reflect the resistance status of Dirofilaria immitis isolates to macrocyclic lactones?* Parasit Vectors, 2017. 10(Suppl 2): p. 480.

19. Blagburn, B.L., et al., *Efficacy of four commercially available heartworm preventive products against the JYD-34 laboratory strain of Dirofilaria immitis.* Parasites & Vectors, 2016. 9(1): p. 191.

20. McTier, T.L., et al., *Microfilarial reduction following ProHeart® 6 and ProHeart® SR-12 treatment in dogs experimentally inoculated with a resistant isolate of Dirofilaria immitis.* Parasites & Vectors, 2017. 10(2): p. 485.

21. (FR3), F.R.R.R.C. *Collecting Infective Larvae of Brugia pahangi, B. malayi, Dirofilaria immitis, and Dirofilaria repens From Infected Mosquitoes*. Available from: http://www.filariasiscenter.org/protocols/Protocols/collecting-infective-larvae-of-brugia-pahangi-b.-malayi-dirofilaria-immitis-and-dirofilaria-repens-from-infected-mosquitoes.

22. (FR3), F.R.R.R.C. *Mosquito Rearing Techniques*. Available from: http://www.filariasiscenter.org/protocols/Protocols/mosquito-rearing-techniques.

23. (FR3), F.R.R.R.C. *Experimental Infection of Dogs, Cats, Ferrets, and Rodents with Dirofilaria immitis, Brugia malayi, B. pahangi, or Dipetalonema reconditum*. Available from: http://www.filariasiscenter.org/protocols/Protocols/experimental-infection-of-dogs-cats-ferrets-and-rodents-with-dirofilaria-immitis-brugia-malayi-b.-pahangi-or-dipetalonema-reconditum.

24. Chen, S., et al., *fastp: an ultra-fast all-in-one FASTQ preprocessor.* Bioinformatics, 2018. 34(17): p. i884-i890.

25. Dobin, A., et al., *STAR: ultrafast universal RNA-seq aligner.* Bioinformatics, 2013. 29(1): p. 15-21.

26. R-Core-Team, *R: A language and environment for statistical computing*. 2022, R Foundation for Statistical Computing: Vienna, Austria.

27. Love, M.I., W. Huber, and S. Anders, *Moderated estimation of fold change and dispersion for RNA-seq data with DESeq2.* Genome Biol, 2014. 15(12): p. 550.

28. Wickham, H., *ggplot2: Elegant Graphics for Data Analysis*. 2016: Springer-Verlag New York.

29. Bourguinat, C., et al., *Genetic profiles of ten Dirofilaria immitis isolates susceptible or resistant to macrocyclic lactone heartworm preventives.* Parasites & Vectors, 2017. 10(2): p. 504.

30. Hübner, M.P., et al., *Evaluation of the in vitro susceptibility of various filarial nematodes to emodepside.* Int J Parasitol Drugs Drug Resist, 2021. 17: p. 27-35.

CHAPTER 5

CONCLUSIONS

Significance

A thorough examination of every life stage is necessary for a comprehensive understanding of filarial parasites. Most *in vitro* studies focus on the MF and L3 life stages of the filarial parasite, *Dirofilaria immitis* (canine heartworm), because the *in vivo* developmental stages of the parasite are not readily available in research settings. While *in vitro* experiments are useful for working out the mechanisms of parasite invasion and worm establishment, little is known about the host-parasite interaction—specifically, the host mechanisms that ultimately determine the parasite's establishment. The best animal models for current *in vivo D. immitis* research are dogs and ferrets, as these studies require a patent infection in a permissive host. Because of the nature of the research and the economics, rodent animal models are typically chosen by researchers for *in vivo* studies; however, prior studies have unsuccessfully attempted to establish infection in immunocompetent mice, rats, and jirds [1, 2].

The hypothesis for this dissertation's research is that the establishment of *D. immitis* in the definitive host is determined by that host's immune response to the presence of larvae. The outcomes of these investigations will close a knowledge gap about the factors influencing filarial host specificity. The findings also shed light on the host's antifilarial processes, which could be useful in the future to find a preventive or therapeutic measure. The findings of these studies will not only have an impact on the field of study on canine heartworms, but they may also inspire

more focused efforts to eradicate other infectious filarial diseases that affect humans and animals.

Three factors make the research in this dissertation novel. First, this is the first study to characterize the early cellular immune response in a Mongolian gerbil (jird) to *D. immitis* IP infection was presented in Chapter 2. This is also the first study to deplete jird peritoneal macrophages and the first to use flow cytometry to investigate the immune response in the gerbil peritoneum using PECs as described in Chapter 3. Differential splicing of SLO-1 is discussed in Chapter 4, which may account for variations in emodepside activity against pertinent *D. immitis* life stages.

This chapter will conclude the dissertation by summarizing the major research findings in connection to the objectives and hypotheses and analyze their significance and usefulness. It will also review the study's limitations and propose opportunities for further investigation.

The brief residency of *Dirofilaria immitis* in the peritoneal cavity of the Mongolian gerbil (*Meriones unguiculatus*)

The Mongolian gerbil, *Meriones unguiculatus*, (jird) serves as an immunocompetent rodent model for another filarial parasite, *Brugia malayi*, a causative agent of lymphatic filariasis [3]. Jirds develop a patent infection after subcutaneous (SC) and intraperitoneal (IP) inoculation of *B. malayi* L3 and developed adult worms are later found in the testes, heart, and lungs with SC infections and in the peritoneal cavity with IP infections [3, 4]. Additionally, microfilariae (MF) are found circulating in the peripheral blood with SC infections and the peritoneal cavity in IP infections [3, 4]. The IP-infected jird model was the ideal control for this study because of the ability to recover all developmental stages of the parasite from a single location [4].

This study is innovative because it is the first to observe the initial immune response of a nonpermissive host, the jird [5], to *D. immitis* IP infection. The objective of this study was to investigate the cellular immune response to infection with *B. malayi* and *D. immitis* larvae in the peritoneal cavity of the jird. We hypothesized that the establishment of *D. immitis* is determined by host immunity after the third larval molt. Identifying the *D. immitis* larval stage for which establishment is prevented by the jird nonpermissive host will provide more insight into host specificity of filarial infections. Jirds were infected by IP injection with either 100 *B. malayi* (n = 20) or *D. immitis* (n = 20) third-stage larvae (L3), for which the jird is permissive or nonpermissive to parasitic establishment, respectively. Necropsies were performed at 1-, 3-, 10-, and 36-days post infection (dpi) (n = 5/timepoint/group). Larvae were recovered by peritoneal lavage at each timepoint, quantified, and stored in formalin for larval-stage morphologic identification. The peritoneal wall and diaphragm were recovered from each jird and stored in ethanol for absolute quantification of larvae using droplet digital PCR (ddPCR).

Dirofilaria immitis L3 were found in the peritoneal wall and diaphragm of jirds 1 dpi, which were examined for their cellular response to infection with *B. malayi* and *D. immitis* L3. The cellular immune response in a naïve jird negative control and *B. malayi* positive control served as a baseline for the evaluation of the jird cellular response to *D. immitis* L3. Jirds infected with *D. immitis* had multifocal mats of neutrophils, macrophages, and lymphocytes, with fibrin and necrotic debris on the muscle surface in contrast with the loose aggregates of cells observed in *B. malayi* tissues. The perimysium and endomysium were expanded by edema, with low to moderate numbers of neutrophils, lymphocytes, and macrophages. Although the negative control displayed perimysium infiltration of macrophages and neutrophils, the *D. immitis* tissue additionally contained lymphocytes and edema of the perimysium. Overall, there

was an increase in inflammation localized around *D. immitis* L3 compared to *B. malayi*-infected peritoneal wall and naïve tissue.

Peritoneal recovery of *D. immitis* larvae in the jird was as expected, with a gradual decline in numbers, but the absence and reappearance of *D. immitis* larvae at 1 and 3 dpi, respectively, was of the utmost interest to the authors. Although the recovery of *B. malayi* larvae was slightly lower at 10% than the expected 23%, this could be due to the overall variability of jird infectivity [6]. Previous studies demonstrated that subcutaneously inoculated *D. immitis* L3 and L4 are found in the skin and muscle of dogs and ferrets up to 58 dpi [1, 7], so the peritoneal wall and diaphragm were excised and submitted for histopathology to potentially locate L3 in the tissues at 1 dpi. Although *D. immitis* L3, along with a few *B. malayi* L3, were observed in the step sections of these tissues, it was highly likely that larvae were overlooked through the process. Notably, there was a clear increase in the presence of inflammatory cells and macrophages that appeared in the tissues with *D. immitis* L3 as compared to the tissues with *B. malayi* L3. These results demonstrate that there is a stronger cellular immune response to *D. immitis* L3 than against *B. malayi* L3.

A major limitation of this research is the jird model. There are almost no immunochemistry markers known to work with gerbils, and characterization of jird peritoneal cells has yet to be published. There are more unknowns than knowns about gerbil immunity, requiring researchers to gain a more basic understanding of jirds before dedicating their efforts to using them as a model. However, the jird was an ideal model for this study, because it is permissive to the establishment of a *B. malayi* intraperitoneal infection, allowing for an easier method of worm recovery than a subcutaneous inoculation method. Although the histopathology results were useful in describing the cellular immune response in the peritoneal wall and

diaphragm to the parasites, ddPCR is a more sensitive test for the absolute quantification of larval DNA as the probability of overlooking larvae through sectioning the tissues was high. Analysis of ddPCR is underway.

The role of macrophages in the immune response to peritoneal infection with *Dirofilaria immitis* larvae in the Mongolian gerbil (*Meriones unguiculatus*)

The jird is nonpermissive to the establishment of *D. immitis*, which can be explained from the perspective of host phylogenetic and geographic specificity. Although the jird is not susceptible to *D. immitis* establishment, investigating the jird immune response to the initial infection of *D. immitis* can provide better insight into the host-parasite interaction, specifically the mechanism of the host cellular response that prevents the establishment of the parasite.

A versatile cell type that plays an essential role in host immunity is the macrophage. Helminth infections trigger type 2 immune responses that prompt the macrophage to undergo alternative activation [8, 9], and macrophages are known to be directly involved in the elimination of filariae [10, 11]. As discussed in Chapter 2, *D. immitis* L3 were found in the peritoneal wall and diaphragm of jirds at 1 dpi, surrounded primarily by macrophages. The objective of this study was to determine the role of macrophages in the immune response to peritoneal infection with *D. immitis* larvae in the jird. We hypothesized that the absence of jird macrophages in the peritoneal cavity would allow L3 to remain in the peritoneal cavity instead of evading the immune response by migrating into tissues.

In this study, jirds (n = 6) were administered clodronate (CL) liposomes (100 µl/10 g body weight) by IP injection for the depletion of peritoneal macrophages prior to IP inoculation with 100 *D. immitis* L3. Another group of jirds (n = 6) were administered phosphate-buffered

saline (PBS) liposomes (100 µl/10 g body weight) by IP injection to serve as a vehicle control prior to *D. immitis* infection. Necropsies were performed at 1 dpi, and L3 were recovered and quantified by peritoneal lavage. Flow cytometry was performed on peritoneal exudative cells (PECs) recovered from the peritoneal lavage fluid, to confirm the absence (or presence in the control group) of macrophages.

More *D. immitis* L3 were recovered from peritoneal macrophage-depleted jirds than from the control group at 1 dpi, supporting the hypothesis that the absence of jird macrophages in the peritoneal cavity would allow L3 to remain in the peritoneal cavity instead of being sequestered in the diaphragm and peritoneal wall. Cell attachment, presumably macrophages, were observed on *D. immitis* L3 in the control group. In the absence of macrophages, there is a significant increase in the presence of neutrophils. Neutrophils are the first cell type to be recruited to the site of infection, followed by non-resident macrophages, so in PECs with macrophage depletion, an increase of neutrophils is to be expected.

There were several limitations to this study. The liposome manufacturer [Liposoma, the Netherlands (clodronateliposomes.com)] provides recommendations for the dose and frequency of administration, but this can be variable across species, age, and size of the animal. There is also not an established protocol for CL liposome IP administration in jirds. Jird PECs have yet to be characterized at the time of writing this dissertation, and the identification of cells and gating strategies were heavily influenced by the success of F4/80 as a jird peritoneal macrophage marker. Imaging flow cytometry was performed, not only to validate the liposome dose and frequency of administration, but to visualize the fluorescence of macrophages tagged with the Alex Fluor 647 F4/80 antibody to confirm its cross-reactivity with jird macrophages. The success of the F4/80 antibody after the imaging flow cytometer allowed the authors to confidently gate

for F4/80^{+} cells by standard flow cytometry, allowing for quantification of the depletion of macrophages from the total PECs recovered from the jird peritoneal cavity.

Dirofilaria immitis stage-specific variations of SLO-1 channel expression through RNA sequencing analysis

There is a loss of efficacy (LOE) concern with ML-resistant *D. immitis* cases increasing in the United States. The first report of LOE occurred in 1998 [12] and has greatly increased since, primarily in the highly endemic areas of heartworm in the southern United States [13]. As the threat of ML-resistant *D. immitis* rises in the United States, there is a need for either a new class of drugs that is effective in killing *D. immitis*, or another target of host immunity to explore to work in tandem with MLs [6]. The target of MLs in *D. immitis* are the GluCls, causing flaccid muscle paralysis of the body, and most importantly the pharynx [13], by opening these channels to the inflow of chloride [14]. Paralysis of the pharynx prevents nutrient absorption, and the *D. immitis* L3 and L4 are removed by the host's immune system. Unlike ML-susceptible gastrointestinal nematodes, ML paralysis of the pharynx is impactful in *D. immitis* and other filarial nematodes due to the ability of these parasites to also absorb nutrients through their cuticles [13].

Emodepside, a cyclooctadepsipeptide, is effective against both gastrointestinal and filarial nematodes. The mode of action of cyclooctadepsipeptides is distinct from other anthelmintic classes [15]; therefore, emodepside is effective against *D. immitis* isolates that are resistant to MLs [16]. Emodepside selectively opens the calcium activated, voltage-dependent potassium channel, SLO-1, and inhibits nematode body muscle contraction [16, 17]. A transcriptomic study was performed to explore the hypothesis that differential splicing of SLO-1

could underlie differences in emodepside activity against relevant *D. immitis* life stages. RNA sequencing was carried out across *D. immitis* microfilariae, and L3 and L4 stages of ML-susceptible isolates, MO and GA, and ML-resistant isolate, JYD. Whole-transcriptome comparisons across strains and stages were conducted, and there is an ongoing survey of SLO-1 channel isoforms across the different isolates and larval stages.

As there were no significant differences in the gene expression of the SLO-1 channel in L3 and L4 of ML-susceptible isolates MO and GA, the effect of emodepside on *D. immitis* L3 and L4 should be equivocally effective. Since there was downregulation in the expression of one SLO-1 gene (gene-DINM_003377) and not the other (gene-DINM_020882) in the comparison of MF with L3, it is unlikely that there is a decrease in efficacy of emodepside due to this downregulation, knowing that emodepside is effective against all stages of *D. immitis in vitro* [18].

The major limitation to this study was the lack of *D. immitis* whole genome assemblies. We used the most recent of the two genomes hosted on Worm base Parasite. There was a recent publication that claims to have made improvements on them [19], but there are no gene annotations available.

Future directions

The jird is a promising immunocompetent nonpermissive rodent model for *D. immitis* due to its permissivity of a related filarial nematode, *B. malayi*. However, due to the lack of gerbil-specific antibody reagents commercially available, a natural next step is to explore available antibodies for cross reactivity. The established flow cytometry protocol developed in these studies and the identification of a cross-reactive macrophage marker removes some of the

unknowns when characterizing jird PECs. Characterizing jird PECs morphologically via cytocentrifuge and quantification of cells via flow cytometry will provide researchers a better understanding of the nonpermissive host cellular immune response to *D. immitis* infection.

Another future direction to explore is the role of macrophages in the establishment of *D. immitis* in jirds by performing an arginase assay to compare naïve jird PECs with naïve PECs cultured with *D. immitis* L3. Understanding the activation of macrophages is the second step to investigating the jird immune response to the initial infection with *D. immitis*. These efforts may provide better insight into the cross-talk between the parasite and the host, specifically the mechanism of the host cellular response that prevents the establishment of *D. immitis*.

Lastly, identifying not only the SLO-1 splice variants, but an annotated whole genome assembly, would allow for a better understanding of gene expression across *D. immitis* larval stages and ML-susceptible and ML-resistant isolates. Identifying specific genes expressed at different stages of larval development can provide a new target for antihelminthics, leading to more targeted eradication efforts of *D. immitis* and other types of human and animal infectious filarial diseases.

References

1. McCall, J.W., et al., *Chapter 4 Heartworm Disease in Animals and Humans*. 2008, Elsevier. p. 193-285.

2. Schorderet-Weber, S. and S. Specht, *In Vivo Models for the Discovery of New Antifilarial Drugs*, in *Human and Animal Filariases*. 2022. p. 391-458.

3. Ash, L.R. and J.M. Riley, *Development of subperiodic Brugia malayi in the jird, Meriones unguiculatus, with notes on infections in other rodents.* J Parasitol, 1970. 56(5): p. 969-73.

4. Mutafchiev, Y., et al., *Intraperitoneal development of the filarial nematode Brugia malayi in the Mongolian jird (Meriones unguiculatus).* Parasitology Research, 2014. 113(5): p. 1827-1835.

5. Wong, M.M., Lim, K. C., *Development of Intraperitoneally Inoculated Dirofilaria immitis in the Laboratory Mongolian Jird (Meriones unguiculates).* The Journal of Parasitology, 1975. 61(3): p. 573-574.

6. (AHS), A.H.S. *American Heartworm Society Canine Guidelines for the Prevention, Diagnosis, and Management of Heartworm (Dirofilaria immitis) Infection in Dogs*. Macrocyclic Lactones 2024.

7. Bowman, D.D. and J. Drake, *Examination of the "susceptibility gap" in the treatment of canine heartworm infection.* Parasites & Vectors, 2017. 10(S2).

8. Van Dyken, S.J. and R.M. Locksley, *Interleukin-4- and Interleukin-13-Mediated Alternatively Activated Macrophages: Roles in Homeostasis and Disease.* Annual Review of Immunology, 2013. 31(Volume 31, 2013): p. 317-343.

9. Rolot, M. and B.G. Dewals, *Macrophage Activation and Functions during Helminth Infection: Recent Advances from the Laboratory Mouse.* Journal of Immunology Research, 2018. 2018: p. 2790627.

10. Remion, E., et al., *Unbalanced Arginine pathway and altered maturation of pleural macrophages in Th2-deficient mice during Litomosoides sigmodontis filarial infection.* Frontiers in Immunology, 2022. 13.

11. Allen, J.E. and P.N. Loke, *Divergent roles for macrophages in lymphatic filariasis.* Parasite Immunology, 2001. 23(7): p. 345-352.

12. Hampshire, V.A., *Evaluation of efficacy of heartworm preventive products at the FDA.* Veterinary Parasitology, 2005. 133(2): p. 191-195.

13. Prichard, R.K., *Macrocyclic lactone resistance in Dirofilaria immitis: risks for prevention of heartworm disease.* International Journal for Parasitology, 2021. 51(13): p. 1121-1132.

14. Wolstenholme, A.J., *Glutamate-gated Chloride Channels*.* Journal of Biological Chemistry, 2012. 287(48): p. 40232-40238.

15. Harder, A., et al., *Cyclooctadepsipeptides—an anthelmintically active class of compounds exhibiting a novel mode of action.* International Journal of Antimicrobial Agents, 2003. 22(3): p. 318-331.

16. Kulke, D., et al., *Characterization of the Ca2+-gated and voltage-dependent K+-channel Slo-1 of nematodes and its interaction with emodepside.* PLoS Negl Trop Dis, 2014. 8(12): p. e3401.

17. Verma, S., et al., *Recording drug responses from adult Dirofilaria immitis pharyngeal and somatic muscle cells.* Int J Parasitol Drugs Drug Resist, 2021. 15: p. 1-8.

18. Hübner, M.P., et al., *Evaluation of the in vitro susceptibility of various filarial nematodes to emodepside.* Int J Parasitol Drugs Drug Resist, 2021. 17: p. 27-35.

19. Gandasegui, J., et al., *Genome structure and population genomics of the canine heartworm Dirofilaria immitis.* Int J Parasitol, 2024. 54(2): p. 89-98.